A COMPREHENSIVE PERFORMANCE INVESTIGATION
OF AN UNDER-FLOOR AIR DISTRIBUTION SYSTEM IN
THE TROPICS

POH KAI SIN

DISSERTATION SUBMITTED IN FULFILMENT
OF THE REQUIREMENT FOR THE DEGREE OF
MASTER OF ENGINEERING SCIENCE

FACULTY OF ENGINEERING
UNIVERSITY OF MALAYA
KUALA LUMPUR

2017

UNIVERSITI MALAYA

ORIGINAL LITERARY WORK DECLARATION

Name of Candidate   :   POH KAI SIN   KGA110097

Registration/Matric No :   MASTER OF ENGINEERING SCIENCE

Name of Degree   :

Title of Project Paper/Research Report/Dissertation/Thesis ("this Work"):
    A Comprehensive Performance Investigation of an Under-Floor
    Air Distribution System in the Tropics

Field of Study   :   HEATING, VENTILATING AND AIR CONDITIONING (HVAC)

I do solemnly and sincerely declare that:

(1)   I am the sole author/writer of this Work;
(2)   This Work is original;
(3)   Any use of any work in which copyright exists was done by way of fair dealing and for permitted purposes and any excerpt or extract from, or reference to or reproduction of any copyright work has been disclosed expressly and sufficiently and the title of the Work and its authorship have been acknowledged in this Work;
(4)   I do not have any actual knowledge nor do I ought reasonably to know that the making of this work constitutes an infringement of any copyright work;
(5)   I hereby assign all and every rights in the copyright to this Work to the University of Malaya ("UM"), who henceforth shall be owner of the copyright in this Work and that any reproduction or use in any form or by any means whatsoever is prohibited without the written consent of UM having been first had and obtained;
(6)   I am fully aware that if in the course of making this Work I have infringed any copyright whether intentionally or otherwise, I may be subject to legal action or any other action as may be determined by UM.

Candidate's Signature   Date

Subscribed and solemnly declared before,

Witness's Signature   Date

Name:
Designation:

ABSTRACT

Under-floor Air Distribution System (UFAD) is the technology that uses an under-floor plenum below a raised floor system to deliver conditioned air into the occupancy space for human comfort in a commercial building. A well-engineered UFAD system can provide the flexibility of restructuring the layout of the interior space, reduce energy consumption, and improve thermal comfort, ventilation efficiency and indoor air quality as compared to the overhead air distribution (OHAD) system. However, the research and technical data on the application of UFAD system in the tropics is very limited. Hence, the application of the UFAD system for human comfort in the tropics is not widely known. This study is divided into three sections to investigate the performance and the application of UFAD system for human comfort, and the integration of a solar photovoltaic (PV) system into the UFAD system in the tropics. First, the fieldwork measurement was conducted to study the thermal environmental and indoor air quality of an existing UFAD system in a high-rise office building in Malaysia. It was found that the air stagnation at the occupancy space is critical as all the air velocities measured at the locations according to the Industry Code of Practice on Indoor Air Quality were well-below the minimum required air velocity of 0.15 m/s. The average air velocities measured are in the range of 0.04 – 0.06 m/s. The airflow pattern of the swirl floor diffuser was then tested at an airflow testing laboratory. Computational Fluid Dynamics (CFD) was used to extend the study on the swirl floor diffuser to various grille designs, diffuser blades and airflow rates to investigate the diffuser's performance according to ASHRAE standard. Finally, the energy consumption of the air-handling unit (AHU) for the UFAD system has been analyzed with the integration of a solar PV system in the tropics. The findings of this study show that the diffuser's design and selection, HVAC system design, construction, operation and maintenance are equally important to produce a UFAD system that achieves significant advantages over the OHAD system.

ABSTRAK

Sistem pengedaran udara bawah lantai (UFAD) adalah satu teknologi yang menggunakan plenum di bawah sistem lantai yang dibangkitkan untuk menyalurkan udara dingin ke ruangan penghuni untuk keselesaan manusia di sebuah bangunan komersial. Suatu sistem UFAD yang baik boleh memberikan fleksibiliti penstrukturan semula susun atur ruangan dalaman, mengurangkan penggunaan tenaga elektrik, dan meningkatkan keselesaan haba, kecekapan pengudaraan dan kualiti udara dalaman berbanding dengan sistem pengedaran udara atas kepala (OHAD). Walau bagaimanapun, data penyelidikan and teknikal mengenai aplikasi sistem UFAD di kawasan tropika adalah terhad. Oleh itu, penggunaan sistem UFAD untuk keselesaan manusia di kawasan tropika tidak diketahui ramai. Kajian ini dibahagikan kepada tiga bahagian untuk menyiasat prestasi dan aplikasi sistem UFAD untuk keselesaan manusia dan integrasi sistem suria fotovoltan (PV) ke dalam sistem UFAD di kawasan tropika. Pertama, pengukuran kerja lapangan telah dijalankan untuk mengkaji haba udara persekitaran dan kualiti udara dalaman sistem UFAD yang sedia ada di dalam sebuah bangunan pejabat bertingkat-tinggi di Malaysia. Kajian didapati bahawa kejadian genangan udara pada ruang penghuni adalah kritikal kerana semua halaju udara yang diukur di lokasi yang ditetapkan berdasarkan Tataamalan Industri Kualiti Udara Dalaman adalah di bawah halaju udara minimum yang dihendaki, iaitu 0.15 m/s. Purata halaju udara yang diukur adalah di antara 0.04 – 0.06 m/s. Kemudian, corak aliran udara dari penyebar pusaran lantai telah dikaji di makmal kajian aliran udara. Dinamik bendalir berkomputer (CFD) telah digunakan untuk melanjutkan pengajian penyebar pusaran lantai dengan pelbagai reka bentuk jeriji, penyebar bilah dan kadar aliran udara untuk menyiasat prestasi penyebar udara berdasarkan piawai ASHRAE. Akhirnya, penggunaan tenaga elektrik unit pengendalian udara (AHU) untuk sistem UFAD telah dianalisis dengan integrasi sistem suria PV di kawasan tropika. Hasil kajian ini

menunjukkan bahawa reka bentuk penyebar udara lantai dan pemilihan, reka bentuk sistem HVAC, pembinaan, operasi dan penyelenggaraan adalah penting sama sekali untuk menghasilkan suatu sistem UFAD yang mencapai kelebihan yang ketara berbanding dengan sistem OHAD.

ACKNOWLEDGEMENTS

First, I would like to deliver my deepest appreciation to my supervisors, Professor Ir. Dr. Yau Yat Huang and Dr. Ahmad Badarudin bin Mohd Badry for their invaluable guidance and support in completing the research work especially when I am conducting it in the transition between full-time and part-time.

From the collaboration with industrial partners, I would like to give my appreciation to Ir. Den Low Han Guan, the director of IAQ Solutions Sdn. Bhd. for providing the opportunity to conduct IAQ audit outside University of Malaya. Besides, I would like to give my appreciation to Mr. Tung Kum Weng, the managing director of Prudentaire Marketing Sdn. Bhd. in giving the technical support and providing laboratory facilities to conduct experimental work. Lastly, I would like to give my appreciation to Mr. Teddy Zhang, the CEO of Eco Geo Solar Sdn. Bhd. in sponsoring solar photovoltaic systems to University of Malaya for research purposes.

I would also like to extend my appreciation to my family members, especially my parents Mr. Poh Chin Meng and Mrs. Lim Siew Looi for their love, encouragement and support. Without them, the study may be halted. Besides, the continuous love and spiritual support from my beloved Ms. Chan Ee Wen and friends have enable me to endure through difficult times.

Finally, I would like to extend thanks to Mr. Arvindt Mariapan, Mr. Ramis A/L K. D. Rada, Mr. Jefferson Chuah Chong Yit, Ms. Anne, Mr. Veer and Mr. Tung You Ming for their help and assistant throughout the research works.

TABLE OF CONTENTS

LIST OF FIGURES

LIST OF TABLES

LIST OF SYMBOLS AND ABBREVIATIONS

ADPI   Air diffusion performance index
AHU   Air handling unit
CAV   Constant air volume
CFD   Computational fluid dynamics
CO   Carbon monoxide
CO_2 Carbon dioxide
FiT   Feed-in tariff
HVAC   Heating, ventilating and air conditioning
IAQ   Indoor air quality
MCB   Miniature circuit breaker
OHAD   Overhead air distribution
PC   Personal computer
PMV   Predicted mean vote
PV   Personal ventilation
SCF   Simple cash flow
SEDA   Sustainable Energy Development Agency Malaysia
SPBP   Simple payback period
UFAD   Under-floor air distribution
VSD   Variable speed drive
VAV   Variable air volume

CMH   cubic meter per hour
mm   millimeter
m/s   meter per second
m   meter
°C   degree Celsius
K   Kelvin
Vc   centerline velocity
VDC   direct current voltage
VAC   alternating current voltage
DC   direct current
W   watt
A   ampere
V   voltage
kWh   kilowatt per hour
RM   Ringgit Malaysia
%   percent

ρ density
t   time
τ tangential viscous stress
σ normal stress
p   pressure
u   velocity component in x direction
v   velocity component in y direction
w   velocity component in z direction
μ dynamic viscocity
λ thermal conductivity
Φ dissipation function
T   temperature

LIST OF APPENDICES

CHAPTER 1 – INTRODUCTION

1.1.   Research Background

Under-floor air distribution (UFAD) system was traditionally designed to serve data centers since year 1950. The application of UFAD system was then extended for human comfort in the 70s. Although this air distribution technology has been available for decades, there was no comprehensive guide or standards available to support the development of this technology. Until recent years, ASHRAE Handbook HVAC Application (ASHRAE, 2015) and various standards such as ASHRAE Standard 62.1, 113 have been amended to include UFAD system (ASHRAE, 2013b, 2013c). ASHRAE then published a UFAD guide on design, construction and operation of under-floor air distribution systems in the year 2013 due to the wide application in North America (ASHRAE, 2013d). This guide is a comprehensive compilation of information supported by decades of extensive research results. It is designed to provide architects, design engineers, building owners and building facility team with a complete understanding of the system. The guide is continuously updated with the latest research findings in the development of this technology.

Thermal comfort and indoor air quality (IAQ) are the two important factors in indoor environmental quality that are related to heating, ventilating and air conditioning (HVAC) system. The concept of air distribution in UFAD system is different from the conventional overhead air distribution (OHAD) system. Thus, the temperature control, air movement and air contamination distribution in the occupancy space are different. A study in the tropics found that thermal discomfort near floor diffusers and air stagnation at the sedentary level far from diffusers are issues of UFAD system that need the attention from design engineers (Sekhar and Ching, 2002). ASHRAE Standard 55 does not have minimum air movement requirement (ASHRAE, 2013a). However, Malaysian Standard

MS 1525:2014 recommended a minimum air movement of 0.15 m/s to avoid air stagnation that will cause human discomfort (Department of Standards Malaysia, 2014).

In UFAD systems, thermal stratification is one of the most important criteria that reduce energy consumption and improve ventilation efficiency. Thermal stratification is produced in a properly designed and controlled UFAD system during cooling operation (Schiavon et al., 2014). In order to achieve thermal stratification, the airflow distribution and momentum from the floor diffusers are the key elements (Raftery et al., 2015; Zhang et al., 2014a). The geometrical designs of the floor diffusers strongly influence these elements. Thus, it is necessary to study various types of floor diffusers and the potential design improvements. Computational fluid dynamics (CFD) analysis is a very useful tool when parametric analysis needed to be conducted. Results can be validated with experiment while further analysis using CFD can reduce the time cost.

On the aspect of energy consumption, HVAC system is the most energy-consuming services in a building. Improving energy efficiency of the system alone is insufficient for the sustainability of the environment. Alternative sources of energy are necessary. Solar photovoltaic cooling systems have been in the interest of researchers worldwide, especially in the countries where solar irradiation is abundance (Ashhab et al., 2013). Solar irradiation can vary significantly in different climatic regions. Malaysia has the advantage of harvesting consistent solar irradiation all year round. The potential application of the solar photovoltaic system in HVAC system is positive.

The feed-in tariff (FiT) was first proposed in the Malaysia Building Integrated Photovoltaic (MBIPV) Project as one of the potential renewable energy policies in the year 2004. The proposal was studied for years to the extent of passing the RE Acts 2011

and SEDA Act 2011. Biomass, Biogas, small hydro and solar photovoltaic are the renewable energies permitted for FiT. Among these options, solar photovoltaic is the fastest and largest renewable energy that has achieved commercial operation (SEDA, 2015). It has greatly improved the market demand for solar photovoltaic system and thus decreases the price of solar photovoltaic panels.

1.2. Problem Statements

Although UFAD system has been designed for human comfort for more than 40 years. It is still not widely used in tropical countries. There are barely few high rise buildings in Malaysia that are designed using UFAD system. The reason of less popularity of designing this system is mainly due to the lack of information for a proper UFAD system's design in the tropics. Thus, building designers tends to go for conventional OHAD system design. Thus, the aim of this study is to provide a comprehensive study of UFAD system so that building designers can have a better understanding and consideration when designing an UFAD system in the tropics.

1.3. Research Objectives

UFAD system has the potential of reducing the operating energy consumption as compared to OHAD system. With the integration of solar PV system, energy consumption from grid can have the potential to be further reduced as solar energy is abundance in the tropics. Thus, the performances of UFAD systems were investigated with the aim to understand and improve thermal environment, indoor air quality, ventilation and energy consumption in the tropics. The objectives of the study are:

    i.   Investigation on the thermal environment and indoor air quality of the office floors served by UFAD system at TM Tower, Kuala Lumpur, Malaysia.

ii. Conducting experiments and CFD simulation on the airflow pattern of a floor swirl diffuser as swirl diffuser is the most widely used floor diffuser.

iii. Analyzing the potential of using solar energy in UFAD system in the tropics through solar irradiation analysis, experimental investigation of solar photovoltaic system, power consumption analysis of AHU and payback period calculation.

1.4. Significance of the Study

The results and findings from this research work will contribute to the following:

i. Thermal environment and indoor air quality audit are conducted. The sick building syndrome (SBS) in relation to the performance of UFAD system in the tropics are presented.

ii. Improvements to reduce SBS in high rise offices served by UFAD system are discussed. This will serve as guidelines to the building owners, operation and maintenance team, building designers and occupants.

iii. Various geometrical designs of floor swirl diffuser are examined through experimental work and CFD simulation. The airflow pattern induced by the variation of floor swirl diffuser will provide fundamental understanding to the air terminal designers during floor swirl diffusers' product development and to the building designers in diffusers selection.

iv. The application of the solar photovoltaic system in HVAC system has been growing in interest. This study will investigate potential to harvest energy through the use of the solar photovoltaic system throughout Malaysia.

v. The energy consumption of UFAD system and the energy generation of the solar photovoltaic system in the tropics is discussed. The results suggested the potential application of hybrid solar-powered UFAD system.

1.5. Scope of the Study

i. The scope of thermal environment study is focused on the implication of physical parameters of air towards the indoor environment quality of the office space.

ii. The airflow patterns of the floor swirl diffuser are tested with unconditioned indoor air. Conditioned airflow patterns are further predicted using CFD modeling.

iii. The energy consumptions of an existing UFAD system and energy generated from the solar photovoltaic system are studied separately. The results give a theoretical feasibility study of using solar photovoltaic energy generation to operate UFAD system. Hence, the unforeseen effects of combining the two systems in operation are not discussed.

1.6. Outline of the Dissertation

i. Chapter one introduces the background, development and issues related to the application of UFAD system. The objectives, significance and limitation of the study are also presented.

ii. Chapter two presents the literature review related to solar photovoltaic system, solar cooling system, UFAD system, sick building syndrome (SBS) and indoor air quality (IAQ).

iii. Chapter three describes the research methodology adopted for IAQ audit of an existing UFAD system in the tropics and the CFD fundamental theories related to the diffuser's airflow study.

iv. Chapter four presents the thermal environment and IAQ investigation of the office spaces served by existing UFAD system in the tropics.

v. Chapter five contains the studies of various geometrical designs of floor swirl diffuser. The results will give an understanding to airflow pattern of the floor swirl diffusers towards the indoor environment.

vi. Chapter six presents the findings from the solar irradiation study throughout Malaysia, solar photovoltaic energy generation, energy consumption of UFAD system and payback period of hybrid solar-powered UFAD system.

vii. Chapter seven concludes the findings with various recommendations.

CHAPTER 2 – LITERATURE REVIEW

2.1   Overview

This chapter presents the literature review of sick building syndrome (SBS), and indoor air quality (IAQ), under-floor air distribution (UFAD) system, heating, ventilating and air conditioning (HVAC) energy demand in commercial building, solar photovoltaic system and solar cooling system. Standards, codes and guidelines related to indoor air quality of office space were compared. Finally, the research purposes were concluded.

2.2   Sick Building Syndrome

Sick building syndrome (SBS) is human health symptoms in association with building indoor environmental quality and the occupants' psychological factor. It can be classified into categories such as mucous-membrane irritation, neurotoxic effects, respiratory symptoms, skin symptoms and chemosensory changes (Redlich et al., 1997). The symptoms are eye irritation, dizziness, headache, sneezing, running nose, dry throat and skin irritation. SBS usually is not attributed to a single cause, which makes identifying a cause difficult (Burroughs and Hansen, 2011).

Numerous studies have shown the connection between various indoor environmental conditions and SBS symptoms (Crook and Burton, 2010; Fisk et al., 2009; Gül et al., 2007; Nakaoka et al., 2014). In these cases, mold has been considered as one of the most significant factors attributing to SBS symptoms. It is the major cause of respiratory allergies such as asthma, rhinitis and bronchitis (Crook and Burton, 2010). Mold is naturally present in the indoor air at a low level. It requires moisture for initial infestation and growth. Thus, humid and dark environments are ideal for the mold to breed. Relative humidity above 70% has been widely recognized as a benchmark for mold infestation and growth (Godish, 2001). Rainwater leakage due to improper building

waterproofing systems, water leaking through pipes, air infiltration through building gaps, moist construction materials, water ponding inside buildings are usually the cause of the high relative humidity and thus encourage the growth of mold inside buildings.

Indoor environmental quality issues that are usually associated with newly-constructed and refurbished buildings are formaldehyde, TVOC and PM_{10} (Nakaoka et al., 2014). Formaldehyde is widely used in building materials, furniture and wooden products. The emission from the new products has been proven to significantly elevate the indoor concentration of formaldehyde and can last for several months (Tang et al., 2009). However, they are less likely to persist if the building's indoor air quality and HVAC system are well-tested and commissioned according to specific guidelines provided for green buildings, such as Leadership in Energy and Environmental Design (LEED) in the US and Green Building Index (GBI) in Malaysia. Mold growth is one of the major factors towards SBS symptoms. Hence, the industry has attributed the SBS symptoms' occurrence to the lack of regular maintenance and services of the building, specifically on the HVAC system. HVAC systems are usually neglected in building maintenance. Regular safety inspections conducted by relevant authorities usually focus on lift and firefighting systems, while the performance of HVAC systems has not been emphasized.

A higher surface temperature of new products will increase the emission rate of formaldehyde and TVOC, and the emission rate usually dissipated through time (An et al., 2010). The indoor air pollution concentration is generally higher compared to outdoors (Salthammer et al., 2010). Fisk et al. (2009) studied the relationship between ventilation rates and SBS. A proper ventilation system is a key solution in removing contaminated air from the indoor space and reduces the prevalence of SBS.

HVAC systems are used to introduce fresh air, mix it with the return air, treat the mixed-air and then supply the treated mixed-air to the occupant space for human comfort. Contaminated air is removed through the exhaust air system or the building gaps when fresh air is introduced. Inadequate ventilation rates or malfunctioning of the HVAC system may lead to ineffective contaminated air removal from the indoor space. Thus, scheduled maintenance of the HVAC equipment is another critical area that should not be overlooked.

Tropical countries experience a relatively high outdoor air temperature and humidity, which attributes to different sets of indoor environmental issues compared to cold climate countries (Zuraimi and Tham, 2008). Malaysia has two monsoonal winds: the south-west monsoon, which is referred as the dry season from May to September, and the north-east monsoon, which is referred as the rainy season from mid-November to March. The annual rainfall is 2500 mm, and there is a relative humidity of about 80% throughout the year (Yau et al., 2013). The changes in outdoor climate conditions should be considered in design, operation and maintenance of HVAC systems. On-going IAQ management plans should be established and implemented in every building to safeguard the health and wellbeing of occupants (Yu and Jeong Tai Kim, 2011).

2.3   Indoor Air Quality

The indoor environmental quality of a building is influenced by thermal environment, indoor air quality (IAQ), lighting and visual environment, and acoustic environment. The thermal environment and IAQ assessments are a performance-based approach used to measure the quality of indoor air in association with the performance of the building and the HVAC systems. The indoor air temperature, relative humidity (RH), air velocity,

carbon monoxide (CO), carbon dioxide (CO_2), formaldehyde, TVOC and PM_{10} are the key parameters in these assessments. The standards for IAQ are usually customized by the authorities in different countries (Cheong and Lau, 2003). The customization is necessary as the environmental conditions vary by region.

2.3.1 Air Temperature

ASHRAE Standard 55 has the most sophisticated standard in defining the comfortable operative temperature for 80% occupant acceptability at the range of 24 – 27 °C during the summer season (ASHRAE, 2013a). Operative temperature considers the dry bulb temperature and mean radiant temperature of the space. The measure of operative temperature is not always available. Thus, local standards usually consider dry bulb air temperature instead of operative temperature. Malaysian Standard MS 1525:2014 recommends the dry bulb temperature to be in the range of 23 – 26 °C with a minimum limit of 22 °C (Department of Standards Malaysia, 2014). Singapore specifies the acceptable dry bulb temperature in the range of 22.5 – 25.5 °C (Ministry of the Environment, 1996).

2.3.2 Relative Humidity

ASHRAE Standard 55 specifies the humidity ratio limit at or below 0.012 kg_{water} / kg_{air} which is equivalent to a relative humidity below 70% at the operative temperature of 22.5 °C and a much lower relative humidity at a higher temperature (ASHRAE, 2013a). The limit is similar to Singapore's standard, which specifies the relative humidity to be below 70% at all acceptable temperature ranges (Ministry of the Environment, 1996). The lower limit of relative humidity is not specified due to the huge fluctuation during winter in cold climate countries. Malaysia specifies the acceptable range of relative humidity as 40 – 70% (DOSH, 2010). Low limit relative humidity in Malaysia is specified due to the

wide acceptability of the high humid environment, and it could cause discomfort when the relative humidity is too low. However, the lower limit can hardly be reached unless in special circumstances, as the outdoor climate is hot and humid in all year round.

2.3.3   Air Movement

ASHRAE Standard 55 specifies a maximum air movement limit of 0.20 m/s in normal circumstances. There is no minimum air movement given in the standard (ASHRAE, 2013a). Similarly, Singapore specifies the air movement to be below 0.25 m/s (Ministry of the Environment, 1996). However, Malaysian Standard MS 1525:2014 recommends the air movement to be in the range of 0.15 – 0.5 m/s with a maximum air movement of 0.7 m/s (Department of Standards Malaysia, 2014). Air stagnation will create thermal discomfort in the local climate.

2.3.4   CO and CO_2

Malaysia specifies the acceptable limit for CO concentrations as 10 ppm. This is similar to Singapore, which specifies 9 ppm. The limit variation is not significant in this study as the office building is prohibited from smoking. There is no source of CO in the building. However, CO_2 concentration is a critical measurement regarding the sufficiency of fresh air intake in the office (Rim et al., 2015). Both standards give a maximum limit of 1000 ppm. The limit should not be exceeded if fresh air intake is sufficient, as the outdoor CO_2 concentration ranges from 350 – 400 ppm (Turanjanin et al., 2014).

2.3.5   TVOC and Formaldehyde

TVOC and formaldehyde are toxic gases emitted from building materials. Formaldehyde has been recognized as carcinogenic to humans. The maximum concentration limit recommended by WHO is 0.08 ppm (WHO, 2010). The limit is similar to Malaysia and

Singapore standards, which both limit concentrations to 0.1 ppm. The concentration limits for TVOC for Malaysia and Singapore standards are both at 3 ppm.

2.3.6   Respirable Particulate

The concentration for PM_{10} for both Malaysia and Singapore standards is 150 µg/m^3. In this measure, particles with aerodynamic diameter of 10µm or below are sampled.

2.4   UFAD System

There are numerous methods of air distribution technologies proposed and studied by researchers (Cao et al., 2014). When compared to the latest innovative technologies available such as stratum ventilation (Z. Lin et al., 2011), under-floor air distribution (UFAD) is no longer a new air distribution technology. This technology was originally used in the data centers where there is a high sensible load and a low latent load. In the 70s, the UFAD system was first introduced into commercial buildings in Germany as noted by David (1984). The advantages of the UFAD system include to improve thermal comfort and ventilation efficiency, reduce energy consumption, reduce floor-to-floor height and provide flexibility for layout reconfiguration (Bauman and Webster, 2001).

The UFAD system uses the space in between the floor slab and raised access floor system to deliver conditioned air to the floor embedded diffusers which supplies to the occupants' space for human comfort (G. Kim et al., 2013). This under-floor ventilation space can also be used to accommodate building facilities across the office space. The evolution of information technology (IT) and internet connectivity has changed the infrastructure requirements in commercial buildings. Data cables and wirings are connected across the office space. This has improved the accessibility for installation,

relocation and servicing, while the cost of reconfiguration is reduced. Thus, UFAD system is becoming more and more popular in high-rise office buildings.

Researchers and designers from developed countries such as USA, Sweden, Poland, Korea and China have increased their attention towards UFAD systems (Zhang et al., 2014b). The focus is mainly on the potential of improving thermal comfort and indoor air quality. Studies on the fundamentals of the UFAD system related to designing, cooling load calculation, thermal stratification, energy consumption remains limited (Schiavon et al., 2011; Schiavon et al., 2014).

In tropical countries, the UFAD system is a relatively new approach. The limitation of the application of the UFAD system in the tropics is due to the lack of research findings, limited available information in standards and design guidelines, a lack of practical experience, and a perceived a higher construction cost by the raised floor system. ASHRAE first published a comprehensive guide for the design, construction and operation for UFAD systems from the latest research and developments of this technology (ASHRAE, 2013d). However, the relevant design and constriction experience of UFAD system is limited. Continuous collective findings from researchers and field experiences will further promote a highly effective UFAD system for the betterment of indoor environment.

2.4.1 Operation of UFAD system

The UFAD system has similar equipment compared to the overhead air distribution (OHAD) system. The conventional OHAD system (also called a mixed system) delivers conditioned air through the ductwork system above the ceiling and supplies conditioned air to the occupancy space from top-to-bottom of the room. However, the UFAD system

uses a similar air handling unit (AHU) to deliver conditioned air into the floor plenum in between raised access floor system and the floor slab. The conditioned air is delivered from the floor plenum to the occupancy space through floor diffusers from bottom-to-top of the room. The schematic diagram of UFAD system is shown in Figure 2.1. It can be designed to operate as a mixed system or thermal stratification system, depending on the air throw and temperature control.
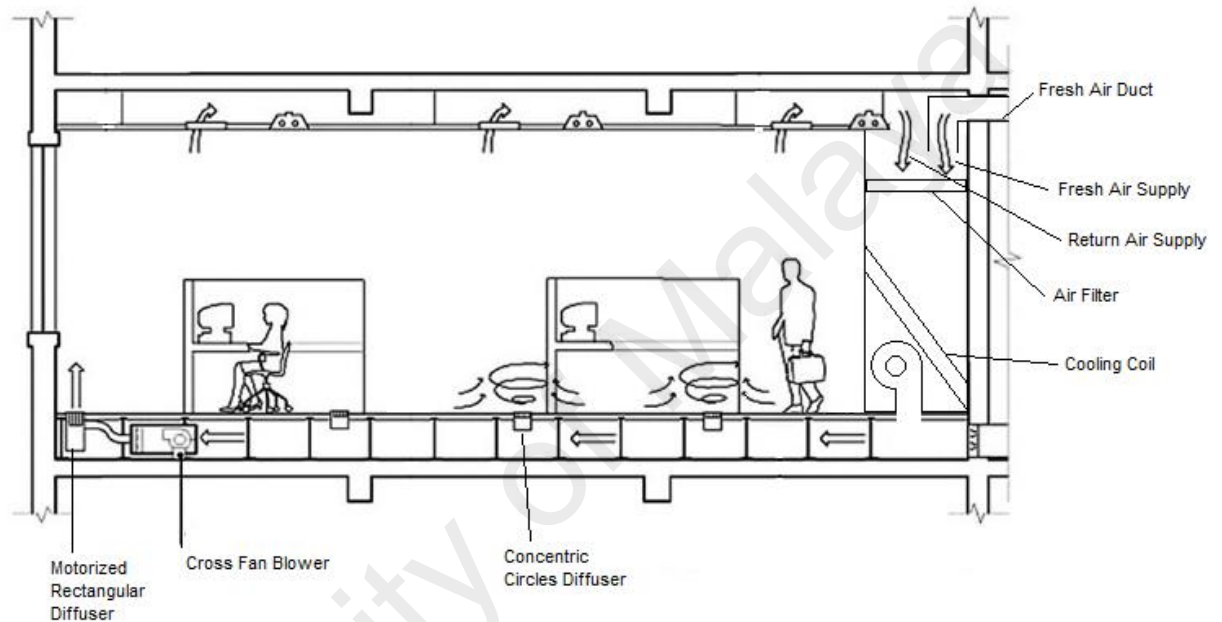
Figure 2.1: Schematic diagram of typical UFAD system. (Ya and Poh, 2015)

The typical raised floor system consists of 0.6 x 0.6 meters concrete-filled steel floor panels installed at the heights of 0.30 – 0.46 meters above the floor slab. Bauman and Webster (2001) described three design configurations for the UFAD system: the pressurized plenum at design pressures of 12.5 – 20.0 Pa, the zero-pressure plenum and the fully ducted system. The most commonly used configuration is the pressurized plenum. The pressurized plenum has potential for air leakage to the adjacent space due to the slightly higher plenum pressure. The issue of air leakage will be explained more at a latter section. Thus, the zero-pressure plenum configuration can reduce the possibility of air leakage. However, this application is very limited due to the complexity of the system.

The fully ducted system is preferred when air leakage is to be avoided. This case is not common either as the use of the ductwork system will jeopardize the benefit of flexibility for future reconfiguration. Besides, the initial and operation costs will increase due to the additional ductwork installation and require a higher fan static operation.

The air supplied from the floor diffusers is closer to the occupants. Thus, the supply air temperature at the diffusers' outlets is maintained at a higher temperature of 17 – 18 °C in contrast with 13 – 14 °C in conventional OHAD system. Larger quantities of floor diffusers are used to supply conditioned air at a lower airflow to reduce thermal discomfort such as cooled feet. Alajmi et al. (2015) investigated the thermal comfort of an office building using predicted mean vote (PMV) and air distribution performance index (ADPI). They concluded that thermal comfort can be achieved with supply air temperature of 21 °C and air velocity of 1 m/s. An UFAD system is usually designed to supply for an area of about 300m^2.

2.4.2   Thermal Stratification

In order to understand thermal stratification, the room can be divided into three zones from the bottom to the top of the room: lower mixed zone, middle stratified zone and higher mixed zone. The height of the lower mixed zone is defined as the elevation at which the supply air from the floor diffuser reaches a terminal velocity of 0.25 m/s. The air in this zone is well-mixed as a high supply air velocity will create turbulences at the lower zone. This characteristic distinguishes a conventional displacement ventilation (DV) system from a UFAD system where the air velocity of the former is lower. The airflow rate and vertical momentum from the floor supply air outlet is key in controlling the height of this zone (Y. J. P. Lin and Linden, 2005). A substantially high vertical momentum will mix the air of the entire room and be detrimental to the middle stratified zone (Y. J. P.

Lin and Tsai, 2014). Thus, ASHRAE Standard 62.1 (ASHRAE, 2013b) acknowledges the importance of air throw on thermal stratification and awarded the highest ventilation effectiveness of 1.2 to the UFAD system that achieved a throw with air velocity of 0.25 m/s and below at the height of 1.4 meter above floor level. The middle stratified zone is the area in between lower and upper mixed zones. In the absence of vertical momentum from the diffusers, the thermal buoyancy in this zone is driven by the thermal plumes of the heat sources. The upper mixed zone is the mixture of contaminated warm air from the thermal plumes and is extracted through the ceiling return. This zone should be open to improve the air distribution of the system (Z. Lin et al., 2009). The upper mixed zone will not exist if the supply airflow rate is higher than the volume of the thermal plumes. Higher supply airflow rate causes two-zone thermal stratification to occur (ASHRAE, 2013d).

The thermal stratification from the floor to ceiling airflow pattern will create a vertical temperature gradient in the space. Experiments have shown that at the airflow rate of 1.5 L/s/m^2, 3 L/s/m^2 and 5 L/s/m^2, the head-to-foot temperature difference are 3.8°C, 1.8°C and 0.7°C respectively (Webster et al., 2002). ASHRAE Standard 55 (ASHRAE, 2013a) specified that the head-to-ankle temperature difference should not exceed 3°C to avoid local thermal discomfort. Thus, UFAD system design should take the airflow rate and heat balance into consideration to achieve thermal stratification while not affecting local thermal comfort.

The control and optimization of thermal stratification is one of the most crucial indications of the performance of the UFAD system's design, energy consumption, thermal comfort and ventilation effectiveness of the system. The heat load from the facades (e.g., windows and walls) affects the indoor thermal stratification. Thus, the design and control of thermal stratification varies in different climate countries. Thermal

stratification has been an emphasis in studies related to UFAD system. Studies are still on-going to provide technical data and understanding to the designers for the implementation of the UFAD system in tropical countries (Zhang et al., 2014b).

2.4.3 The Performance of UFAD System

The main purpose of the HVAC system is to provide occupants a comfortable and safe indoor environment. With the increasing awareness on environmental protection, green energy, and CO_2 emissions, the energy consumption of HVAC systems has become another key measure in regards to its performance (Khalid et al., 2015). Thus, indoor environmental quality and energy consumption are the two main area in the performance of UFAD systems. Among the factors in indoor environmental quality, thermal comfort and indoor air quality are the two major factors related to UFAD systems (Sekhar and Goh, 2011). Both factors involve the measure of temperature, relative humidity, velocity, and air contamination in the occupants' space. On the aspect of energy consumption, two major considerations that should be included specifically for UFAD systems during the design and construction stages are heat gain from the floor slab and air leakage.

Xue and Chen (2014) conducted a case study on the influence of heat transfer through the floor slab on the performance of UFAD systems. The results showed that the total energy cost for UFAD systems is higher than a well-mixed system due to the heat transfer through the slab. The study included the energy cost for heating and cooling. The increase of chiller and fan energy consumption was proven by Lee et al. (2012). Thus, Pasut et al. (2014) studied the application of using fabric and metal ductwork to reduce the rise of supply air temperature due to the heat gain from the slab. They used the ductwork to deliver conditioned air to the plenum near the perimeter. This reversed the

typical temperature distribution of UFAD system in which the air at the perimeter is colder than the air at the interior zone.

Although the UFAD system theoretically has several advantages over the conventional OHAD system as described earlier, actual UFAD systems in the buildings have not maximized these advantages (Gupta and Woods, 2007). Air leakage is the major issue in existing UFAD system. There are two types of air leakage: air leakage through the building structures into other building spaces and air leakage through the raised floor panels into the conditioned spaces. This is a construction issue. Unfortunately, the cooling capacity sizing of the AHU has to compensate for this air loss. However, the consequences of this issue are thermal discomfort due to unequal air distribution, energy wastage due to higher AHU cooling capacity, difficulty for maintenance teams to reseal the raised floor system after servicing and indoor air quality issues due to the possible air contamination at the air leakage pathway to the unconditioned spaces.

The operations of UFAD systems should be optimized. Alajmi et al. (2013) investigated the performance of an existing UFAD system in Kuwait. The results concluded that inefficient operation of a UFAD system caused an additional 30% energy consumption compared to the best optimized operation setting. Although the existing system does not operate at its optimum performance, it is proven that the energy consumption of the UFAD system is still lower than conventional OHAD system.

2.4.4   The Type of Floor Diffusers

In the current HVAC market, the UFAD system is not common in Malaysia. As a result, the types of floor diffusers available in the local market are limited. However, western countries have a wide-range of floor diffusers, and it is not difficult to import or produce

locally when there is demand. Manufacturers in Malaysia have sufficient technology to create various types of diffusers when the market requires. Floor diffusers can be categorized into 6 types: round omnidirectional diffusers, selective directional diffusers, displacement flow diffusers, linear diffusers, ducted diffusers and terminal units (ASHRAE, 2013d). The installation method can be floor pressurized plenum, ducted system or incorporated with a fan terminal unit. Regardless of the types of diffusers, the air outlet can be designed as a constant-air volume (CAV) or variable-air-volume (VAV) system. CAV systems are ideally used in lobbies and corridors where occupancy rate is transient. VAV systems are preferable for seated occupancy areas where control can be personalized. Floor swirl diffusers which is a type of round omnidirectional diffusers with diffuser blades beneath the grille are the most widely used floor diffuser in the market (Trox, 2015). Thus, it is selected for this research study.

2.5   HVAC Energy Demand in Commercial Building

The building sector is estimated to consume 20 – 40% of the total energy consumption worldwide (L. Pérez-Lombard et al., 2008). Among the building services available, HVAC system is the most energy consuming service (Luis Pérez-Lombard et al., 2011). It accounts for 40 – 60 % of the total energy consumption of a building. Ürge-Vorsatz et al. (2015) estimated that HVAC systems will continue to grow significantly by triple to fivefold in developing countries in order to meet the need of thermal comfort and indoor air quality. Given that the energy consumption of buildings will continue to grow, especially at a much higher rate in developing countries, it is important to emphasize energy efficiency of buildings, especially on the HVAC system. Day et al. (2009) estimated that a 1 – 3% annual efficiency improvement on the cooling systems in the UK alone will reduce 340,000 tons of CO_2 emission by 2030. The significance in tropical countries will be much higher due to the year-round cooling requirement.

The improvement of technology in HVAC systems and the increment of living standards of humans has made air conditioning affordable by every individual. In fact, it has become a necessity product at most public areas such as shopping complexes, restaurants, offices, hotels, etc. Some building developers include the installation of an air conditioning system as part of the development when middle to upper class condominiums and landed houses are constructed for residential purposes.

Tropical countries such as Malaysia have a hot and humid climate. The outdoor air temperature on normal days can go up to 40°C. It is unhealthy to have long hours of outdoor activities between 10 a.m. to 5 p.m. Hence, people spend most of the time on activities in indoor environment (Hwang and Kim, 2013). HVAC systems are used to control indoor air temperature, humidity, cleanliness, air quality and ventilation of a space to meet the requirement for human comfort (McQuiston et al., 2005). Hence, HVAC systems are important and necessary to maintain a comfortable indoor environment.

The energy consumption of HVAC system is also significant in tropical countries, where higher energy is required to lower down the higher temperature difference from 30 – 40°C outdoor temperature to a comfortable indoor temperature of 23 – 25°C. Figure 2.2 shows the energy consumption distribution of residential, hotels, shopping complexes and offices in Malaysia. It shows that the energy consumption for HVAC system is significant, especially for shopping complexes and offices, which operate mostly during the day.
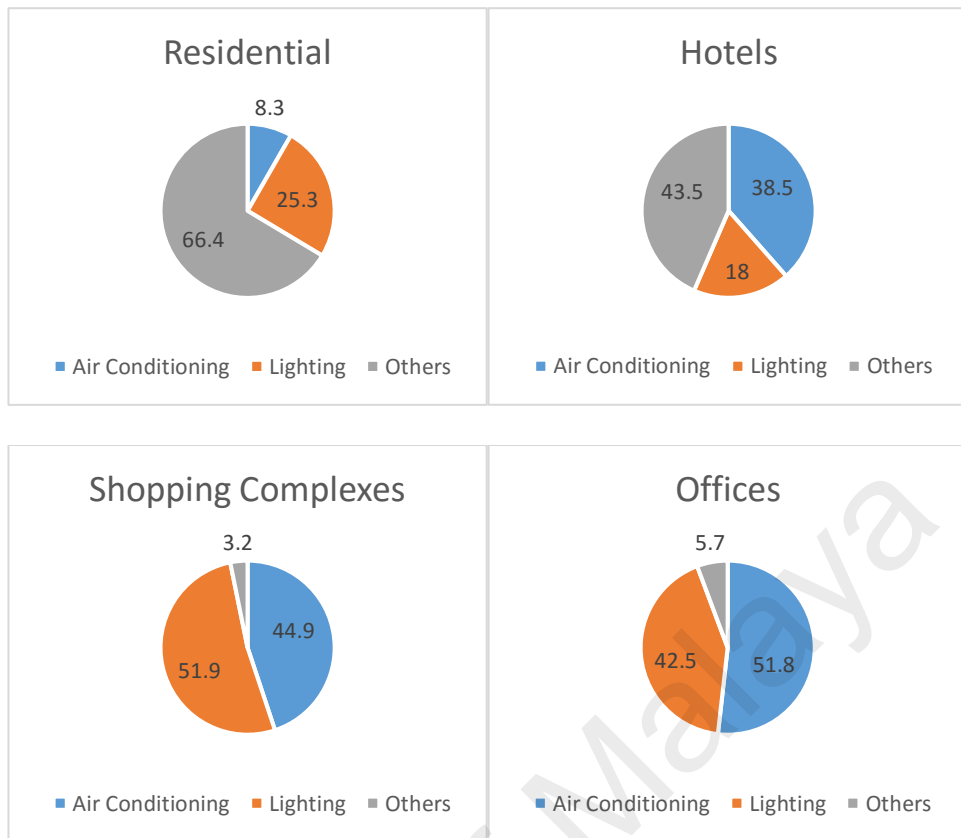
Figure 2.2: Energy consumption distribution of various types of buildings in Malaysia.
(Ahmadzadehtalatapeh, 2011)

2.6   Solar Photovoltaic System

Energy demand has been increasingly competitive for the past decades. The price crises of coal, oil and gas have led scientists and engineers to explore for alternative sources of energy. Renewable energy in the market has growth considerably in the last decade. Statistics show that renewable energy sources account for 14% of total global energy supply (Manzano-Agugliaro et al., 2013).

Solar photovoltaic is a renewable energy approach that converts solar irradiation to electricity using photovoltaic materials (Parida et al., 2011). It is one of the most promising renewable technologies used worldwide and has great potential in tropical countries due to the tremendous sunlight available (Ismail et al., 2015). Malaysia, a tropical country located at 3°08'N 101°42'E receives an average of 6 hours sunlight daily

(Ministry of Science Technology and Innovation, 2012). Exploration for solar photovoltaic energy is significant in this region. Economic and local climate studies receive high interest among the researchers due to the great influence of regional conditions on the development of the solar photovoltaic system (Liu et al., 2012; Peng et al., 2013; Radhi, 2012; Zogou and Stapountzis, 2011). Figure 2.3 shows the solar irradiation mapping in Malaysia.
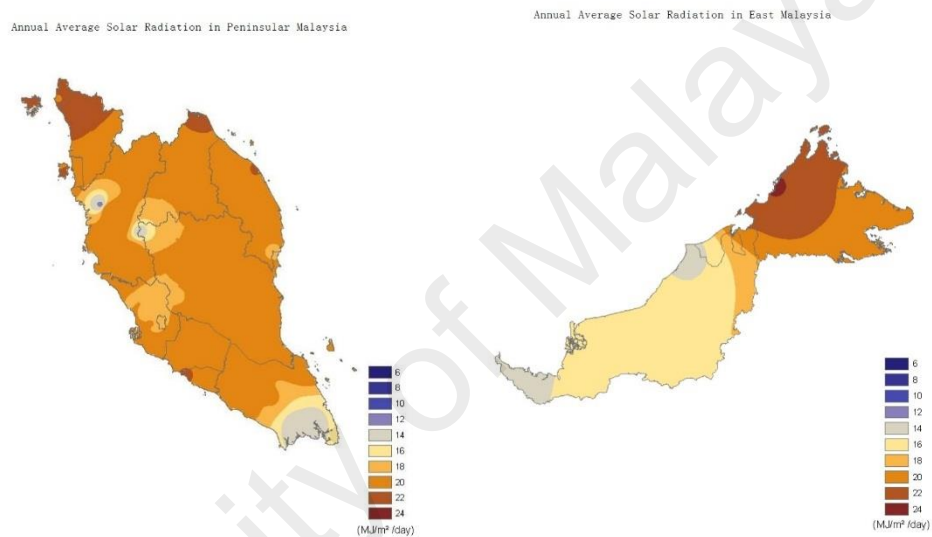
Figure 2.3: The solar irradiation mapping in Malaysia.

(Mekhilef et al., 2012)

The solar photovoltaic system is reliable and pollution-free. It uses sunlight to produce electricity. This makes the system widely applicable for most electric appliances (Pandey et al., 2016). There are two categories of solar photovoltaic systems: the on-grid system and the off-grid system. The basic components in a solar photovoltaic system include photovoltaic panels, an inverter and battery (for off-grid systems). The on-grid system connects solar panels to a utility grid through a DC – AC inverter. The electricity generated from the solar photovoltaic system will be used while the excessive electricity generated will be returned to the grid. However, when the electricity supply from the solar

photovoltaic system is insufficient for the demands, grid electricity will cut in to meet the energy demands. Off-grid systems connect to appliances directly without utility grid. This system is very useful in rural areas where the utility grid cannot be reached. Batteries are usually available in this system to store the excess electricity generated for use when the solar irradiation is insufficient to generate electricity (National Renewable Energy Laboratory, 2001).

Political policies which stimulate the market growth are seen to be the market drivers for solar photovoltaic system. Hoffmann (2006) pointed out that the solar photovoltaic market has a great future for both on-grid and off-grid systems, depending on the long-term financial schemes provided by the government. Renewable energy (RE) policies such as feed-in tariffs (FiT), tenders and tax incentives are among the policies that drive the impressive growth of solar photovoltaic systems in the market. Among these policies, FiT is the most popular policy, adopted by 65 countries worldwide. By the end of 2010, about 87% of the photovoltaic system worldwide was estimated to be installed through this scheme (Kilinc-Ata, 2016).

After the RE Act 2011 and SEDA Act 2011 were established and the FiT policy was adopted in Malaysia, more than 160 MW capacities of the solar photovoltaic system were in operation under the FiT policy by the end of the year 2014. This accounted for more than 65% total capacity in operation among the renewable energy sources such as biogas, biomass, small hydro and solar photovoltaic for individual and non-individual categories (SEDA, 2015). The Green Technology Financing Scheme (GTFS) and soft loans support the initial cost for the solar photovoltaic system, while FiT gives incentive based on the electricity generation (Muhammad-Sukki et al., 2012). According to a

projection simulation study, a total of 10 – 16 GW power generation from solar photovoltaic system are expected by the year 2050 (Ahmad et al., 2015).

2.7   Solar Cooling System

Solar cooling is the concept of using solar energy to operate a cooling system that provides a cooling effect for indoor environments. This technology has existed for many years. Due to the immature market demand and the high equipment cost, the technology advancement and market growth is slow. Coal, oil and gas price crises have brought up the renewable energy market demand, therefore, the solar cooling system has once again captured the attention of researchers (Ashhab et al., 2013).

Solar cooling systems can be divided into solar electrical cooling systems and solar thermal cooling systems. The solar electrical cooling system as shown in Figure 2.4 is an electrical driven refrigeration system. The system is the combination of solar photovoltaic panels and an electric refrigeration system (Fong et al., 2010). The solar thermal system includes solar absorption cooling systems, solar adsorption cooling systems and solar desiccant cooling systems. These thermal driven solar cooling systems normally use flat-plate solar collectors or evacuated tubes to collect heat from the sun. Solar cooling systems highly depend on solar irradiation, climate conditions and geographical locations. The solar cooling system usually integrates with a grid power supply to achieve energy savings. Solar cooling systems can have up to 40-50% of energy saving potential in southern European and Mediterranean areas (D. S. Kim and Infante Ferreira, 2008).
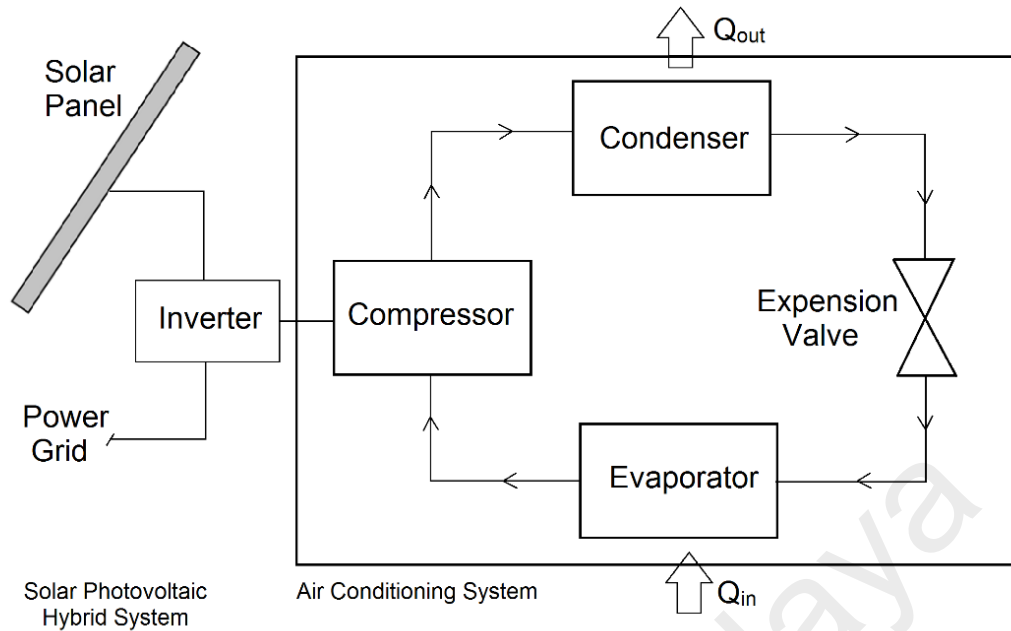
Figure 2.4: A typical schematic diagram of solar electrical cooling system.
(Fong et al., 2010)

Hartmann et al. (2011) compared solar photovoltaic cooling systems with solar adsorption cooling systems in European climates. Primary energy, economic, investment cost and macroeconomic impacts were investigated. Results showed that solar photovoltaic cooling system outperformed the solar adsorption cooling system. The cost for solar adsorption chiller and its system is about 40% higher, and the solar collection area has to six times larger than the solar photovoltaic system in order to achieve a similar energy saving.

Otanicar et al. (2012) compared the future projection costs of solar electric and solar thermal systems, including solar photovoltaic cooling systems, desiccant cooling systems, LiBr solar absorption cooling systems, NH_3 solar absorption cooling systems and solar adsorption cooling systems. The study concluded that the continuous drop of the price of solar photovoltaic panels would give the solar electric cooling system a more prevailing future compared to a solar thermal cooling system. The solar thermal cooling

system has a stable cost projected in the next 20 years, unless there is a technology breakthrough which significantly improves the coefficient of performance (COP) of the system.

Cooling demand is influenced by the exposure of solar radiation. Higher solar radiation requires a higher energy consumption in order to meet the cooling load. Hence, solar cooling systems which use solar energy to operate an air-conditioning system often come to our mind as an ideal solution (Bilgili, 2011). However, when it comes to the feasibility of the solar cooling system in the market, high cost and low performance of the system are stumbling blocks that hinder this system from rapid growth. Although research has shown that solar photovoltaic cooling system has promising potential in the future, the solar energy output of the system highly depends on local climate conditions. Thus, the performance and economic study should be conducted according to regions.

2.8   Summary

HVAC system is a high energy consuming system in a building. As HVAC systems have become a necessity in the tropics, it is important to improve the energy efficiency of the system and explore the alternative sources of energy for the system. Solar energy is widely available in tropical countries. The intensity of solar radiation is also proportional to cooling load. Thus, the feasibility of using solar electricity and solar thermal energy to operate a cooling system has drawn the attention of researchers. Among the solar based systems, the solar photovoltaic system is one of the most promising methods available. Hence, the application of a solar photovoltaic system on an electric driven refrigeration system has been studied in various countries. The studies are mainly on economic aspect and payback period.

A comfortable indoor environment and building energy efficiency are the key considerations for a sustainable building. The UFAD system is one of the innovative ventilation technologies that has the potential to improve indoor environment while reducing energy consumption. However, it is not widely used in the tropics due to the immaturity of the technology. The design and construction considerations are different from the conventional OHAD system. The UFAD system should be incorporated into the building design during the initial planning of a new building. A refurbishment plan to convert an existing OHAD system to UFAD system is nearly impossible. Thus, research on the UFAD system should be emphasized on the design and construction in the promotion of its application.

Yun and Kim (2014) proved that the operation of comfortable indoor environment can lead to energy savings. Another example of energy efficiency through optimum HVAC operation is proven by Alajmi et al. (2013). The performance measurements of the UFAD system are indoor environmental quality and energy consumption. Therefore, the study of the UFAD system in the areas of thermal environment, indoor air quality and energy consumption is favorable in order to provide guidance for the design and construction of UFAD systems in the tropics.

CHAPTER 3 – RESEARCH METHODOLOGY

3.1   Overview

This chapter describes the fundamental methodology and theories related to the study and equipment used for the physical work. The details of the specific methodology are explained in respective chapters later. The overall workflow to achieve the objectives of the performance investigation on the UFAD system in the tropics is summarized sequentially as follows:

i.   Preliminary inspection of the building

The TM Tower, located in Kuala Lumpur, is one of the earliest built high-rise buildings that uses the UFAD system in Malaysia. The building was selected for this case study. A walkthrough and inspection of the office area was led by the office's facility manager. As-built drawings review and discussion with the building's operation and maintenance team was conducted. These two processes were crucial to understand the system design, operation and scheduled maintenance prior to deciding sampling points for assessment.

ii.   Fieldwork planning and data acquisition

As agreed with the office's facility manager, the fieldwork was carried out during office hours from 8.30am – 5.30pm. Thermal environment, indoor air quality (IAQ) and power consumption data were collected for further analysis.

iii.   Analysis of the data collected.

The thermal environment and IAQ data was analyzed and compared with local standards and guidelines, such as Industry Code of Practice on Indoor Air Quality 2010 (DOSH, 2010) and Malaysian Standard MS 1525:2014 (Department of Standards

Malaysia, 2014). Power consumption data of the AHU was used to analyze the payback period of hybrid solar-powered UFAD system.

iv.   Experimental investigation on the floor swirl diffuser

The floor swirl diffuser was modeled, fabricated and tested in the laboratory of Prudentaire Marketing Sdn Bhd for data comparison and verification in the CFD model. Measurements taken included air temperature, relative humidity, room surface temperature and air velocity.

v.   Modelling and airflow simulation of the floor swirl diffuser

Various geometrical designs of floor swirl diffusers were investigated by CFD modeling to examine the effect of the airflow pattern. The floor swirl diffuser was modeled using SolidWorks 2012 software. Simulations were performed using FLUENT in ANSYS Workbench.

vi.   Study on the solar irradiation in Malaysia

Solar irradiation was studied through the data obtained from the Malaysian Meteorology Department (MMD). Seven critical cities in Malaysia were selected in the study as a representative for the country. The results were compared with a sub-tropical country, taking Hong Kong as a representative country.

vii.   Experimental investigation of solar photovoltaic system

The power consumption of the UFAD system in TM Tower was evaluated by data logging the power consumption of the AHUs used in the UFAD system in TM Tower. Experimental data logged from the solar PV at University of Malaya was studied. Payback period of hybrid solar-powered a UFAD system was calculated.

3.2   IAQ Assessment Methodology

Indoor air quality (IAQ) of offices served with the UFAD system was studied according to the typical assessment methodologies used in tropical regions (Cheong and Lau, 2003; DOSH, 2010; Ministry of the Environment, 1996). There are 4 stages for the complete assessment, as shown in Table 3.1.

Table 3.1 – Stages of Assessments Methodology. (Cheong and Lau, 2003)

Preliminary Stage	**Understand building background** Review architecture drawing Walkthrough • Feedback from occupants • Identification of area of studied and observe problem area

Sampling Stage	**On-site data collection**
	• Objective measurements
	  ▪ Physical
	  ▪ Chill water
	  ▪ Supply air rate
	  ▪ Fresh air rate
	• Subjective assessment
	  ▪ Field inspection
	  ▪ Questionnaires survey (not in this study)

Evaluation Stage	**Data Analysis** • Objective Parameters • Observation data **Comparisons with Standards/ Regulations** **Determine implication and causes**

Recommendation Stage	**Remedial measures**
	• Activity management
	• Design intervention
	• Strategies and source control
	  ▪ Isolation
	  ▪ Removal
	  ▪ Dilution

3.3 Equipment for IAQ Fieldwork Assessment and Experimental Measurement

Table 3.2 – Equipment used for fieldwork and experiment.

Parameters	Equipment	Descriptions
Temperature Relative humidity Air velocity	*Alnor Thermo Anemometer Model 440-A*	The hot wire anemometer measures air velocity, temperature and relative humidity. It is sensitive to the flow accounted to cosine law. Thus, it senses the flow normal to the wire axis only. *Operating range* Temperature: -10 to 60 °C RH: 5 to 95% Velocity: 0 to 30 ms^{-1} *Accuracy* Temperature: ± 0.3 °C RH: ± 3% Velocity: ± 3% of reading or ± 0.015ms^{-1}, whichever is greater *Resolution* Temperature: ± 0.1 °C RH: 0.1% Velocity: 0.01 ms^{-1}
Temperature Air velocity	*TSI VelociCalc Air Velocity Meter*	The hot wire anemometer measures air velocity and temperature. It is sensitive to the flow accounted to cosine law. Thus, it senses the flow normal to the wire axis only. *Operating range* Temperature: -17.8 to 93.3 °C Velocity: 0 to 30 ms^{-1} *Accuracy* Temperature: ± 0.3°C Velocity: ± 3% of reading or ± 0.015ms^{-1}, whichever is greater
Temperature		This thermal couple thermometer is a micro controller based tester. *Operating range* Temperature: 0 to 50 °C *Accuracy* Temperature: ± 0.3% + 1 °C *Resolution* Temperature: 0.1 °C

	Center 309 – Thermomether (K Type, 4 Inputs, Datalogger)	
Carbon monoxide Carbon dioxide	*ALNOR Indoor Air Quality Instruments-Model CF930*	This device simultaneously measures and data logs multiple parameters, which are carbon dioxide (CO_2), carbon monoxide (CO), temperature, humidity, and calculates dew point, wet bulb temperature and % outside air.
Aerosol (Dust)	*TSI DuskTrakII Aerosol Monitor (Model 8532)*	This device measures the mass of aerosol in different sizes, which are 1μm, 2.5μm, 4μm and 10μm, by using different size-selective impactors, running on the factory default setting of 3.0 L/min to achieve correct cut points.
TVOC	*Portable VOC Monitor PGM-7600*	This device is a handheld photoionization detector (PD) for volatile organic compound (VOC) measurement. *Accuracy* 0 – 2000 ppm: ± 2 ppm or 10% of reading >2000 ppm: ± 20% of reading
Formaldehyde	*PPM Formaldemeter htV-m*	This device measures the levels of hazardous formaldehyde vapours, even under extremes of temperature and humidity. *Operating Range* Temperature: 0 to 40 °C, RH: 15 to 90% *Concentration Range* 0 – 10ppm as standard (0- 12.3 mg/m³ at 25°C) *Resolution* 0.01 ppm *Precision* 2%

3.4   Computational Fluid Dynamics (CFD)

3.4.1   The Governing Equations General Form of Governing Equations

Computational fluid dynamics (CFD) analysis is based on the governing equations of conservation of mass, momentum, and energy. Fluid motions are predicted through solving these three mathematical transport equations of the physical laws using computer-aided programs. (Tu et al., 2013)

Conservation of mass:

$$\frac{\partial \rho}{\partial t} + \frac{\partial(\rho u)}{\partial x} + \frac{\partial(\rho v)}{\partial y} + \frac{\partial(\rho w)}{\partial z} = 0 \tag{1}$$

The equation above is the partial differential form of continuity equation. The component u, v and w represent the fluid velocity in respective direction of x, y and z in Cartesian coordinate system. In satisfying the physical behavior, a decrease of velocity in a particular direction will increase the velocity in adjacent direction. The transfer of mass is balanced.

Conservation of momentum:

The momentum equation is derived from Newton's second law of motion. The forces acting on a fluid are similarly represented into three directions in the Cartesian coordinate system. Each direction has its independent scalar relation and equation represented by x, y and z. There are two types of forces in the system, namely body forces and surface forces. The body forces are external forces that may affect the rate of change of the initial fluid momentum and thus are introduced into the equations as additional source terms. The surface forces are due to the normal stresses and tangential viscous stress acting on the surfaces.

x-momentum equations,

$$\rho \frac{Du}{Dt} = \frac{\partial \sigma_{xx}}{\partial x} + \frac{\partial \tau_{yx}}{\partial y} + \frac{\partial \tau_{zx}}{\partial z} + \sum F_x^{body\ forces} \qquad (2)$$

y-momentum equations,

$$\rho \frac{Dv}{Dt} = \frac{\partial \tau_{xy}}{\partial x} + \frac{\partial \sigma_{yy}}{\partial y} + \frac{\partial \tau_{zy}}{\partial z} + \sum F_y^{body\ forces} \qquad (3)$$

z-momentum equations,

$$\rho \frac{Dw}{Dt} = \frac{\partial \tau_{xz}}{\partial x} + \frac{\partial \tau_{yz}}{\partial y} + \frac{\partial \sigma_{zz}}{\partial z} + \sum F_z^{body\ forces} \qquad (4)$$

where σ_{xx}, σ_{yy} and σ_{zz} are the normal stresses due to pressure and normal viscous stress components acting perpendicular to the volume.

Conservation of energy:

The energy equation is derived from the first law of thermodynamics. In order to relate with the continuity equation and momentum equations, the time rate of change of energy is represented in *x*, *y* and *z* directions as shown below:

$$\rho \frac{DE}{Dt} = \frac{\partial}{\partial x}\left[\lambda \frac{\partial T}{\partial x}\right] + \frac{\partial}{\partial y}\left[\lambda \frac{\partial T}{\partial y}\right] + \frac{\partial}{\partial z}\left[\lambda \frac{\partial T}{\partial z}\right] - \frac{\partial(up)}{\partial x} - \frac{\partial(vp)}{\partial y} - \frac{\partial(wp)}{\partial z} + \Phi \qquad (5)$$

The dissipation function, Φ, represents the energy work done on the fluid, which is then converted into heat.

$$\Phi = \frac{\partial(u\tau_{xx})}{\partial x} + \frac{\partial(u\tau_{yx})}{\partial y} + \frac{\partial(u\tau_{zx})}{\partial z} + \frac{\partial(v\tau_{xy})}{\partial x} + \frac{\partial(v\tau_{yy})}{\partial y} + \frac{\partial(v\tau_{zy})}{\partial z} + \frac{\partial(w\tau_{xy})}{\partial x} +$$

$$\frac{\partial(w\tau_{yz})}{\partial y} + \frac{\partial(w\tau_{zz})}{\partial z} \qquad (6)$$

3.4.2 Flow Solver

There are two types of numerical flow solving methods available: the pressure-based solver and the density-based solver. The primary variables in a pressure-based solver are momentum and pressure or pressure correction. Pressure and momentum are solved

simultaneously in a pressure-based coupled solver. The algorithm in a pressure-based solver constraints the mass conservation of the velocity field by solving the pressure and pressure correction equations, which are derived from the continuity and momentum equations. This is widely applicable to low speed incompressible flow. In a density-based solver, the equations of continuity, momentum, energy and species are solved in vector form. It is applicable for analysis such as high speed compressible flow when there is a strong coupling or interdependency between these criteria. In this study, the flow is incompressible and is in single phase, and the pressure-based coupling approach was selected as the solver.

The Semi-Implicit Method for Pressure-Linked Equations (SIMPLE) algorithm is a widely used pressure-based solver in estimating indoor airflow patterns at steady-state condition. This method uses a guessed initial pressure and velocity values to calculate the velocity field using the momentum equations. The pressure equation is then generated using the predicted velocities to calculate the pressure field. The initial pressure under-relaxation factor is used to minimize the effect of non-linearity of the pressure field calculated. The under-relaxed pressure field is used for the next iteration until the solution has converged to the desired setting. The pressure equation is described below:

$$p^{new} = p^{old} + \alpha_p(p^p - p^{old}) \tag{7}$$

where p^{old} is the guessed initial pressure value or pressure value from the previous iteration, p^p is the pressure value from the pressure equation, p^{new} is the final pressure field use for next iteration and α_p is the pressure under-relation factor.

3.4.3 Turbulence Model

The turbulence k-ε model is the most widely used turbulence model in industrial flow and heat transfer simulations (ANSYS, 2013). It solves two model transport equations

separately to obtain turbulence kinetic energy per unit mass, k and dissipation rate, ε. The standard k-ε has been proven successful for indoor environment CFD application. The transport equations are shown below:

Turbulence kinetic energy, k:

$$\frac{\partial}{\partial t}(\rho k) + \frac{\partial}{\partial x_i}(\rho k u_i) = \frac{\partial}{\partial x_j}\left[\left(\mu + \frac{\mu_t}{\sigma_k}\right)\frac{\partial k}{\partial x_j}\right] + G_k + G_b - \rho\varepsilon - Y_M + S_k \quad (8)$$

Dissipation rate, ε:

$$\frac{\partial}{\partial t}(\rho\varepsilon) + \frac{\partial}{\partial x_i}(\rho\varepsilon u_i) = \frac{\partial}{\partial x_j}\left[\left(\mu + \frac{\mu_t}{\sigma_\varepsilon}\right)\frac{\partial\varepsilon}{\partial x_j}\right] + C_{1\varepsilon}\frac{\varepsilon}{k}(G_k + C_{3\varepsilon}G_{b)} - C_{2\varepsilon}\rho\frac{\varepsilon^2}{k} +$$

$$S_\varepsilon \tag{9}$$

Turbulent viscosity, $\mu_t = \rho C_\mu \dfrac{k^2}{\varepsilon}$ $\qquad\qquad\qquad\qquad$ (10)

where G_k = generation of turbulence kinetic energy due to the mean velocity gradients, G_k = generation of turbulence kinetic energy due to buoyancy, Y_M = contribution of the fluctuating dilatation in compressible turbulence to the overall dissipation rate, $C_{1\varepsilon}, C_{2\varepsilon}$ = constants of 1.44, 1.92 and C_μ = constants of 0.09, σ_k, = Prandtl number for k, 1.0, σ_ε = Prandtl number for ε, 1.3, and S_k, S_ε = source terms.

Through years of application, some other variations were derived from this standard k-ε model (Stamou and Katsiris, 2006). The variations are re-normalised group (RNG) k-ε and realizable k-ε. The RNG k-ε model is an enhancement from the standard k-ε model to improve the accuracy for rapid strained flow and swirl flow by additional terms in k and ε transport equations. The realizable k-ε model is another enhancement from standard k-ε model. This model has a different formulation for turbulent viscosity, which causes this model to outperform other variation in several cases. Thus, the CFD

results from these turbulence models were compared in the study to obtain the most suitable turbulence models in the study.

RNG k-ε model has an additional term in the epsilon equation. The additional term is $R_\varepsilon = \frac{C_\mu \rho \eta^3 (1-\frac{\eta}{\eta_0})}{1+\beta\eta^3}\frac{\varepsilon^2}{k}$, where $\eta \equiv \frac{Sk}{\varepsilon}, \eta_0 = 4.38, \beta = 0.012$. The transport equations for RNG k-ε model are shown below:

Turbulent kinetic energy, k:

$$\frac{\partial}{\partial t}(\rho k) + \frac{\partial}{\partial x_i}(\rho k u_i) = \frac{\partial}{\partial x_j}\left(\alpha_k \mu_{\epsilon jf} + \frac{\partial k}{\partial x_j}\right) + G_k + G_b - \rho\varepsilon - Y_M + S_k$$

(11)

Dissipation rate, ε:

$$\frac{\partial}{\partial t}(\rho\varepsilon) + \frac{\partial}{\partial x_i}(\rho\varepsilon u_i) = \frac{\partial}{\partial x_j}\left(\alpha_\varepsilon \mu_{\epsilon jf} + \frac{\partial\varepsilon}{\partial x_j}\right) + C_{1\varepsilon}\frac{\varepsilon}{k}(G_k + C_{3\varepsilon}G_{b)} -$$

$$C_{2\varepsilon}\rho\frac{\varepsilon^2}{k} - R_\varepsilon + S_\varepsilon$$

(12)

Turbulent viscosity:

$$d\left(\frac{\rho^2 k}{\sqrt{\varepsilon\mu}}\right) = 1.72\frac{\hat{v}}{\sqrt{\hat{v}^3 - 1 + C_v}}dv$$

(13)

$$\hat{v} = \frac{\mu_{\epsilon jf}}{\mu}, C_v \approx 100$$

(14)

where G_k = generation of turbulence kinetic energy due to the mean velocity gradients, G_k = generation of turbulence kinetic energy due to buoyancy, Y_M = contribution of the fluctuating dilatation in compressible turbulence to the overall dissipation rate, $C_{1\varepsilon}, C_{2\varepsilon}$ = constants of 1.42, 1.68, σ_k, = Prandtl number for k, σ_ε = Prandtl number for ε, and S_k, S_ε = source terms.

For the realizable k-ε model, the k equation is similar to standard k-ε model. However, the ε equation is different from those in the standard and RNG k-ε models. The turbulent viscosity in this model is also different from the previous two models as C_μ is not a constant. It has been shown that C_μ is a function of mean strain, rotation rates, angular velocity of the system rotation, and the turbulence fields of k and ε. The transport equations for are shown below:

Turbulent kinetic energy, k:

$$\frac{\partial}{\partial t}(\rho k) + \frac{\partial}{\partial x_j}(\rho k u_j) = \frac{\partial}{\partial x_j}\left[\left(\mu + \frac{\mu_t}{\sigma_k}\right)\frac{\partial k}{\partial x_j}\right] + G_k + G_b - \rho\varepsilon - Y_M + S_k \quad (15)$$

Dissipation rate, ε:

$$\frac{\partial}{\partial t}(\rho\varepsilon) + \frac{\partial}{\partial x_j}(\rho\varepsilon u_j) = \frac{\partial}{\partial x_j}\left[\left(\mu + \frac{\mu_t}{\sigma_\varepsilon}\right)\frac{\partial\varepsilon}{\partial x_j}\right] + \rho C_1 S_\varepsilon - \rho C_2\frac{\varepsilon^2}{k+\sqrt{v\varepsilon}} +$$

$$C_{1\varepsilon}\frac{\varepsilon}{k}C_{3\varepsilon}G_b + S_\varepsilon \quad\quad\quad\quad\quad\quad\quad (16)$$

where $C_1 = max\left[0.43, \frac{\eta}{\eta+5}\right], \eta = S\frac{k}{\varepsilon}, S = \sqrt{2S_{ij}S_{ij}}$

Turbulent viscosity, $\mu_t = \rho C_\mu\frac{k^2}{\varepsilon}$ $\quad\quad\quad\quad\quad\quad\quad\quad (17)$

where G_k = generation of turbulence kinetic energy due to the mean velocity gradients, G_k = generation of turbulence kinetic energy due to buoyancy, Y_M = contribution of the fluctuating dilatation in compressible turbulence to the overall dissipation rate, $C_{1\varepsilon}, C_2$ = constants, σ_k, = Prandtl number for k, σ_ε = Prandtl number for ε, and S_k, S_ε = source terms.

$$C_\mu = \frac{1}{A_0 + A_s kU^*/\varepsilon} \quad\quad\quad\quad\quad\quad\quad\quad (18)$$

where $U^* \equiv \sqrt{S_{ij}S_{ij} + \tilde{\Omega}_{ij}\tilde{\Omega}_{ij}}$, $\tilde{\Omega}_{ij} = \Omega_{ij} - 2\varepsilon_{ijk}\omega_k$, $\Omega_{ij} = \overline{\Omega_{ij}} - \varepsilon_{ijk}\omega_k$,

$\overline{\Omega_{ij}}$ is the mean rate-of-rotation tensor viewed in a moving reference frame with the

angular velocity of ω_k , $Ao = 4.04$, $As = \sqrt{6}cos\emptyset$

3.4.4 Convergence Control

Convergence control is one of the key criteria to the accuracy of the simulation results. The approach in convergence control is observed by the residuals of continuity, x-velocity, y-velocity, z-velocity, energy, turbulence kinetic energy and dissipation rate. Low criteria will increase the number of iterations and time required. Thus, the solution cost increased.

The residual's control depends on the application. In this case, the recommended residual for continuity, x-velocity, y-velocity, z-velocity, turbulence kinetic energy and dissipation rate equations is (10^{-3}) while the residual for energy equation is (10^{-6}) (Srebric and Chen, 2002). The default under-relaxation factors is recommended.

3.4.5 Boundary Condition

Wall, Ceiling and Floor

The wall, ceiling and floor surfaces of the laboratory were not exposed to outdoor and sunlight heat sources; however, the outer surfaces were exposed to unconditioned indoor temperature. Thus the temperature of each surface was measured as isothermal and prescribed in the setup. The surfaces were stationary and no-slip wall. The relative velocity between the surfaces and the air near to the surface is assumed to be zero.

Air inlet

There are 3 types of inlet boundary conditions: velocity inlet, pressure inlet and mass inlet. In these cases, the velocity inlet is specified as the system is incompressible flow. The air inlet is the source of momentum defined as velocities in x, y and z direction. The velocity magnitude, initial pressure, temperature, turbulence kinetic energy and dissipation rate were specified. Turbulence kinetic energy and dissipation rate were obtained through turbulence intensity and viscosity ratio. The inlet air temperature was measured through experiment.

Air outlets

There were 4 air outlets specified at the corners of the room in order to observe balanced velocity profiles from the air inlet. The outlet velocity was calculated though the mass balance equation of the system. The air return was a free system. Hence, the static or gauge pressure of the environment into which the flow exits was equal to zero. Backflow turbulent intensity and viscosity ratio were specified. The outlet air temperature was measured through experiment.

3.4.6 Modelling

In the current study, the diffuser was modeled using SolidWorks 2012 software and fabricated using laser-cut sheet metal. The diffuser's prototype is shown in Figure 3.1. The structure of the design was based on the models of Trox (2015) and Prudentaire (2015). There are three sizes of floor swirl diffusers available in the market: 150mm, 200mm and 250mm nominal diameter. The 250mm nominal diameter diffuser was selected in this study due to the wide application. The prototype was fabricated using sheet metal with support from Prudentaire Marketing Sdn Bhd for experimental purposes. The same model was imported into Ansys to conduct simulation.
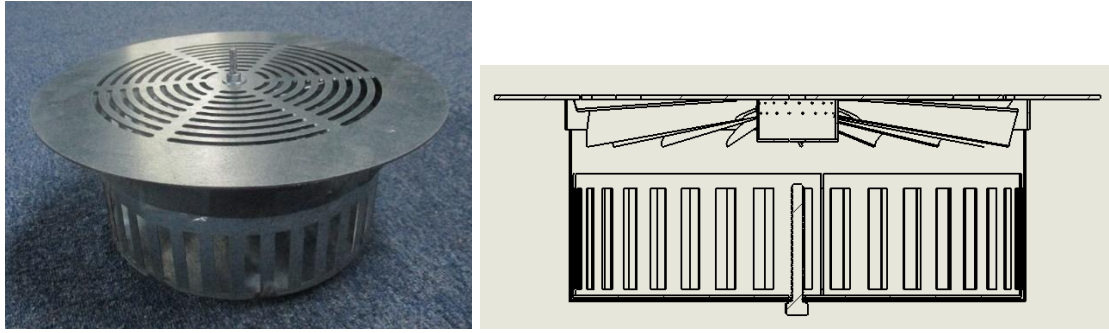
Figure 3.1: Prototype (left) and section view (right) of tested floor swirl diffuser.

3.4.7 Meshing

In the current study, the airflow simulation of the floor swirl diffuser was conducted in 3-dimensional analysis. Unstructured tetrahedral mesh can easily fill an arbitrary volume and is very useful for complicated geometry. Thus, the fluid domain of floor swirl diffuser is more convenient to discretize in tetrahedral mesh (Aziz et al., 2012). It will generate a higher number of mesh elements and nodes as compared to structured hex mesh.

The number of mesh elements is one important factor that influences the accuracy of the CFD results. However, the results should be independent from the discretization. It was necessary to compare the differences of results with a wide range of grid sizes. Typically, the CFD results are compared through different grid sizes with 1.5 to 2 times increment from the coarser mesh (Wilcox, 2006). Errors of the results were reduced as the number of mesh elements increases. The appropriate grid size modeling was obtained when the variation of results fell within an acceptable range. In order to reduce the number of mesh elements and nodes to avoid unnecessary time cost, the mesh element at the inlet, outlets and diffuser were refined. The size change of adjacent cells was kept below 120% and the maximum skewness kept below 0.95. The simulation was initially started with a course mesh. Then it was repeated with finer mesh until the discretization error is acceptable. The section view of the mesh elements is shown in Figure 3.2.
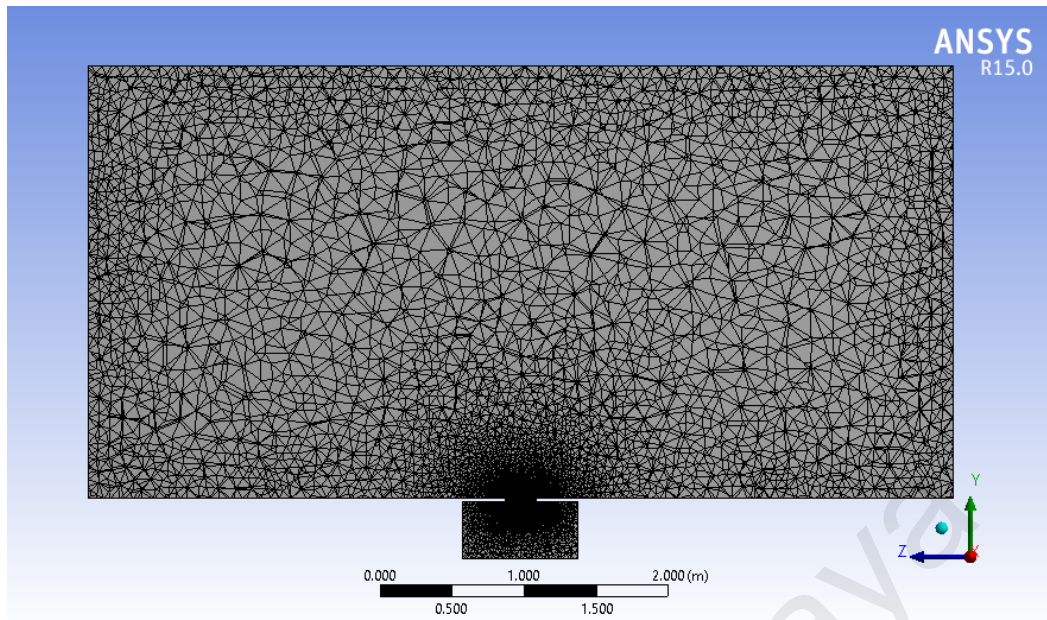
Figure 3.2: Section view of the mesh elements.

3.4.8   Verification

Verification is different from validation. Validation is to ensure the accuracy of the CFD model in representing the actual situation, while verification is to find the most appropriate mathematical model that could represents the conceptual description and obtains accurate solutions (AIAA, 1988). In verification, the comparison between experimental measurement and simulation solution can be made quantitatively and qualitatively. In quantitative assessment, air velocity, temperature, species concentrations, turbulence kinetic energy and Reynolds stresses should be compared (ASHRAE, 2009). This study does not include the comparison on species concentrations, turbulence kinetic energy and Reynolds stresses. After the quantitative assessment, the airflow pattern of the experiment and simulation is compared qualitatively through smoke test and section view in simulation. The judgment also includes referring to mathematical models studied in literatures. The simulation results in quantitative assessment can be slightly deviated. However, the mathematical model can be considered acceptable as long as the predicted trends are consistent qualitatively (Srebric and Chen, 2002).

3.5 Methodology for the Study of Solar Under-Floor Air Distribution System

This section has two major investigations. First, the solar irradiation across Malaysia is investigated as a representative of the tropics. Second, the economic feasibility of using a solar photovoltaic system in a UFAD system is investigated through an experimental study on the solar photovoltaic system, energy consumption data collection of the existing UFAD system and the payback period calculation using the Simple Payback Period (SPBP) method.

3.5.1 Solar Irradiation in Malaysia

Solar irradiation data was obtained from the Malaysian Meteorology Department (MMD) as the equipment to collect solar irradiation data from the sunlight is expensive and not feasible in the current study. Figure 3.3 shows a map of Malaysia with the seven locations indicated for this solar irradiation study. The seven locations are Bayan Lepas, Kuala Terengganu, Cameron Highlands, Subang, Kuantan, Senai and Kota Kinabalu. Bayan Lepas is located in northern Malaysia. The data from Bayan Lepas represents the northern region of Malaysia. Kuala Terengganu and Kuantan represented the major cities at the east coast of peninsular Malaysia. Cameron Highlands is located at a higher altitude with relatively low temperature, thus representing high altitude in Malaysia. Subang is located at the Klang Valley of Malaysia, the major city hub of Malaysia, and represents the central region of Malaysia. Senai in Johor represents southern Malaysia. Kota Kinabalu is a major city located in Sabah and thus represents East Malaysia. These cities were selected in this study because of the importance of economic development in these cities and their uniqueness, which can be a representative to other cities in Malaysia.
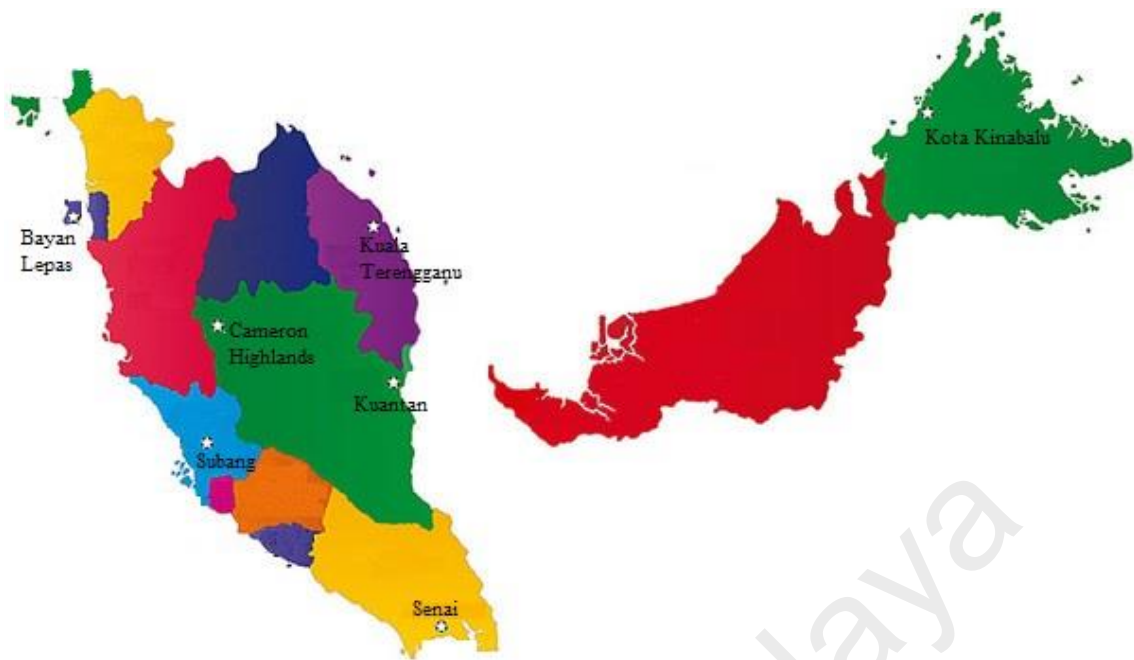
Figure 3.3: The map of Malaysia indicating the seven locations selected in this study.

3.5.2 Experimental Setup of the Solar Photovoltaic System

The test-rig in this experiment was a 1 kW on-grid solar photovoltaic system, which consists of 6 sets of Solarland SLP230-20 polycrystalline silicon photovoltaic panels connected in series to the utility grid installed on the roof top of HVAC&R Laboratory, Faculty of Engineering at University of Malaya as shown in Figure 3.4. The size of each panel is 1655 x 992 mm. The system combines for a total of 1.38 kW actual power output, which is equivalent to 140 W/m^2.

The ideal tilt-angle of solar panels is 0° face up to the sky for maximum output performance. However, the poo of birds and dust from the outdoor air accumulates on the surface of the panels through time and affects the energy output. Regular cleaning s creates a substantial cost for the maintenance. Fortunately, Malaysia is a tropical country with regular rainfall. Thus, solar panel installation is practically adjusted to a tilt-angle of 16° facing south in order for rainwater to clean the surface. The south direction is selected because Malaysia is located at 3.1° north of equator.

Figure 3.5 shows the schematic diagram of the on-grid solar photovoltaic system. Solar photovoltaic panels are connected in series to surge protective device (SPD) with fuses and switches to cut off the power manually when necessary for the safety reasons. The system is then connected to the GW1500-SS solar inverter as shown in Figure 3.6. A miniature circuit breaker (MCB) was installed after the inverter to protect against overloading and short circuits. Lastly, it is connected to the building's MCB power supply and to the building electricity load.

Figure 3.4: Experimental setup of the 1 kW on-grid solar photovoltaic system.
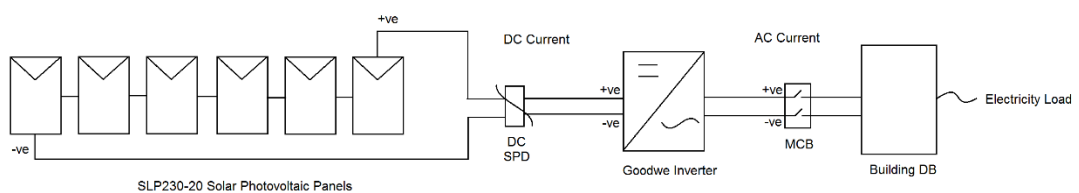
Figure 3.5: Schematic diagram of the on-grid solar photovoltaic system.

Figure 3.6: GW1500-SS solar inverter by Goodwe Power Supply Technology Co. Ltd.

The electrical characteristics of this system are shown in Table 3.3. The technical electrical data was obtained at the standard test condition (E=1000W/m^2, TC=25°C and Am=1.5). An individual solar photovoltaic module is 30.2V. The connection of the system was in series, which makes up to a total of 181.2VDC before reaching the inverter. The DC voltage is inverted into 240VAC, the same as the building power grid supply.

Table 3.3: Electrical characteristics of solar photovoltaic panel SLP230-20

Maximum power (Pmax)	230W
Voltage at Pmax (Vmp)	30.2V
Current at Pmax (Imp)	7.62A
Open-circuit voltage (Voc)	36.9V
Shor-sircuit current (Isc)	8.31A
Number of diode	6
Number of cells	60
Max system voltage	1000V DC
Temperature coefficients of Isc	0.0877%/°C
Temperature coefficients of Voc	-0.3522%/°C
Nominal operating cell temperature	47±2°C
Output tolerance	0/+5W

Power generated from the solar photovoltaic system was analyzed using the voltage and current data collected from the inverter through a USB AM-BM cable connected to a PC. EzExplorer software developed by Goodwe was installed onto the PC running 24 hours to collect real time data from the solar photovoltaic system and stored on the PC. The data collected included time, date, VDC, DC current, VAC, AC current, frequency, AC power output, inverter temperature, etc. The data collection and analysis were conducted for 12 months.

3.5.3   Simple Payback Period (SPBP)

The simple payback period (SPBP) method is adopted in this study (Rodrigues et al., 2016). This SPBP method is widely used to identify the time required to repay the initial cost of investment. Discount and interest rates are not included in the calculation, which makes it an easily understandable method to estimate the profitability to invest in the solar

photovoltaic cooling system. The annual simple cash flow (SCF) as shown below had to be developed prior to the analysis of the payback period.

$$SCF_y = Cash\ inflow_y - Cash\ outflow_y$$

$$SCF_y = \sum_{y=1}^{Y}(T_g \times E_g)_y - \sum_{y=1}^{Y}(T_e \times E_e + M)_y$$

where T_g is the tariff for electricity generated (RM), E_g is the annual electricity generated (kWh), T_e is and the tariff for grid electricity (RM), E_e is the annual electricity imported from the grid (kWh), M is the maintenance cost (RM).

The solar panels have a 25 year warranty from the manufacturer. No maintenance on the panels is required due to no moving parts and rainfall cleaning the surface frequently. However, it is necessary to consider the cost to replace the solar inverter and cost of operation and maintenance. Thus, it is logical to assume the maintenance cost per year to be 2.5% of the initial cost of the solar photovoltaic system (Rodrigues et al., 2016).

The solar panel is warranted with at least 80% power output in 25 years of use (Solarland, 2012). Thus, the worst case performance degradation rate is assumed to be at 0.8% per year. The assumed performance degradation rate in this study is similar to the international recommended linear degradation rate of 0.7. Thus, the assumption is valid. Finally, the SPBP (in years) was calculated as "n" below when the initial cost plus simple cash flow of the solar photovoltaic UFAD system equals the simple cash flow of the conventional UFAD system as shown below:

$$\sum_{y=1}^{n} SCF_{sol} + I = \sum_{y=1}^{n} SCF_{conv}$$

where n is the years of SPBP, SCF_{sol} is the simple cash flow of solar photovoltaic UFAD system, SCF_{conv} is the simple cash flow of the conventional UFAD system and I is the initial cost of solar photovoltaic system.

3.5.4   Feed-in Tariff (FiT)

Feed-in Tariff (FiT) is a subsidy program initiated by Sustainable Energy Development Agency Malaysia (SEDA), a government agency. This program provides subsidies to successful applicants who install renewable energy power generation systems, including solar photovoltaic systems, at their respective building. This subsidy program is effective for 21 years from the first year of the commencement date. This program boasted the development of the solar photovoltaic system in Malaysia. Hence, it is included in the SPBP calculation.

The FiT rate for each renewable energy is different. In our case study, the rate is adopted from solar PV (non-individual $\leq$ 500 kW). The FiT rate is calculated by the formula below:

$$FiT\ Rate = Basic\ FiT\ rates + Bonus\ FiT\ rates$$

where the basic FiT rates are qualified based on the installed capacity. There are four types of bonus FiT rates provided. The bonus FiT rates are given if the solar photovoltaic system is used as installation on buildings or building structures, or used as building materials, or use of locally manufactured or assembled solar PV modules, or use of locally manufactured or assembled solar inverters.

3.6   Summary

A thorough investigation on the existing UFAD system of a high rise building is important to have a complete understanding of the actual system's operation in the tropics. In order to have a good understanding of the system's operation, the exisiting system is investigated using a typical IAQ field assessment methodology in the tropics. Then, CFD computational tool that combines fundamental theories of fluid dynamics and mathematics in analyzing the behavior of fluid flow is used to analysis the flow patterns of the floor diffuser. The relevancy of the solution output to the actual scenario is directly influenced by modeling, discretization, solver selection and input of boundary conditions. Thus, it is important to understand the fundamental governing equations of CFD, background theories of flow solvers, types of turbulence models, and boundary conditions in order to obtain reliable results to achieve the objectives of this study. Finally, the energy consumption of UFAD system and energy generation from solar PV system is studied.

CHAPTER 4 – THERMAL ENVIRONMENTAL AND INDOOR AIR QUALITY CASE STUDY OF AN UNDER-FLOOR AIR DISTRIBUTION SYSTEM IN TM TOWER, MALAYSIA

4.1 Overview and Background of the Building

Menara Telekom, also called TM Tower, is the third highest skyscraper in Malaysia. The construction was completed in the year 2001 and officiated in the year 2003 with a height of 310 m and 55 floors. The total floor area of the building is 148,800 m^2. It is the tallest building in Malaysia after KLCC Twin Towers and KL Tower. The façade is shaped to represent a sprouting "bamboo shoot", a traditional food of local communities in rural areas in Malaysia. TM Tower was a pioneered building that uses under-floor air distribution (UFAD) system for human comfort in Malaysia. The building is mainly office floors, designed with 22 unique open sky gardens at every third floor.

The heating, ventilating and air-conditioning (HVAC) system of the building is served by chilled water supplies from Bangsar district cooling plant. Chilled water is channeled through the underground from Bangsar district cooling plant to LG4 of TM Tower, where four heat exchangers are used to supply the second cycle of chilled water to LG3. Water pumps at LG3 supply the chilled water to Level 29, where another heat exchanger system is used to supply chilled water to serve Level 29 – 56.

Each floor is divided into North (N) and South (S) wing offices. One precool air handling unit (PAHU) is served to precool outdoor air at each office wing. Precooled outdoor air is then supplied to the five air handling units (AHUs) inside the office, which combines it with the ceiling return air to go through cooling coils and deliver the mixed air for human comfort according to the design concept of UFAD system.

In this study, thermal environment and indoor air quality (IAQ) assessments were conducted at five office spaces, which are 33N, 33S 34N, 34S and 35S, with the aim to identify the performance of the existing UFAD system in the tropics after more than 10 years of operations. Table 4.1 shows the floor area of each office space. The interior of the office is designed as open plan office with low partition walls. A few small rooms are partitioned out as meeting rooms at the inner section and periphery of the office space. Figure 4.1 shows the interior of the open plan office. Five AHUs are installed throughout the office area on each office wing.

Table 4.1: The floor area of each office space.

Office Wing	Working Area (ft²)
Level 33 North	9310.5
Level 33 South	9310.5
Level 34 North	9171.0
Level 34 South	9171.0
Level 35 South	8676.0

Figure 4.1: Photo shows the interior of the open plan office space.

4.2 Assessment Methodology

The assessment methodology was guided by the thermal environment and IAQ assessments generally used in Malaysia and Singapore (Cheong and Lau, 2003; DOSH, 2010; Ministry of the Environment, 1996). The assessment was divided into objective and subjective measurements. However, this study focused on objective measurements, while subjective measurements including questionnaires and statistical analysis were not conducted. The assessment procedures are generally divided into 4 stages: preliminary, sampling, evaluation and recommendation.

4.2.1 Preliminary Stage

The assessment procedure was started with a walk-through survey and inspection of the HVAC plant room where the incoming and the outgoing district chilled water and the heat exchanger system were located. The walk-through was led by the building operation and maintenance team. A comprehensive discussion with the team and a detailed review on the HVAC as-built drawings were crucial to understand the routine operations and maintenance of the HVAC system. A walk-through and inspection of the office area was led by the office tenant. Feedback from the occupants was arbitrary collected during the walk-through to grasp an understanding on if sick building syndrome (SBS) occurred. The location of fresh air inlets, PAHU, AHU, supply and return air grilles, the air distribution and the possible source of indoor air pollutants in the office were located and inspected prior to the planning of assessment sampling points.

4.2.2 Sampling Stage

The thermal environment data (indoor air temperature, relative humidity and air velocity) and IAQ data (CO, CO_2, formaldehyde, TVOC and PM_{10}) were collected in this study. Noise level in the office space was collected due to the relation with the airflow rate and performance of the floor swirl diffusers. Fresh air intake was measured in relation with the CO_2 levels in the office space. Within the five office spaces examined in this study, eight sampling locations were selected at each office space as shown in the typical floor plan in Figure 4.2. Point 1 to 5 are located at the open office area. Point 6 is located at the pantry area. Point 7 to 8 are located at the partitioned meeting rooms. The sampling height was fixed at 110 mm above floor level, a height which is suitable for both sedentary and standing activity (ASHRAE, 2013a).

Indoor thermal environment is closely related to outdoor climate conditions, while CO_2 concentration is influenced by the occupancy's activity. These parameters fluctuate throughout the day. Hence, they were measured at 4 different time zones throughout the office hours to observe the profile changes and thus identify the effectiveness of the HVAC system. The time zones are divided as follows: 1 (9am – 11am), 2 (11am – 1pm), 3 (1pm – 3pm) and 4 (3pm – 5pm). At each time zone, the data was taken based on the average of half-hour surrogate measurements at an interval of five minutes for a period of a half-hour (DOSH, 2010). The equipment used for fieldwork assessment is shown in Chapter 3 and thus not repeated here.
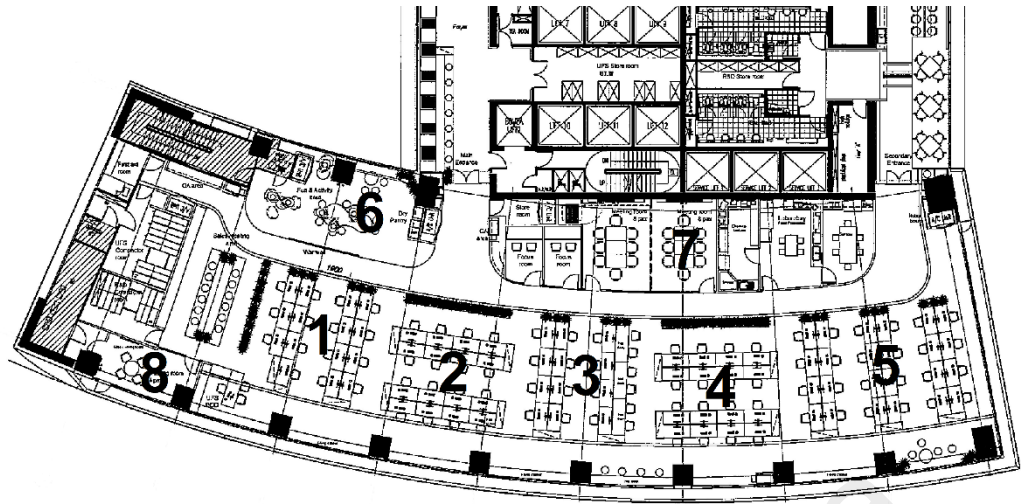
Figure 4.2: Typical floor plan showing the location of the sampling points in the office space.

(Pua, 2013)

Outdoor fresh air is supplied by the external ducting installed at the lobby's ceiling of each floor. The air is precooled by a PAHU unit at the ceiling before it is conducted to five AHU units in the office. According to ASHRAE Standard 41.2 – Standard Methods for Laboratory Airflow Measurement – the traverse technique can be used to measure air flow inside ducts using a pitot tube (ASHRAE, 1992). The measuring point must be at least 7.5 duct diameters downstream, and at least 3 duct diameters upstream from any turns or flow obstructions. Figures 4.3 and 4.4 show the standard flow measurement.
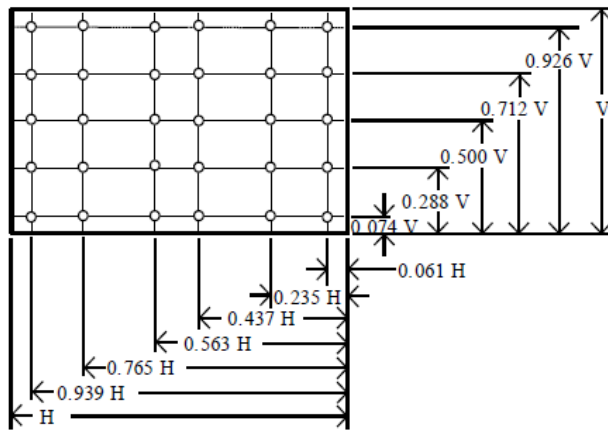
Figure 32: Location of Measuring Points for Traversing a Rectangular Duct using Log-Tchebycheff Method

For this duct, a 30-36" horizontal dimension requires 6 points (or 6 traverse lines). For this duct, a vertical dimension less than 30" requires 5 points (or 5 traverse lines).

# of Points or Traverse Lines per Side	Position Relative to Inner Wall
5	0.074, 0.288, 0.500, 0.712, 0.926
6	0.061, 0.235, 0.437, 0.563, 0.765, 0.939
7	0.053, 0.203, 0.366, 0.500, 0.634, 0.797, 0.947

Figure 4.3: Traverse Method (Log Tchebycheff Rule) for rectangular duct.

(TSI, 2012)
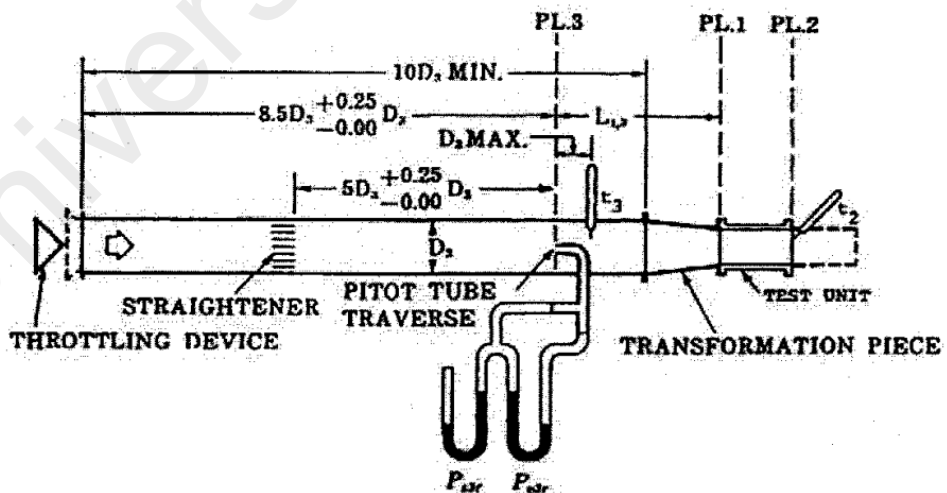
Figure 4.4: Outlet duct setup for the pitot traverse in the outlet duct.

(ASHRAE, 1992)

56

The duct size is measured at 0.94 X 0.36 meters, which is equivalent to 0.65 meters diameter by the calculation using the formula shown below.

$$\text{Equivalent Diameter} = \text{sq root of } 4HV / Pi$$

where:

H = horizontal duct dimension

V = vertical duct dimension

Pi = 3.14

Hence, the minimum duct length required is 6.5 m. Note that the maximum duct length is 5.5 m at the site with the assumption of ignoring the split duct for the lift lobby supply air. Due to the short duct length, assumptions were made in this measurement. The assumptions were that fresh air flow inside the ducting is laminar flow, the influence of the split duct to the supply air on the air flow turbulence at the lift lobby is negligible and the fresh air at the measuring station is fully-developed. Based on the required duct length ratio, the measuring point was fixed at 4 m from the PAHU unit as shown in Figure 4.5. Figure 4.6 shows the measuring conditions at the site.

To minimize the destructible condition at the fresh air duct, the full traverse method was carried out only at Level 35S. The Correction Factor was developed from this measurement, and then applied to the rest of the office wings measured. The measurements at Levels 33N, 33S, 34N and 34S were only conducted at the centre-point of the duct. The actual volumetric flow rate was calculated by multiplying the results with the Correction Factor developed.
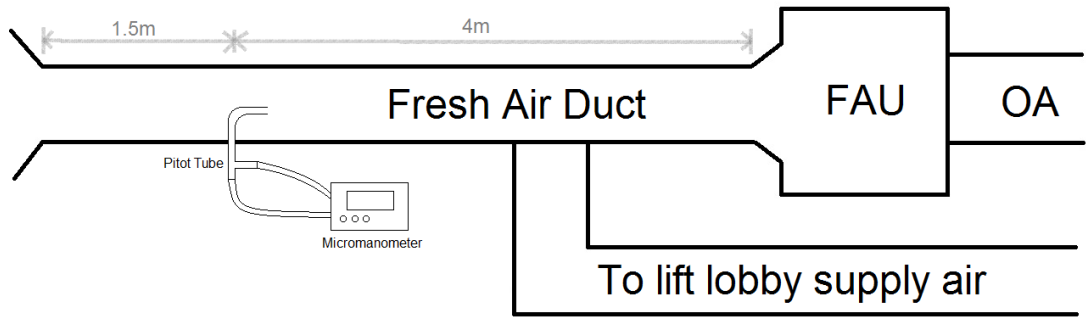
Figure 4.5: Traverse measuring station at the fresh air duct.

Figure 4.6: Site measuring conditions.

4.2.3 Evaluation Stage

The standards and regulations referred to in this study are the Industry Code of Practice on Indoor Air Quality 2010 (DOSH, 2010), ASHRAE Standard 55-2013 (ASHRAE, 2013a), and the Malaysian Standard MS 1525:2014 (Department of Standards Malaysia, 2014). Based on the measurements obtained, the causes of SBS symptoms were discussed and determined.

Table 4.2: Thermal environment design guideline in Malaysian standard MS 1525:2014 (Department of Standards Malaysia, 2014)

Parameter	Threshold Limits
Dry bulb temperature	23 – 26 °C
Relative humidity	55 – 70 %
Air velocity	0.15 - 0.5 m/s

Table 4.3: Acceptable range of thermal environment and IAQ parameters in industry code of practice on indoor air quality 2010.

Parameter	Threshold Limits
Dry bulb temperature	23 – 26 °C
Relative humidity	40 – 70 %
Relative air velocity	0.15 - 0.5 m/s
CO concentration	10 ppm
CO_2 concentration	1000 ppm
Formaldehyde	0.1 ppm
Particulate (PM_{10})	0.15 mg/m^3
TVOC	3 ppm

4.2.4 Recommendation Stage

In final stage, remedial strategies were recommended to improve the indoor air quality and to enhance thermal comfort. A re-audit is recommended once the remedial work is performed to ensure the health and well-being of the occupants is safeguarded.

4.3 Thermal Environment

4.3.1 Indoor Air Temperature and Relative Humidity

The recommended indoor air temperature in the Malaysian Standard MS 1525:2014 (Department of Standards Malaysia, 2014) and Industry Code of Practice on Indoor Air Quality 2010 (DOSH, 2010) have the same range of 23°C – 26°C. This range is similar to the Singapore guidelines which have a range of 22.5 – 25.5°C (Ministry of the Environment, 1996). The occupants in the tropics can perceive a higher RH than those in the sub-tropics. However, an RH above 70% will encourage mold growth and subsequently causes SBS. Thus, all the three standards, code and guidelines do not allow the RH to be exceeded 70%.

Figure 4.7 shows the indoor air temperature and the RH of the office spaces. Most of the office spaces have relatively low indoor air temperatures at or below 23°C. The low air temperature is attributed to the failure of the chilled water valve actuators. The malfunctioning chilled water valve actuators allow the chilled water to continue to cool the space even when the temperature set-point is achieved. The low indoor air temperature causes the RH to be high. The indoor air temperature and the RH are inversely related. The phenomenon of the low indoor air temperature, and the high RH can be seen mostly at points 6, 7 and 8 where the pantry area and meeting rooms are located. These places are not usually occupied. The heat load is much less compared to the open-plan office. Data fluctuation can also be seen at different time zones in these areas where the

movements of occupants are random. These areas were over-cooling at certain time zones.

Points 1 to 5 seem to have a much stable indoor air temperature and RH, except for 35S

where the office space is partly occupied and has more human movement due to the nature

of work.
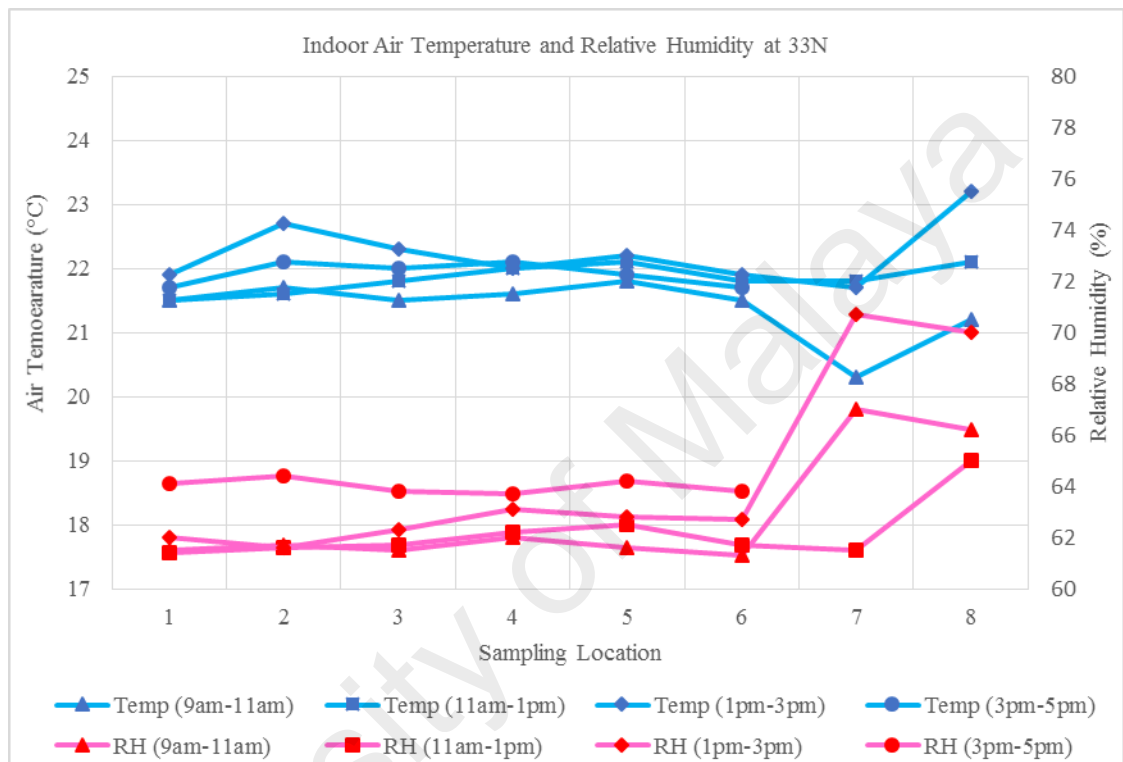
(a) Office space 33N
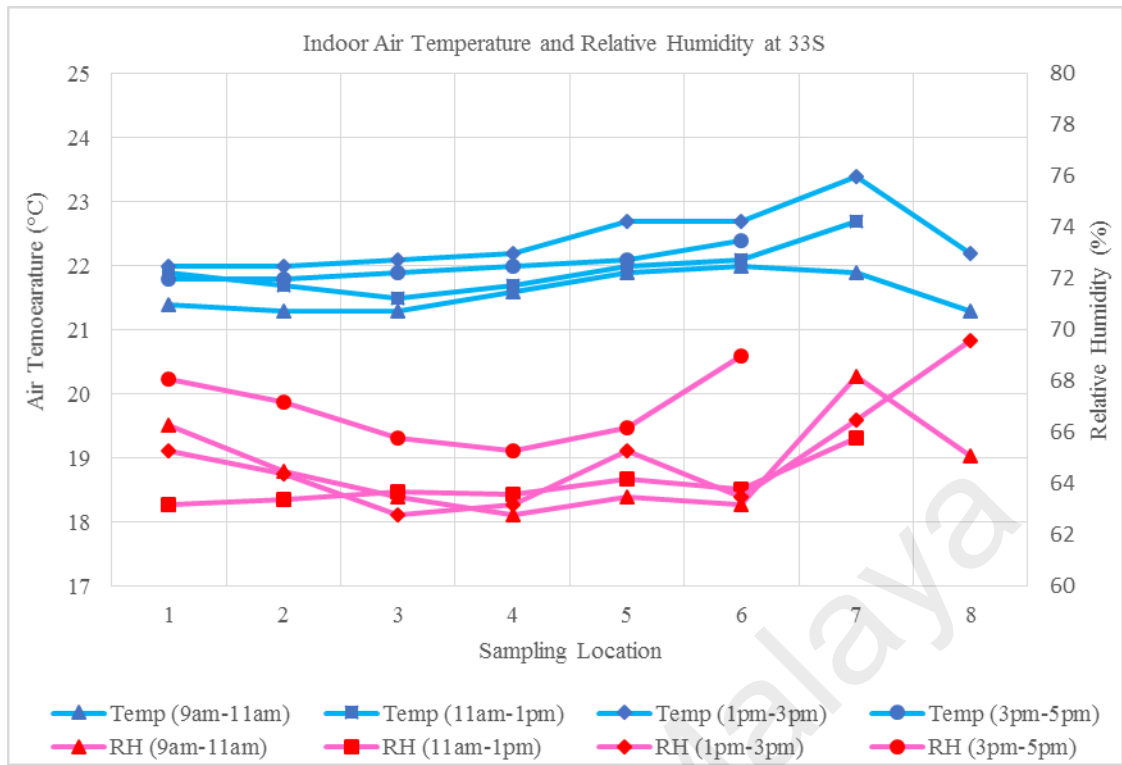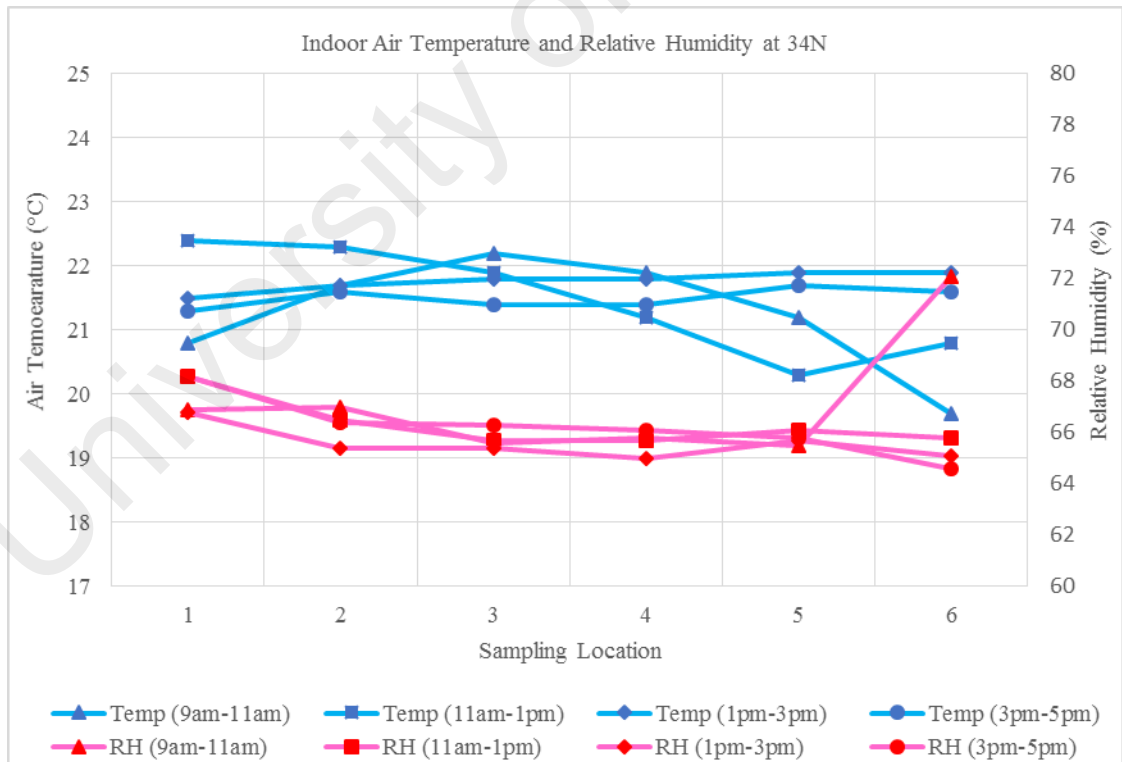
(b) Office space 33S
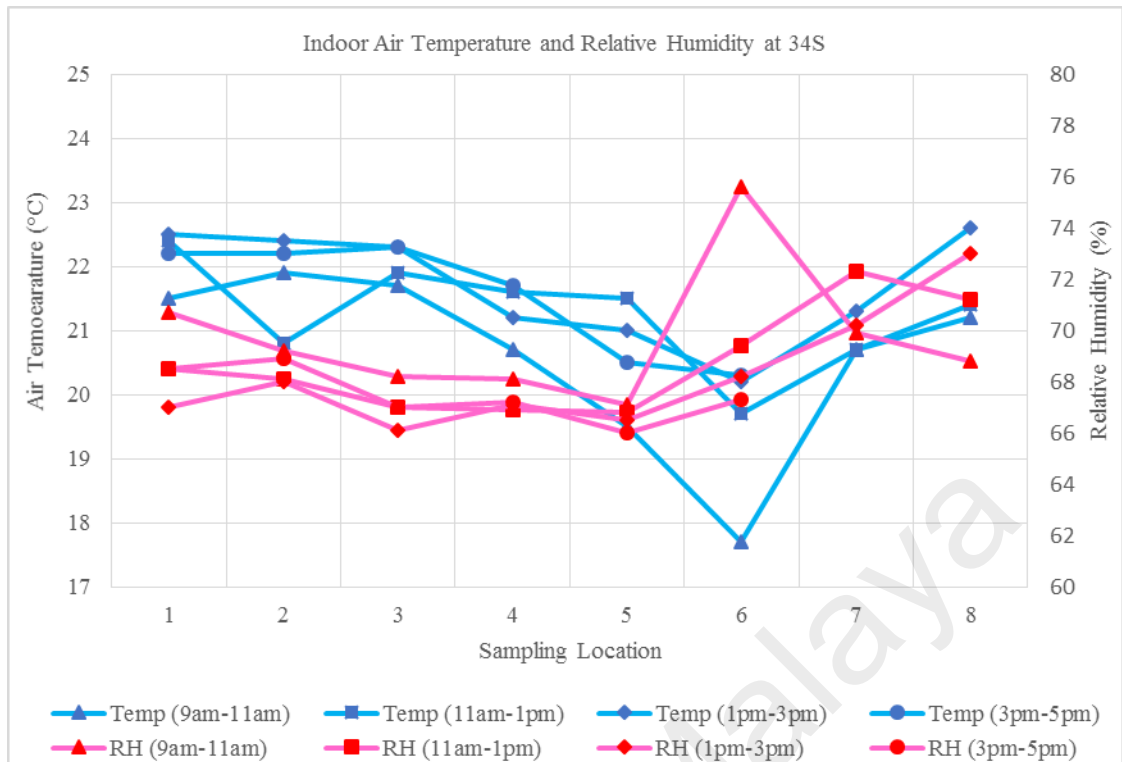
(c) Office space 34N
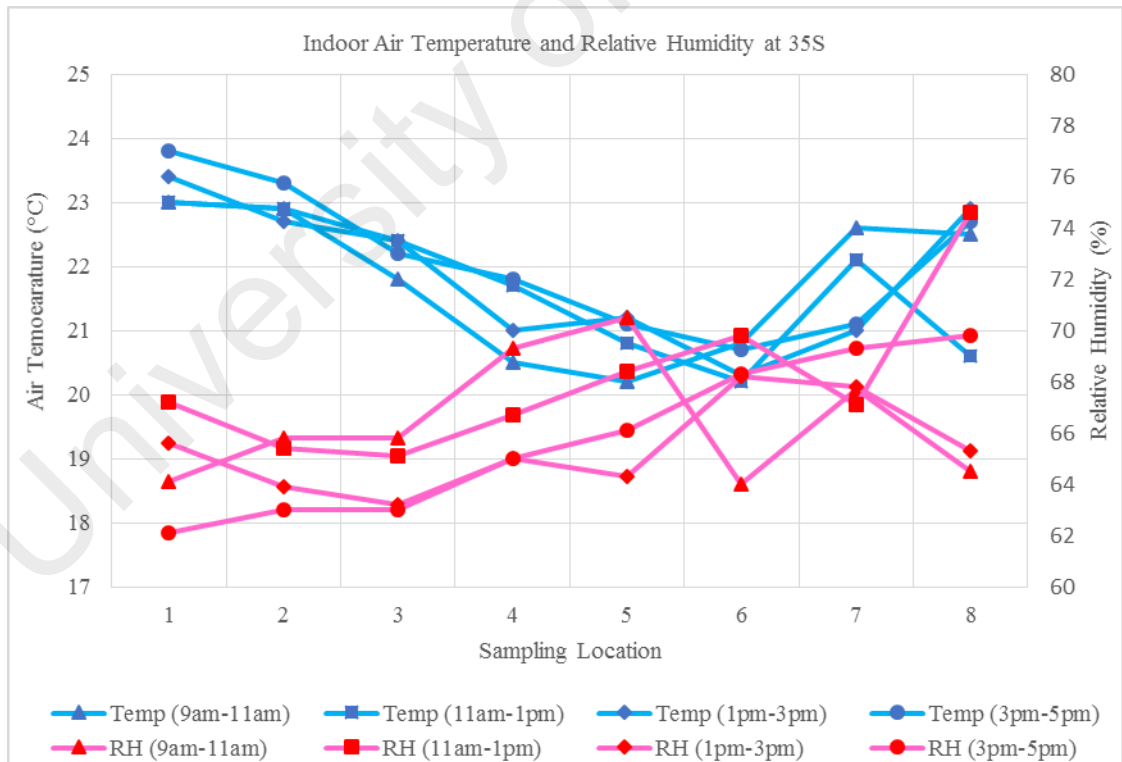
(d) Office space 34S

(e) Office space 35S

Figure 4.7: Indoor air temperature and relative humidity of the office space: (a) office space 33N (b) office space 33S (c) office space 34N (d) office space 34S (e) office space 35S.

Figure 4.8 shows the distribution of the humidity ratio at different time zones. The humidity ratio of the office space is in the range of 9.52 – 12.59 g_{water}/kg_{air} with most of the data falling in between 10.0 – 11.5 g_{water}/kg_{air}. This moisture level is equivalent to a relative humidity of 56.8 – 65.2% at an indoor air temperature of 23°C, which proves the effectiveness of dehumidification of the AHU cooling coil. Hence, RH can be maintained within a good range if the temperature does not decrease below the comfort level.
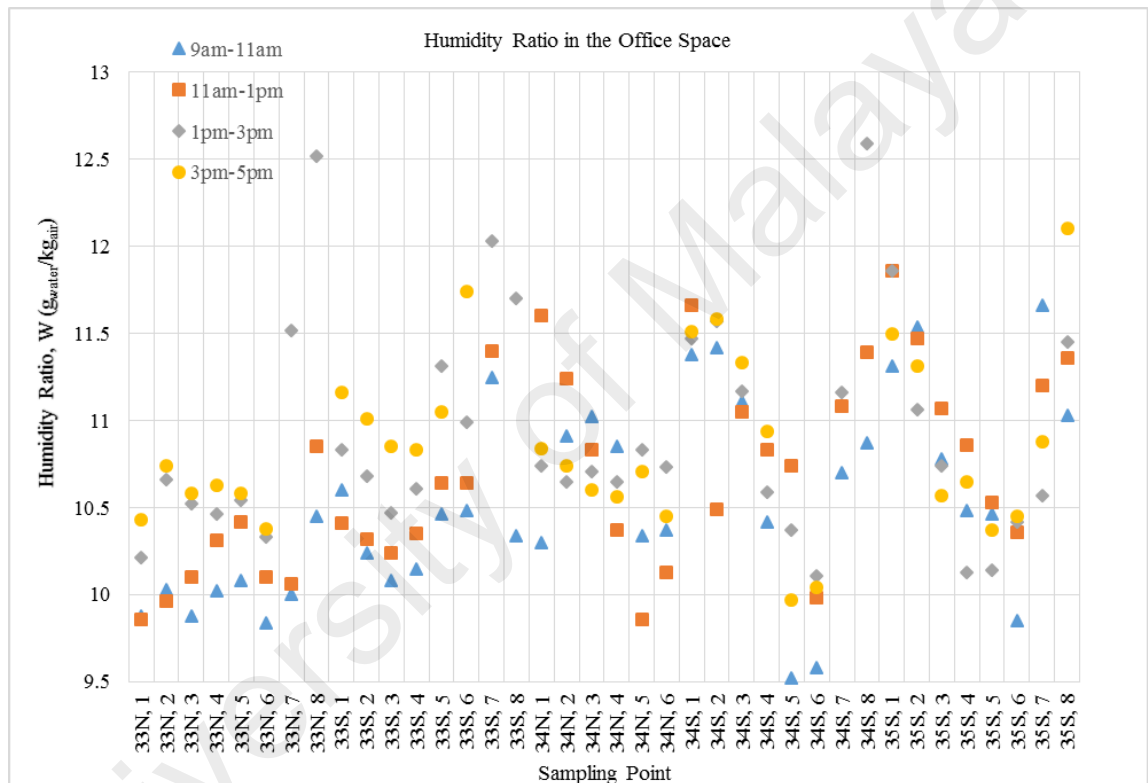
Figure 4.8: The distribution of the humidity ratio at different time zone.

4.3.2 Air Velocity

The air velocity of the office space is shown in Table 4.4. It is much lower compared to that of the thermal comfort requirement. Low air movement causes human discomfort and feeling stuffy. It is noteworthy that occupants in the tropics are used to a damped environment and sweating. A higher air velocity acting on the human body will improve thermal comfort (Li et al., 2010).

It was observed that most of the floor grilles have broken or missing diffuser blades. It is pertinent to mention that without the diffuser blades, the conditioned air will not spread out to the space and will not effectively create an air-mixing at the occupied space. Besides, the diffuser blade plays a significant role in creating air stratification. ASHRAE 62.1 has rated a higher air ventilation effectiveness of 1.2 for the UFAD system, in which the terminal velocity of 0.25 m/s is achieved at 1.4 m or less above the floor level (ASHRAE, 2013b). Without the diffuser blades, conditioned air will eject vertically with a much higher velocity. The upper stratified zone is not formed when the supply air jet exceeds the heat plumes within the space. As a result, the ventilation effectiveness is reduced.

Table 4.4: The air velocity of the office space.

Office Space	Air Velocity (m/s)
Level 33N (max, min, average)	0.10, 0.01, 0.04
Level 33S (max, min, average)	0.07, 0.02, 0.04
Level 34N (max, min, average)	0.11, 0.01, 0.04
Level 34S (max, min, average)	0.11, 0.03, 0.06
Level 35S (max, min, average)	0.08, 0.04, 0.05

4.4   Indoor Air Quality

The IAQ parameters in association with occupants' health are CO, CO_2, formaldehyde, TVOC and PM_{10}. The interior office spaces were newly renovated. Hence, a complete IAQ assessment is important, especially on the formaldehyde, TVOC and PM_{10}, which are closely related to materials and adhesives used in furniture. The IAQ results are shown in Table 4.5.

TVOC was not detected in the office space. However, the formaldehyde that was detected exceeded the threshold limit of 0.1 ppm. The office had recently moved in new wooden tables and partitions, which might be the cause of the unusually high formaldehyde level. Formaldehyde, which used widely in many wood products, is carcinogenic to humans as reported by IARC (IARC, 2012). The short-term effects are skin, eye and nose, and throat irritations. A prolonged exposure could be cancerous. The cancer effects in associated to formaldehyde are nasopharynx cancer, leukemia and nasal sinuses cancer (Liteplo et al., 2002; WHO, 2010). Thus, 0.75 – 0.2 ppm has been the threshold limit in many countries (OSHA; SCOEL, 2008). However, the formaldehyde emission rate decreases through time. A higher ventilation rate and higher temperature increase the formaldehyde emission rate (An et al., 2010). Smoke spill fans, which are available at the office spaces, are suggested to flush out the indoor air to be replaced with the outdoor air during off-hours. The HVAC system should be switched off during the air flushing, as a higher temperature can effectively enhance the formaldehyde emission and remove it from the office spaces.

The average PM_{10} in the office spaces were in the range of 0.116 – 0.143 mg/m^3, which is below the threshold limit of 0.15 mg/m^3. The maximum PM_{10} were recorded at 0.198 – 0.427 mg/m^3 for a short interval of time, which is above the threshold limit. This could be due to the movements of the occupants. However, because the average PM_{10} is below the threshold limit, the results are acceptable.

The CO and CO_2 are the parameters used to measure the air pollutants that have been created from the human activity. The CO levels were far below 10 ppm. This was expected, as the office spaces do not have any potential activities and sources that emit CO, such as smoking.

The CO_2 concentration gradually increased from morning to evening in the same office space as shown in Figure 4.9. Office spaces in 33N, 34N and 34S had CO_2 concentrations that exceeded the threshold limit of 1000 ppm for most of the time, while 33S exceeded the threshold limit of 1000 ppm at time zone 3. The CO_2 concentration in 35S was within the safe margin between 676 – 749 ppm as the office is not fully occupied. Note that the outdoor CO_2 concentration can vary between 350 and 400 ppm (Turanjanin et al., 2014). Hence, exceeding the limit of 1000 ppm shows a major CO_2 concentration increase compared with the levels normally measured at outdoor. This indicates that the fresh air supply is insufficient. When inspected, it was discovered that the fresh air supply unit and the PAHU were not operating during the evening, although the occupancy rate remained the same. A separate test was performed to measure the duct fresh air flowrate using the traverse method at the latter part of this chapter, and it determined the sufficiency of the designed fresh air supply meeting the requirement of ASHRAE Standard 62.1 (ASHRAE, 2013b). Hence, the CO_2 sensor is encouraged to be used for the PAHU control to avoid human maneuver in switching off the fresh air supply, as well as providing optimum control of the fresh air supply to reduce power wastage.

Table 4.5: The indoor air quality parameters measured at the office space.

Indoor air quality	33N	33S	34N	34S	35S
CO (ppm) (max, min, average)	(2.5, 0.2, 0.9)	(2.0, 0.2, 0.9)	(1.5, 0.2, 0.6)	(2.3, 0.2, 0.8)	(2.0, 0.2, 0.8)
CO_2 (ppm) (max, min, average)	(1352, 818, 1113)	(1130, 720, 948)	(1256, 772, 1021)	(1128, 764, 1014)	(818, 635, 716)
Formaldehyde (ppm) (max, min, average)	(0.30, 0.21, 0.26)	(0.29, 0.23, 0.27)	(0.37, 0.32, 0.34)	(0.18, 0.13, 0.15)	(0.28, 0.24, 0.25)
TVOC (ppm) (max, min, average)	(0, 0, 0)	(0, 0, 0)	(0, 0, 0)	(0, 0, 0)	(0, 0, 0)
PM_{10} (mg/m^3) (max, min, average)	(0.427, 0.131, 0.143)	(0.198, 0.118, 0.128)	(0.308, 0.108, 0.116)	(0.293, 0.057, 0.120)	(0.280, 0.119, 0.126)
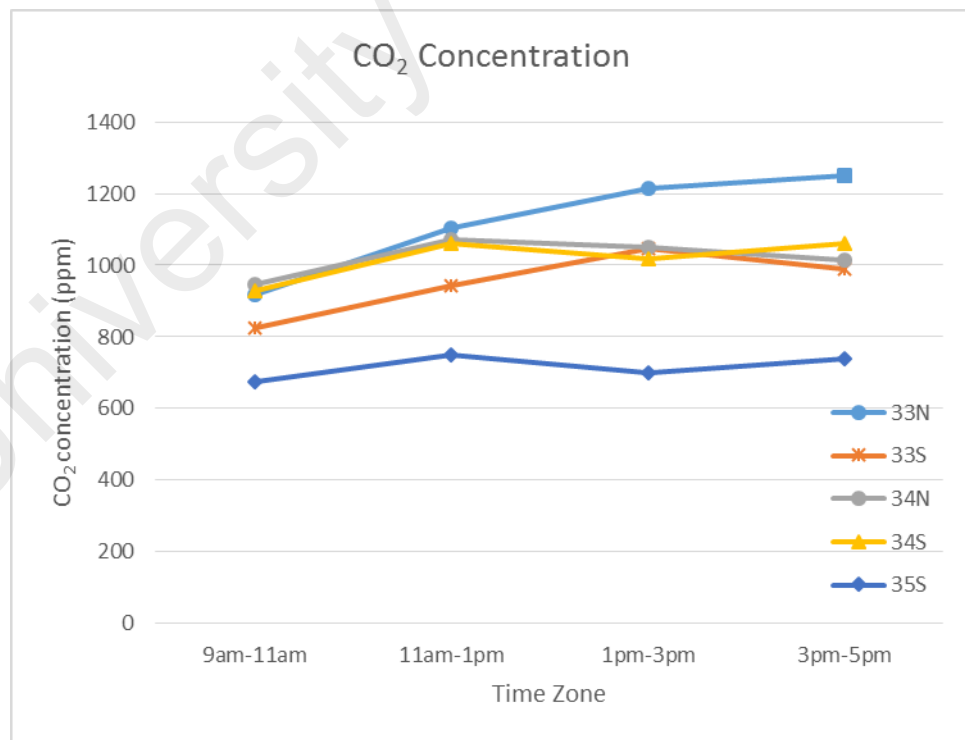
Figure 4.9: CO_2 concentration of the office space at different time zone.

4.5 Fresh Air Measurement

Based on ASHRAE Standard 42.1, 35 measuring points are required. Table 4.6 shows the Traverse volumetric flow rate measurement on the fresh air duct at Level 35S with units in cubic feet per minute (CFM). Table 4.7 shows the results developed from the measurements taken. By comparing the average volumetric flow rate with the centre-point volumetric flow rates, the Correction Factor is 1.0049. Table 4.8 shows the results for Levels 33N, 33S, 34N and 34S with the corrected values by multiplying with the Correction Factor developed.

According to the ASHRAE Standard 62.1 the minimum amount of fresh outdoor air recommended for office spaces is 20 CFM/person. Each office wing is occupied with roughly 90 occupants. Based on the results indicated in the graph shown in Figure 4.10, the amount of fresh air at most of the office wings is generally sufficient.

Table 4.6: Traverse measurement at the fresh air duct at level 35S.

2839	2840	2758	3413	4308	4632	4480
3037	2954	2924	3550	4183	4488	4265
3024	2721	3033	3352	4034	4129	3907
3048	2834	2968	3338	3541	3661	3585
2440	2521	2861	2909	2939	3156	3220

Table 4.7: Fresh air data for level 35S.

Air Temperature (°C)	19.30
Relative Humidity (%)	89.50
Average Volumetric Flow Rate (cfm)	3368.34
Correction Factor with Centre Point	1.0049
Area of L35S (ft^2)	8676.00
Floor height (ft)	10.00
Air change (hr^{-1})	2.33

Table 4.8: Fresh air data for level 33N, 33S, 34N and 34S.

Level	33N	33S	34N	34S
Air Temperature (°C)	18.80	15.60	16.50	19.20
Relative Humidity (%)	89.60	92.10	88.90	89.30
Volumetric Flow Rate at Centre-Point (CFM)	4059.00	2735.00	1951.00	2167.00
Corrected Volumetric Flow Rate (CFM)	4078.79	2748.33	1960.51	2177.57
Floor Area (ft^2)	9310.50	9310.50	9171.00	9171.00
Floor height (ft)	10.00	10.00	10.00	10.00
Air change (hr^{-1})	2.63	1.77	1.28	1.42
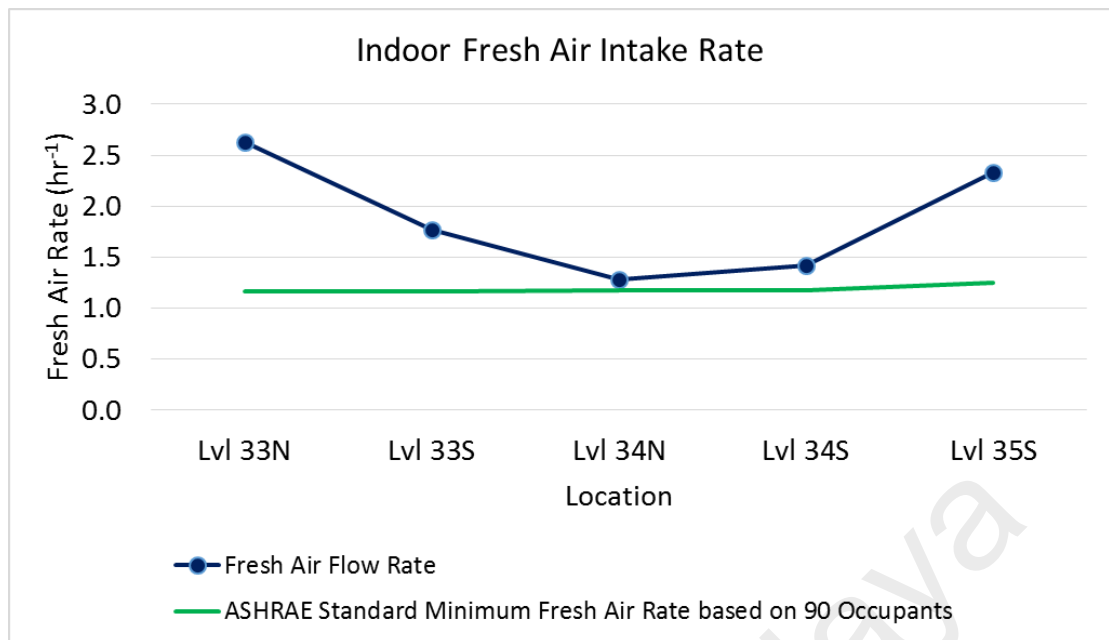
Figure 4.10: Fresh air flow rates at each office space.

4.6 Noise Level

There is no specific requirement for the noise level control for office spaces. However, too much unwanted sound or levels too quiet may not be desired for occupants' comfort. Maxwell quoted ASHRAE and recommends that the noise range for office spaces is between 49 to 58 dBA. As a comparison to this recommended range, the results are shown in Figure 4.11. In general, the current noise level in the office spaces was acceptable with the exceptions of few locations either exceeded or below the recommended noise range.

Noise Level at Level 33N

Noise Level at Level 33S

Noise Level at Level 34N
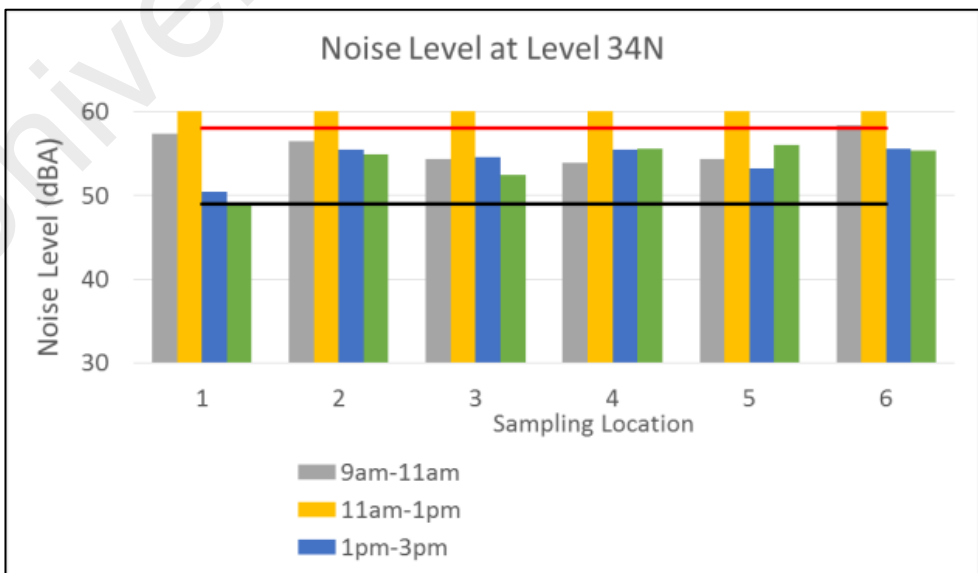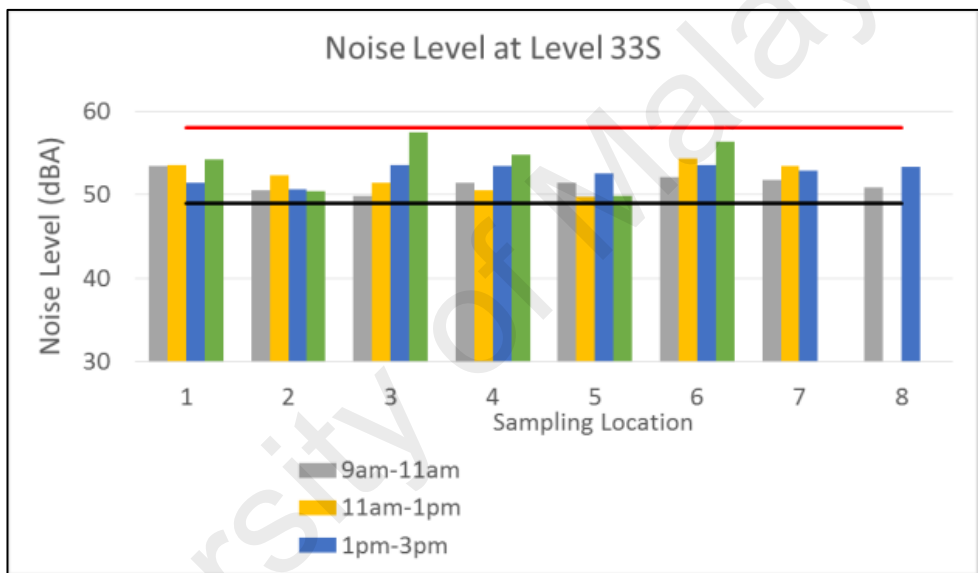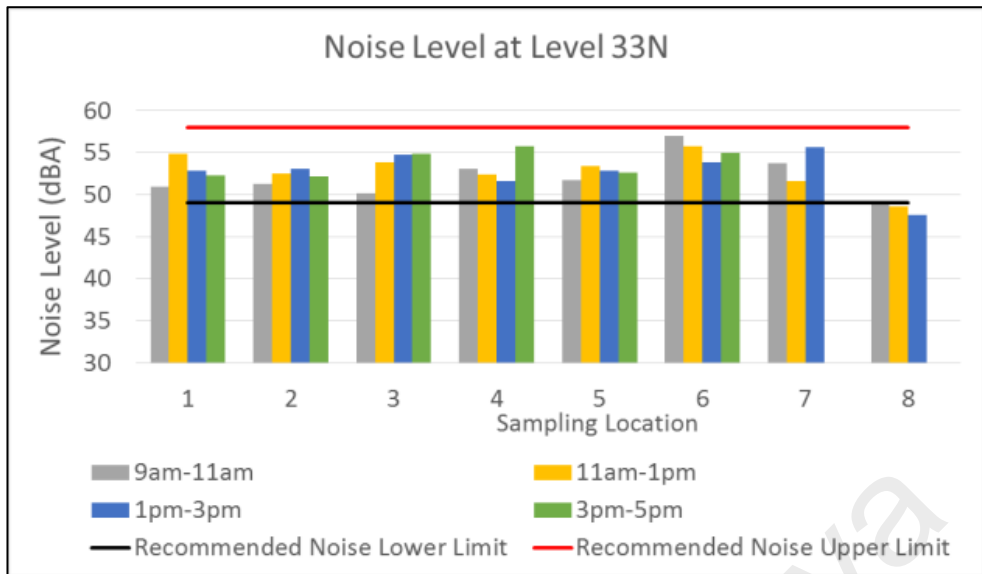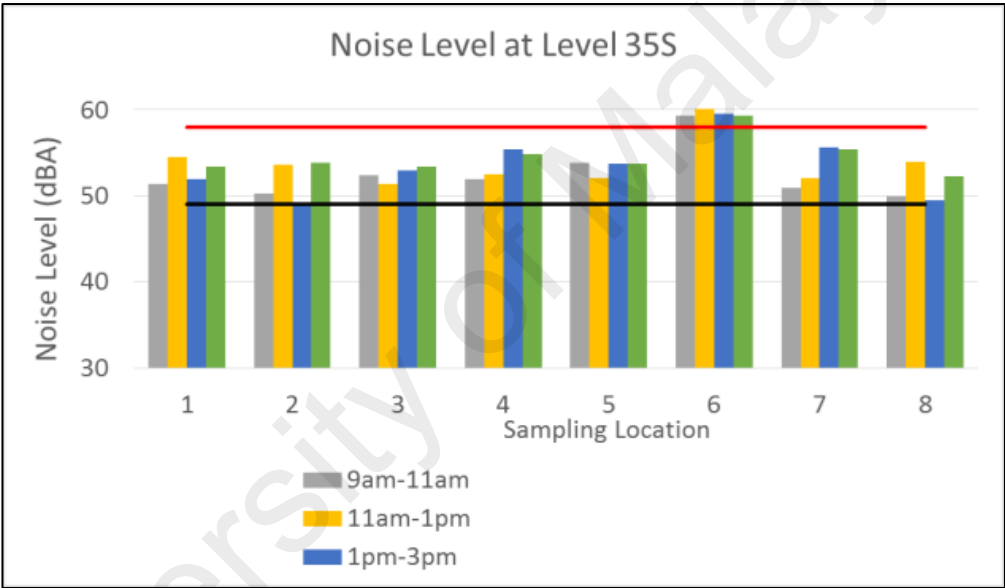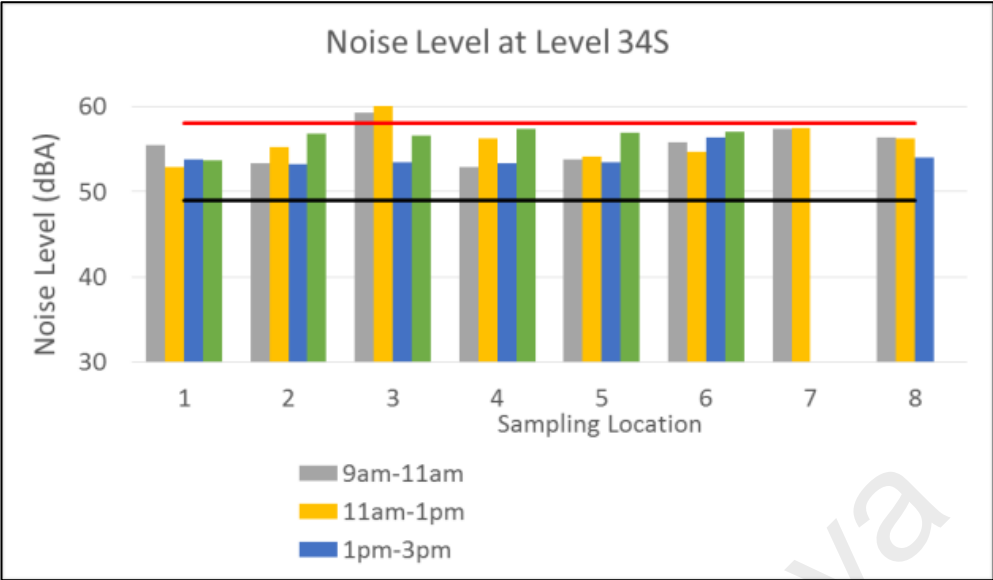
Figure 4.11: Noise level at each sampling location of the office spaces.

4.7   Visual Inspection

Figure 4.12 shows the under-floor condition of the UFAD system. From observations, the ground is clean and dry. There was no possible water leakage that would lead to poor indoor air quality. Conditions were good.

Figure 4.12: Under-floor condition.

Most of the floor diffusers were not equipped with the diffuser blade shown in Figure 4.13. It is noted that many diffuser blades were broken or missing. The diffuser blade attached below the grille is to distribute the airflow into the office space. Without the diffuser blades, the conditioned air directly flows into the office space like a jet air without distribution. Consequently, air stagnation is created at certain locations, and occupants will feel stuffy due to the lack of the air movement.

Figure 4.13: Missing, broken and the improper installation of the floor diffuser.

The conditions inside the AHU units were corroded and mold growth was serious as shown in Figure 4.14. These units are old and conditions were not well maintained. Besides, the chilled water actuator which functioned to regulate the chilled water flowrate is damaged. The temperature regulation is not functioning which caused the indoor air temperature to be low while the relative humidity exceeded the threshold limit.

Figure 4.14: The internal conditions of the AHU units.

4.8 Summary

An evaluation of the performance of the existing UFAD system in the tropics in the area of thermal environment and indoor air quality was successfully carried out. The causes of SBS after more than 10 years of the system's operation have been identified. The findings of the current work can serve as an important guide to ventilation design that must be considered when using the UFAD system in the tropics. The significant findings and strategies recommended are as follows:

- ➤ The high air velocity at each individual diffuser causes the air to flow into the office space vertically without spreading into the space to create air-mixing at the occupied zone. This was shown with a relatively low air velocity in the office space. The diffuser blades at each floor grille should be streamlined to follow the airflow pattern in the office space and to reduce the air stagnation. A further experimental investigation and simulation were performed in the following chapter to study the effectiveness of the floor swirl diffuser.

- ➤ Malfunctioning chilled water valve actuators cause the indoor air temperature to be over-cooled. This has contributed to a high indoor RH above 70%, which can be detected at most unoccupied areas, where the heat load is much less. It has promoted the infestation and the growth of mold in the offices in places such as carpet and return air grille. Note that mold growth is seen as a major SBS symptom that affects the health and well-being of occupants. The replacement of chilled water valve actuators is critical.

- ➤ CO_2 sensors and controls are recommended to be used to avoid human maneuver in switching off the fresh air supply. Besides, it will provide an optimum control of fresh air supply to reduce power wastage. Providing a constant fresh air supply can be energy consuming.

- It is suggested that smoke spill fans, which are available within the office spaces, should be applied to replace indoor air with the outdoor air during the off-hours. The air flushing procedure is recommended during warm and dry weather to avoid introduction of humid outdoor air. Relative humidity should be observed during and after the procedure. HVAC systems should be turned off during the air flushing as a higher temperature can effectively enhance the formaldehyde emission and remove it from the office space.

- IAQ management plan shall be established and implemented. As part of the plan, the practice to conduct IAQ assessment once in every three years is recommended to ensure the health and well-being of the occupants are safeguarded.

- The maintenance team has a crucial role to ensure the indoor air quality is maintained up to the required standard. A scheduled checking and maintenance work should be in place, so that HVAC&R systems can function based on the intended designs.

CHAPTER 5 – AN INVESTIGATION OF THE AIRFLOW PATTERN OF FLOOR SWIRL DIFFUSER

5.1 Overview

In the previous chapter, it was observed that floor diffusers play an important role on the airflow patterns of the rooms. Air velocity, grille design, diffuser blades are important parameters that will influence the air movement. Thus, the geometrical design of floor swirl diffuser is further examine in this chapter.

UFAD diffusers are used to deliver conditioned air from the floor plenum to the occupants' space for human comfort in UFAD system. Generally, UFAD diffusers are categorized into six types: round omnidirectional diffusers, selective directional diffusers, displacement flow diffusers, linear diffusers, ducted diffusers and terminal units (ASHRAE, 2013d). Despite the fact that there are various UFAD diffusers available in the market since the emerging of this air distribution technology in 1990s, there is limited research work studied on the geometry of the UFAD diffusers.

It is known that a well-designed UFAD system can reduce energy consumption, reduce floor to floor height, improve thermal comfort, improve ventilation efficiency and provide flexibility in reconfiguring the interior layout of the building (Bauman and Webster, 2001). One of the most crucial factors that influence the thermal comfort and ventilation efficiency of the indoor environment is the geometry of the UFAD diffusers.

Y. J. P. Lin and Tsai (2014) found that supply airflow rate has a strong connection with the supply air momentum flux and thus affects the gradient of the vertical temperature profiles of the indoor environment. The study describes the throw height as the level where the temperature at the supply air outlet area is equal to the temperature of

that height in the other area. Results show that a higher airflow rate will produces a lower thermal stratification.

Schiavon et al. (2014) studied thermal stratification in perimeter zones using linear bar grilles and VAV directional diffusers. Their study describes the relationship between the non-dimensional parameter, Γ, and the dimensionless temperature ratio, Φ, of the diffusers. Gamma, Γ, is the ratio of buoyancy forces to the vertical momentum forces, while phi, Φ, is the dimensionless temperature at a specific height in the room. The results showed that thermal stratification by using VAV directional diffusers is generally higher than linear bar grilles. However, the thermal stratification of UFAD diffusers is generally lower compared to displacement ventilation (DV) system. Thus, it is suggested that the ventilation performance of a UFAD system can be comparable to a DV system when a large number of diffusers are used. The diffusers with lower airflow rate will have a lower throw height and produce less mixing. Raftery et al. (2015) studied the least commonly used floor DV diffusers which delivers air mostly with horizontal air momentum. The thermal stratification based on the dimensionless temperature ratio, Φ, showed that the floor DV diffuser produce a comparable results to the DV system.

ASHRAE Standard 62.1 awards the highest ventilation effectiveness of 1.2 to the UFAD system that achieves thermal stratification (ASHRAE, 2013b). Thermal stratification can be achieved by having low-velocity unidirectional airflow with vertical thermal stratification or airflow vertical throw of less than or equal to $0.25\,\text{ms}^{-1}$ at the height of 1.4 m above the floor. The ventilation effectiveness of UFAD system will be downgraded to 1.0 if the system does not achieves thermal stratification nor the required air throw, and thus the performance will be similar to conventional overhead air distribution (OHAD) system.

However, there is little information about the airflow pattern due to the geometry of the UFAD diffuser. The objective of this study is to investigate the performance of the floor swirl diffuser through various aspects such as the airflow rate, number of diffuser blades, angle of attack of diffuser blades and grille thickness. A widely used 250 mm nominal diameter floor swirl diffuser was selected in this study. The study was mainly conducted in CFD simulation with experimental work carried out for data comparison and validation. This study will provide some guidelines to the building design engineers and the air terminal design engineers about the geometry of floor swirl diffuser design that will impact the indoor airflow pattern of the environment.

5.2 Assumptions

1. The testing laboratory had achieved steady state condition after 5 hours of fan operation since the temperature differences between room surfaces dropped below 0.1°C.

2. The study is assumed to be in isothermal condition since the heat generated from two T-5 fluorescent light is far from the airflow pattern studied. The temperature difference between supply air, return air and average room temperature fell within 1°C.

5.3 Experimental Measurement

The experimental work was carried out in the air terminal testing laboratory in Prudentaire Marketing Sdn Bhd. The laboratory was located inside a building with all the walls, ceiling and floor exposed to ambient room temperature. Thus, the indoor environment was controllable. The purpose of this experiment was to validate the CFD simulation in

studying various geometrical designs that will affect the airflow pattern of floor swirl diffuser.

The experimental setup for the testing of floor swirl diffuser is shown in Figure 5.1. A single inlet centrifugal fan with airfoil wheels running by a 3-phase induction motor was used to supply air to the diffuser. The fan was installed with variable speed drive (VSD) to control the airflow rate by motor frequency. The fan capacity was substantially larger compared to the testing required airflow rate of a unit of floor swirl diffuser. Hence, a variable air volume (VAV) system with actuator and damper was used to further regulate the airflow rate to the testing requirement. A smoke inlet was available at the flexible duct to conduct the smoke tests. The smoke generator and set up for smoke test is shown in Figure 5.2. The smoke was supplied into the ducting system after the VAV control. The schematic diagram of the experimental setup in the laboratory is shown in Figure 5.3. The air was supplied from the outer room into the laboratory using the centrifugal fan while the return air exited the laboratory through the return opening.

Boundary conditions of the laboratory were measured prior to the testing conducted. The surface temperature of the walls, ceiling and floor was measured by taping the sensors of the Center 309 K-type thermocouple on the surfaces using reflective aluminum tape. The average room temperature was measured by swinging a Alnor Model 440-A hot-wired anemometer at the reference point in the lab. After the fan was operated to deliver a constant airflow of 290 CMH with a fluctuation of less than 10%, measurements were taken every one hour. The steady-state condition was achieved at the 5th hour of fan operation as the supply air temperature, average room air temperature and return air temperature did not vary more than 1°C (ASHRAE, 2013c). The hourly temperature difference of the room surface temperatures also dropped below 0.1°C after

5 hours. The measurements recorded are shown in Table 5.1. The only heat source in the testing laboratory was the two T-5 fluorescent lights. However, they were excluded from numerical modeling due to the fact that the heat generated was insubstantial (Yau and Ding, 2014) and the lighting was located at the top corner of the lab. Thus, the heat generated did not affect the diffuser's airflow pattern which comes from the floor level. Hence, the case can be assumed to be in isothermal condition.

Figure 5.1: Experimental setup for the testing of floor swirl diffuser in laboratory. (Top: floor diffuser installed on the floor plenum with measuring tools, bottom left: supply air VSD fan, bottom right: VAV actuator and damper for airflow rate control).
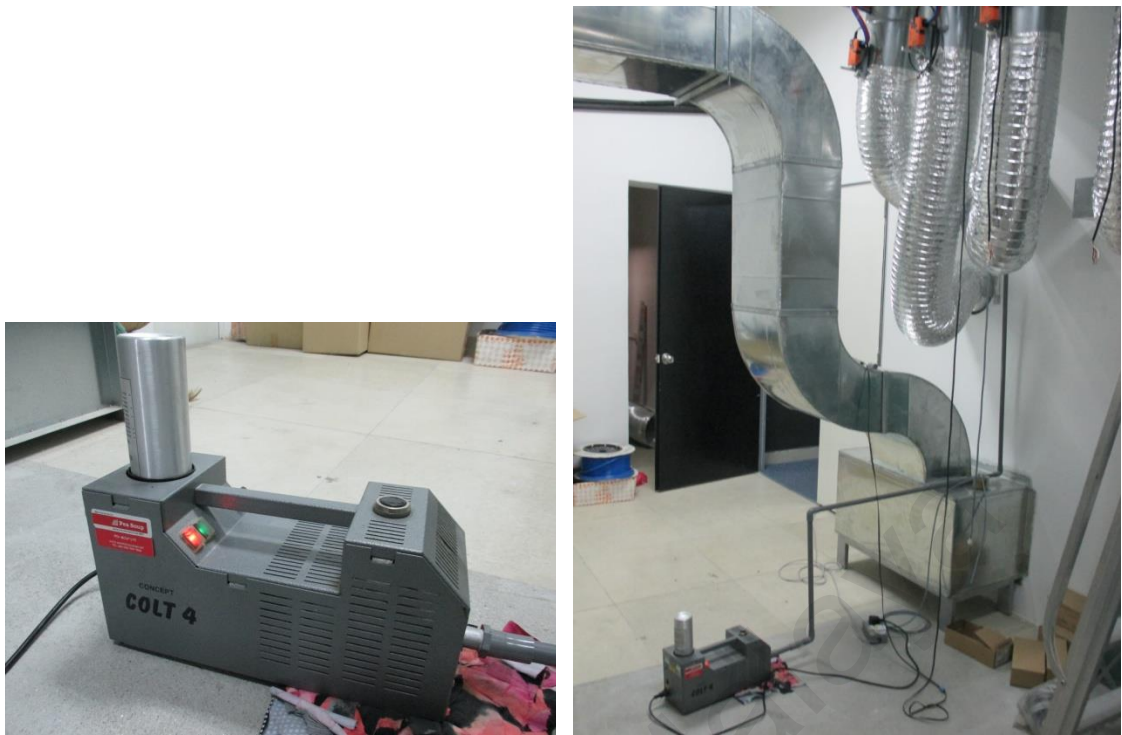
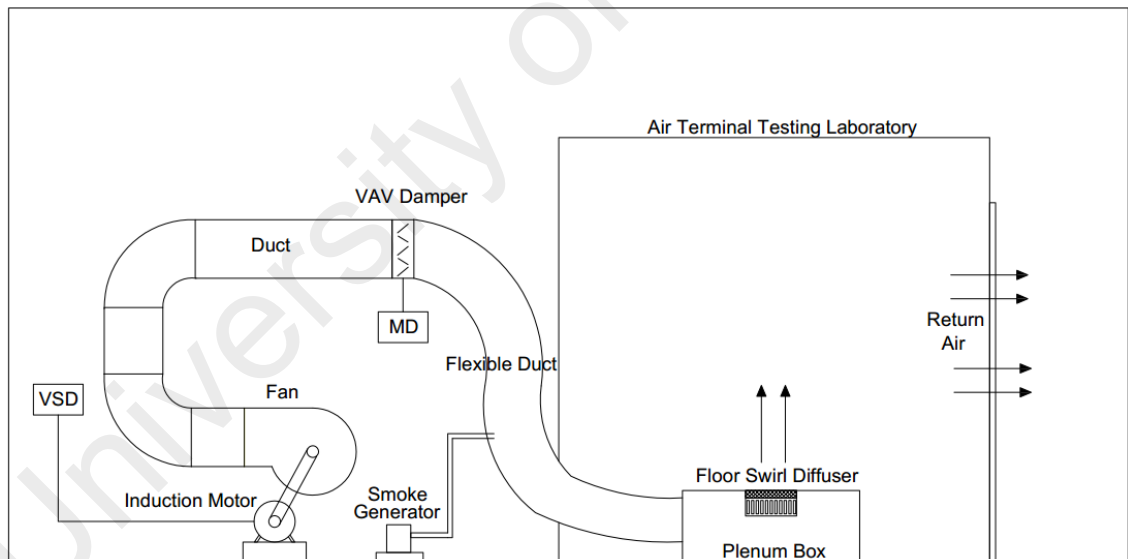Figure 5.2: Smoke generator (left) and the setup for smoke test (right).

Figure 5.3: Schematic diagram of the experimental setup in the laboratory.

Table 5.1: Laboratory air and surface temperature measurement.

Hour	1st	2nd	3rd	4th	5th
Supply air temperature (°C)	28.8	30.0	30.6	31.1	30.9
Return air temperature (°C)	28.6	29.4	30.2	30.2	30.3
Room air temperature (°C)	28.0	29.0	29.5	29.8	29.9
Wall 1 surface temperature (°C)	29.2	29.3	30.0	30.2	30.2
Wall 2 surface temperature (°C)	29.0	29.3	29.9	30.2	30.1
Wall 3 surface temperature (°C)	28.9	28.9	29.1	29.3	29.4
Wall 4 surface temperature (°C)	28.4	28.4	29.0	29.1	29.2
Ceiling surface temperature (°C)	29.5	29.5	30.3	30.7	30.7
Floor surface temperature (°C)	28.6	28.5	29.0	29.4	29.3

The diffuser was installed on the H 420 mm x W 800 mm x D 800 mm plenum box as shown in Figure 5.1. The centerline air velocity, air temperature and relative humidity were recorded every 10 seconds for a period of 2 minutes (Zhang et al., 2014a). Measurements were taken at an incremental height of 100 mm above the diffuser up to 2000 mm. The average data recorded is shown in Table 5.2 while the raw data collected is shown in Appendix D.

Table 5.2: Experimental measurement of the average temperature, relative humidity and air velocity above floor swirl diffuser at 290 CMH.

Height (m)	Average		
	Temperature (°C)	**Relative Humidity (%)**	**Air Velocity (ms⁻¹)**
0.1	30.90	53.75	0.24
0.2	30.83	53.81	0.21
0.3	30.80	53.95	0.25
0.4	30.64	54.33	0.29

0.5	30.54	54.65	0.33
0.6	30.40	54.93	0.45
0.7	30.33	55.23	0.44
0.8	30.27	55.48	0.48
0.9	30.20	55.73	0.48
1.0	30.20	55.86	0.48
1.1	30.26	55.78	0.50
1.2	30.10	56.41	0.46
1.3	30.10	56.74	0.48
1.4	30.10	57.09	0.47
1.5	30.00	57.36	0.44
1.6	30.23	57.04	0.41
1.7	30.07	57.47	0.41
1.8	30.00	57.81	0.37
1.9	30.00	58.05	0.34
2.0	30.00	58.55	0.29

5.4   CFD Simulation

5.4.1   Mesh Independence Study

Seven unstructured tetrahedral meshing with different mesh elements were performed on the model in relation to the relevance center in ANSYS meshing to study the mesh independency of the results. The details of the mesh elements are shown in Table 5.3. Typically in mesh independence studies, the meshing increment step is 1.5 times from the coarser mesh. However, this increment step is not viable when the mesh element exceeds 3×10^6 cells. The computational time is costly. Hence, a low incremental step of up to 1.24 times was used in fine mesh setting to produce more than 5×10^6 cells. A higher increment step of up to 2.58 times was used in coarse mesh to reduce the number

of analyzing models in this study. The computer used to run the simulation was incorporated with Intel core i7-4510U CPU @ 2.00GHz processor, 8.00GB RAM and 64-bit Window 10 Pro operating system. Due to the limited computational power available, the mesh was studied from coarse mesh of about 200,000 cells until the room temperature difference of two consecutive mesh elements dropped below 0.01°C.

Figure 5.4 shows that the room mean temperature was consistent for mesh V, VI and VII. Further analysis was conducted to compare the center plane velocity profiles of the three meshes. Figure 5.5 and 5.6 show the comparison between mesh V & VI, and mesh VI & VII respectively. The plane velocity profile is almost identical for the case in mesh VI &VII. Thus, the model can be considered to be mesh independence at mesh VI.

Table 5.3: The unstructured tetrahedral mesh in mesh independence study.

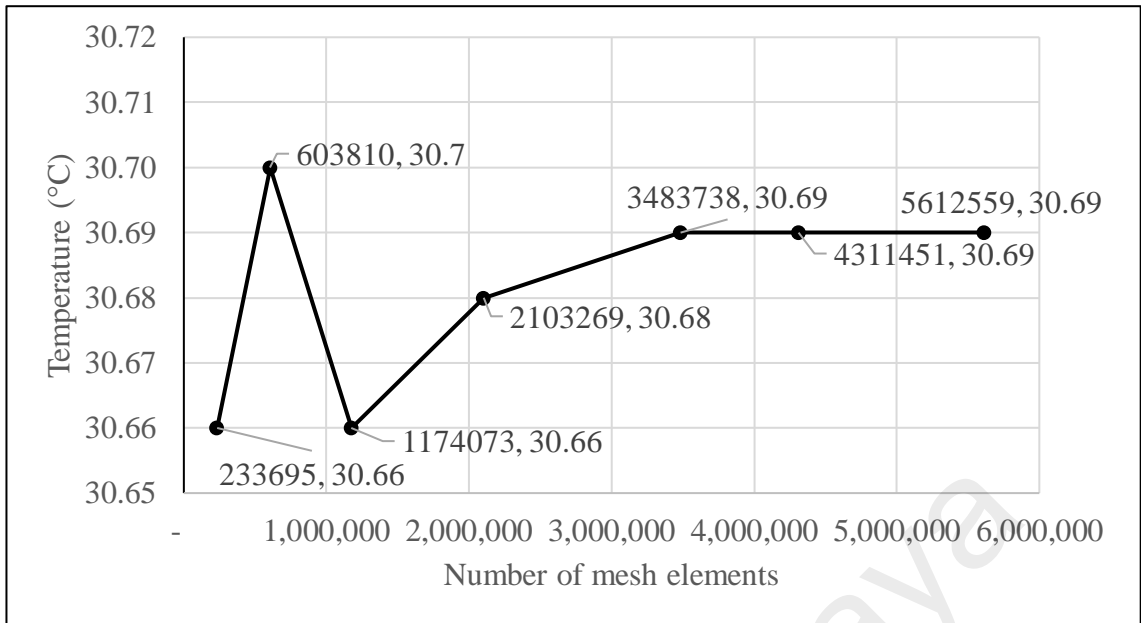| Mesh	Relevance center	Mesh element	Nodes	Increment step
I	Coarse	233,695	43,646	2.58
II	Medium	603,810	111,606	
				1.94
III	Fine, Relevance 0	1,174,073	217,359	
				1.79
IV	Fine, Relevance 50	2,103,269	382,442	
				1.66
V	Fine, Relevance 80	3,483,738	623,420	
				1.24
VI	Fine, Relevance 90	4,311,451	766,523	
				1.30
VII	Fine, Relevance 100	5,612,559	990,285	

Figure 5.4: Room mean temperature at different mesh elements.
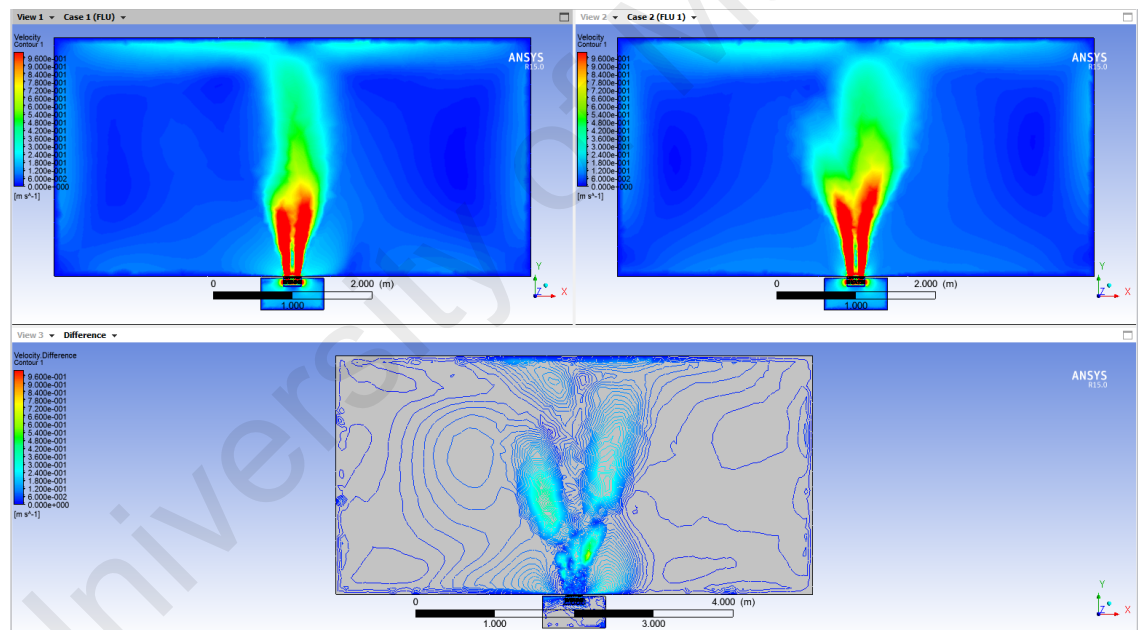

Figure 5.5: Plane air velocity for Mesh V (top left), plane air velocity for Mesh VI (top right) and air velocity differences between Mesh V and VI (bottom).
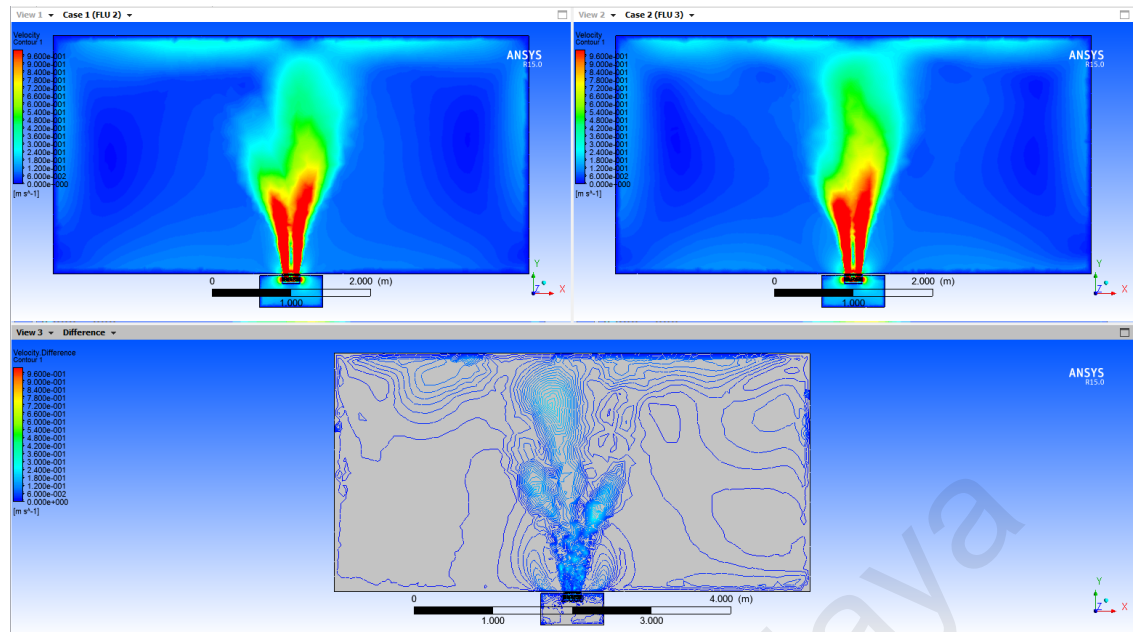
Figure 5.6: Plane air velocity for Mesh VI (top left), plane air velocity for Mesh VII (top right) and air velocity differences between Mesh VI and VII (bottom).

5.4.2   Data Verification

CFD investigation of diffuser airflow pattern was problematic due to the complex geometry of the diffuser, and because the size of the diffuser was relatively small compared to the room dimensions. A correct turbulence model is crucial to accurately predict the turbulent airflow pattern and the heat transfer between the inflow and the room. Hence, data comparison and verification are important to ensure that the numerical modeling could best represent the physical model.

The standard k-ε turbulence model has been widely used for diffusers' airflow prediction in OHAD systems such as round diffusers, square diffusers and swirl diffusers (Aziz et al., 2012; Hu, 2003; Sajadi et al., 2011). In this study, standard k-ε, RNG k-ε, and realization k-ε were compared with the experimental measured data. The plane airflow pattern was then compared with the smoke test data to find the most suitable turbulence model for this investigation.

For comparison and verification purposes, centerline air velocity was extracted from the simulation to compare with the experimental measurement. Figure 5.7 shows the vertical centerline air velocity profiles of the measured and the predicted data for various turbulence models. No perfect agreement between the measured and predicted data was expected. However, both the standard and RNG k-ε model showed a similar centerline air velocity pattern to the measured data. In fact, the RNG k-ε model had a closer prediction to the measured data at the location near to the floor swirl diffuser outlet. There was a drop at around $y/H = 0.20$ and a spike at around $y/H = 0.40$ in all turbulence models. This fluctuation was observed mainly due to the swirl mechanism that causes difficulty measuring turbulence flow using the existing tools (hot-wire anemometer). Hence, the predicted models are acceptable.
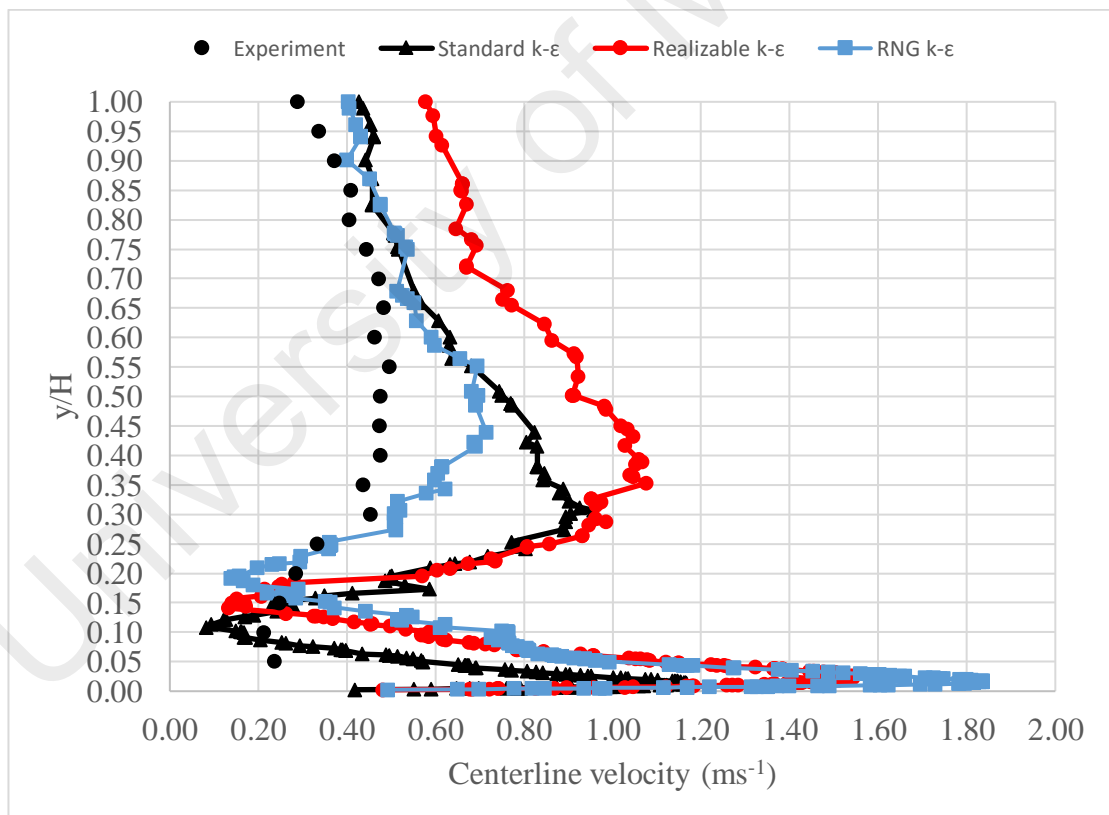
Figure 5.7: Vertical centerline air velocity profile of actual model and predicted various turbulence models.

Figures 5.8 – 5.13 show the plane air velocity profiles and streamline air velocity profiles for standard, RNG and realizable k-ε turbulence model. When compared to the

photos taken during the smoke test as shown in Figure 5.14, standard k-ε turbulence model showed the closest match to the actual airflow pattern. Hence, standard k-ε turbulence model was safely used for this floor swirl diffuser model investigation.
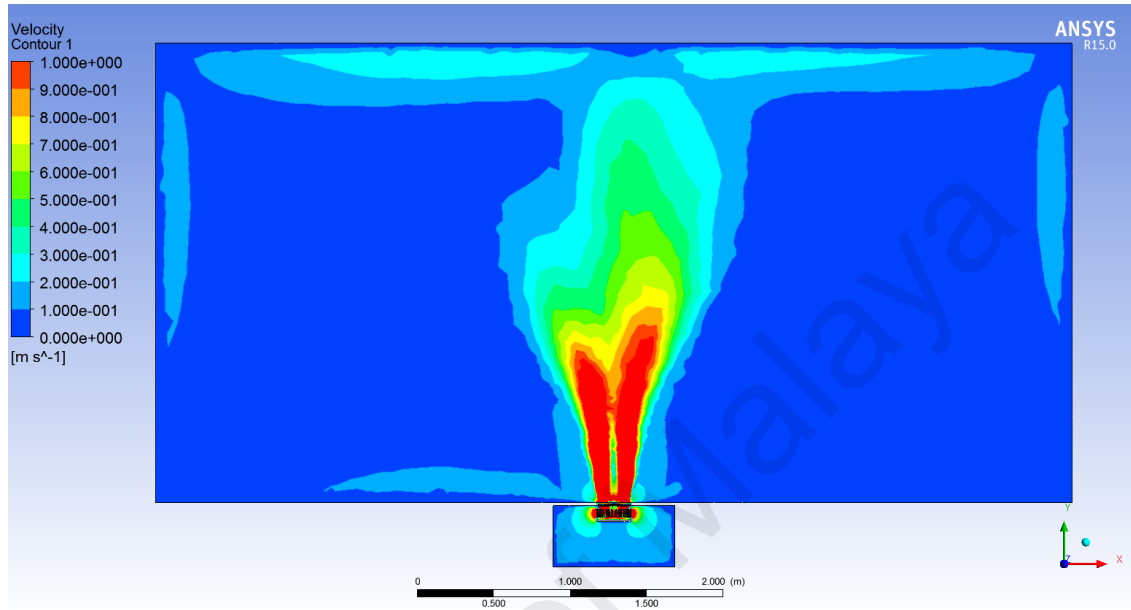
Figure 5.8: Plane air velocity profile for standard k-ε turbulence model.

Figure 5.9: Streamline air velocity profile for standard k-ε turbulence model.
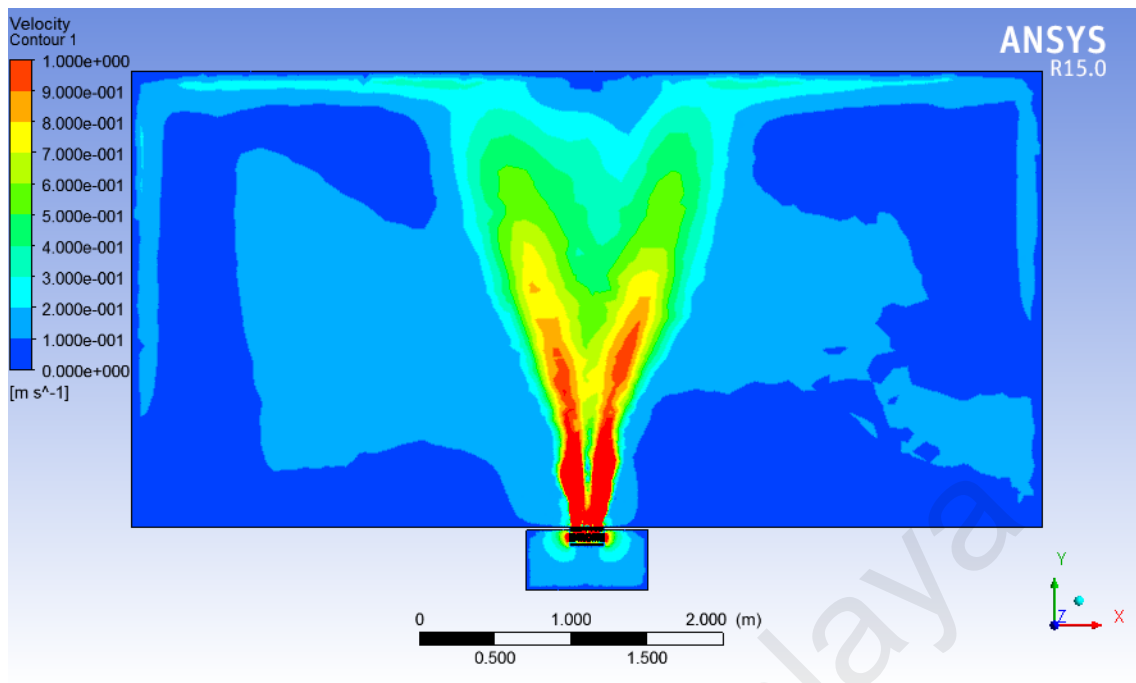
Figure 5.10: Plane air velocity profile for RNG k-ε turbulence model.
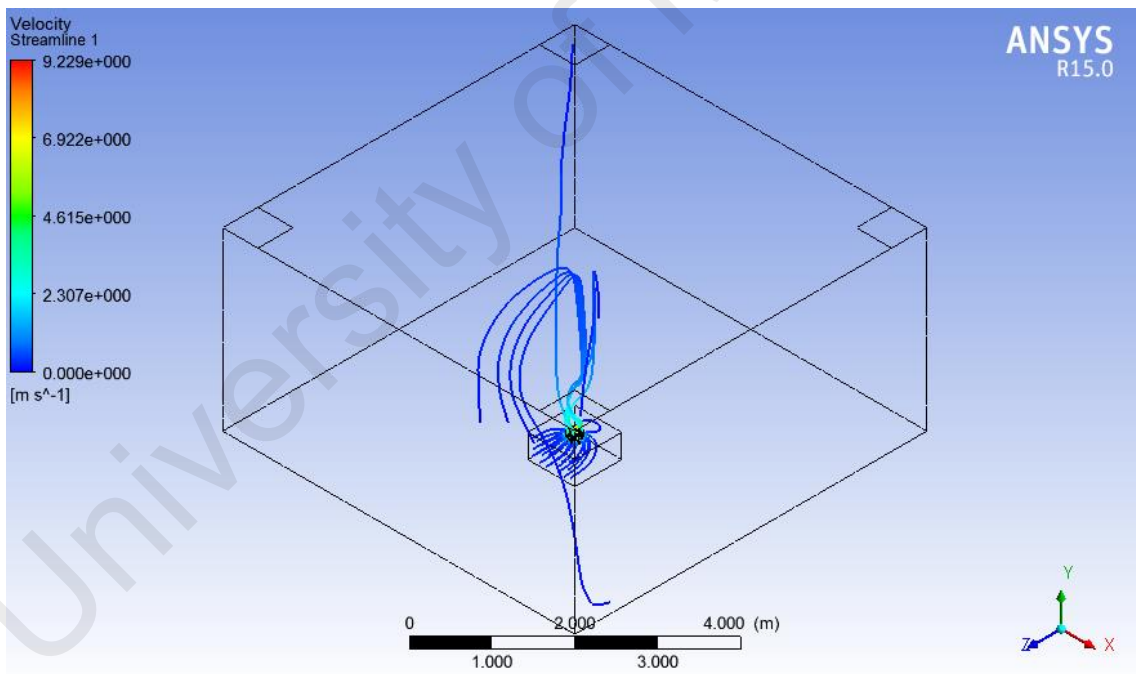
Figure 5.11: Streamline air velocity profile for RNG k-ε turbulence model.
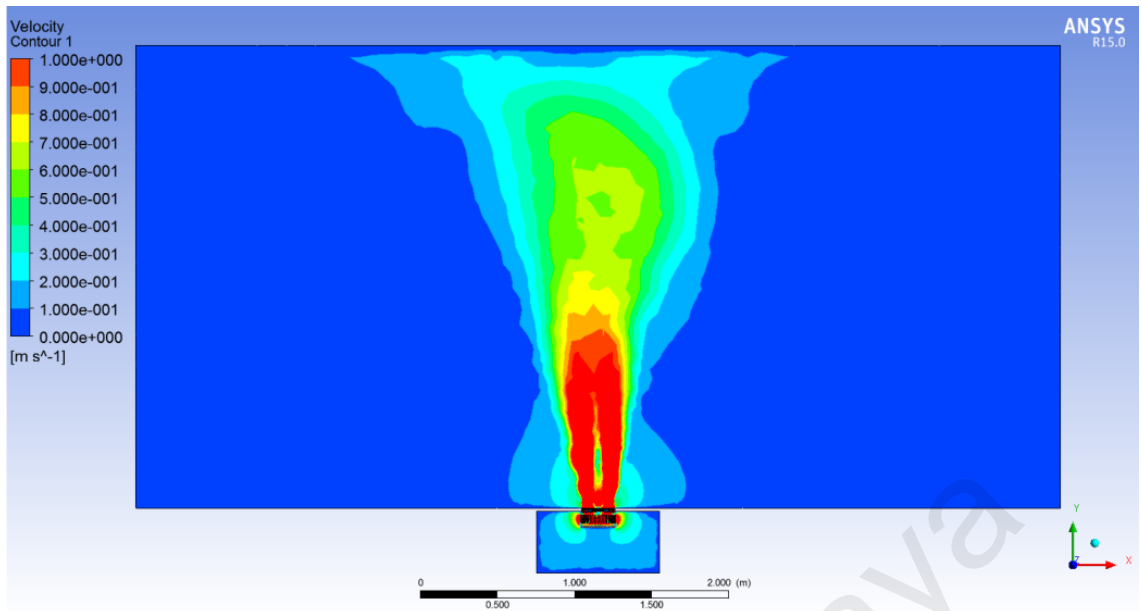
Figure 5.12: Plane air velocity profile for realizable k-ε turbulence model.
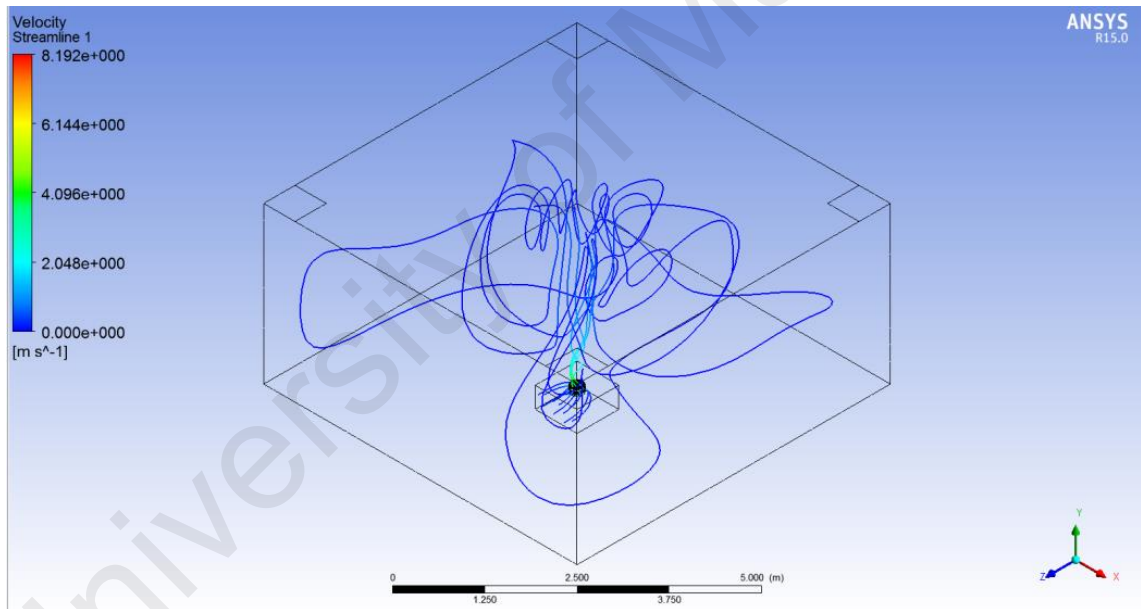
Figure 5.13: Streamline air velocity profile for realizable k-ε turbulence model.

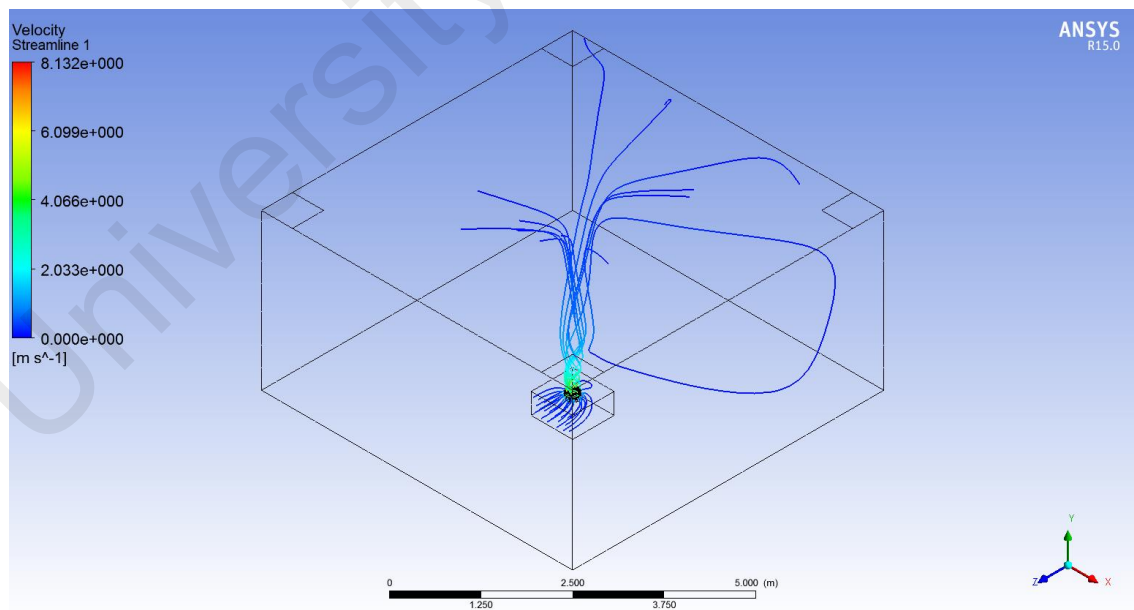| (a) | (b) | (c) | (d) |
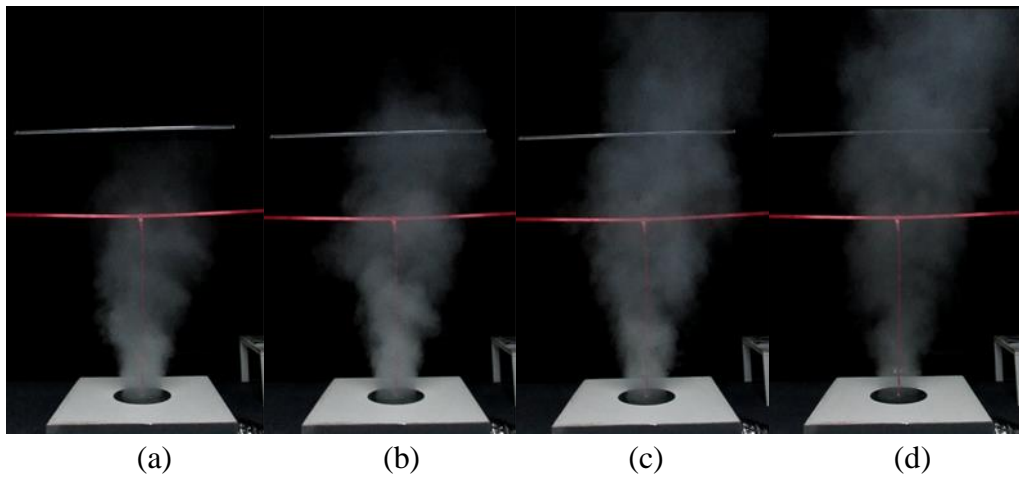
Figure 5.14: Photo snapped during the smoke test at (a) 10 seconds, (b) 11 seconds, (c) 13 seconds and (d) 14 seconds.

5.4.3   Numerical Modeling

The numerical study was conducted to study the airflow pattern of various floor swirl diffuser designs. The floor swirl diffuser and the room were developed using SolidWorks 2012 software and imported into Design Modeler in ANSYS Workbench 15.0. The floor swirl diffuser was then subtracted from the volume of the room to remain with the fluid domain. The boundary surfaces of the fluid domain were then defined.

The ANSYS meshing program was used to mesh the fluid domain and simulated using FLUENT software. The setup of the boundary conditions from Mohammed (2013) is referred. The boundary conditions and the setting of the FLUENT numerical solver are shown in Table 5.4 and 5.5.

Table 5.4: Boundary conditions of the CFD simulation.

Boundary	Details
Supply air inlet	Airflow rate = 100, 195, 290 CMH Air temperature = 18°C Relative humidity = 60%
Exhaust air outlet	4 numbers of 600 x 600 mm ceiling exhaust air outlet at 0 Pa gauge pressure
Walls	Surface temperature = 28.5°C
Ceiling	Surface temperature = 27°C
Floor	Surface temperature = 27°C
Grille	Adiabatic
Air plenum	Adiabatic

Table 5.5: Numerical solver setting of the CFD simulation.

Category	Details
Mesh elements	Approximately 4×10^6 tetrahedral mesh elements
Solver	Pressure based velocity formulation and steady state
Model	Heat transfer calculation is included in energy equation. Viscous model = Standard k-ε Near wall treatment = Standard wall functions Constants: C_{mu} = 0.09, $C_{1\varepsilon}$ = 1.44, $C_{2\varepsilon}$ = 1.92, TKE Prandtl number = 1, TDR Prandtl number = 1.3, Energy Prandtl number = 0.85, Wall Prandtl number = 0.85
Air properties at temperature of 18°C and RH of 60%	Density, ρ = 1.2073 kg/m^3 Specific heat, C_p = 1005 J/kg.K Thermal conductivity, k = 0.02624 W/m.K Viscosity, v = 1.846 x 10^{-5} kg/m.s
Solution methods	Scheme: SIMPLE Gradient: Least squares cell based Pressure: Second order Momentum: Second order upwind

	Turbulent kinetic energy: Second order upwind
	Turbulent dissipation rate: Second order upwind
	Energy: Second order upwind
Solution controls	*Under-Relaxation Factors (default)*
	Pressure = 0.3
	Density = 1
	Body Forces = 1
	Momentum = 0.7
	Turbulent Kinetic Energy = 0.8
	Turbulent Dissipation Rate = 0.8
	Turbulent Viscosity = 1
	Energy = 1
Convergence criteria	Continuity, x-velocity, y-velocity, z-velocity, k, $\varepsilon = 1 \times 10^{-3}$
	Energy = 1×10^{-6}

The fluid domain in the room was meshed in unstructured tetrahedral elements as shown in Figure 5.15. The wall was not inflated in layers because the diffuser tested was in the middle of the room. Air movement was minimal near the wall. The air velocity decreased more than 4 times from the inlet to the 4 exhausts located at each corner of the room.
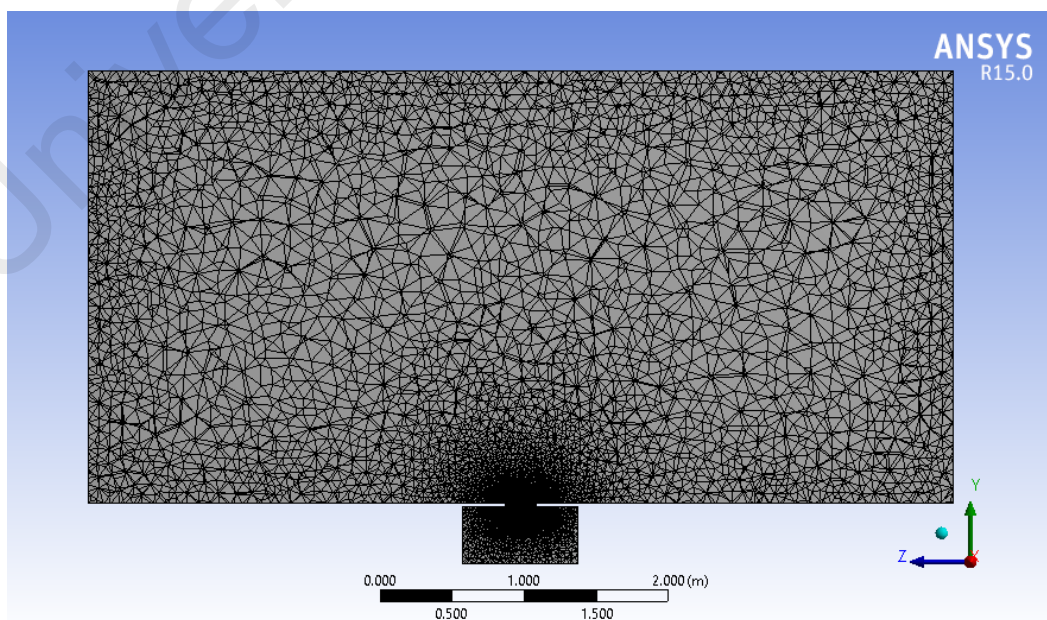
Figure 5.15: Section view of the mesh elements for the 290 CMH airflow case simulation at fine mesh relevance center of 90.

5.4.4 The Effect of Airflow Rates

This study was conducted with an airflow rate of 100, 195 and 290 cubic meter per hour (CMH), which is the lowest to the highest recommended airflow rates used for a 250 mm nominal diameter floor swirl diffuser. As indicated by Y. J. P. Lin and Tsai (2014), the airflow rate has a strong influence on vertical temperature profiles where higher airflow rate lowers the thermal stratification. For the purpose of understanding the thermal stratification of the UFAD system in terms of vertical velocity profiles, a comparison on the centerline air velocity is reported in Figure 5.16.
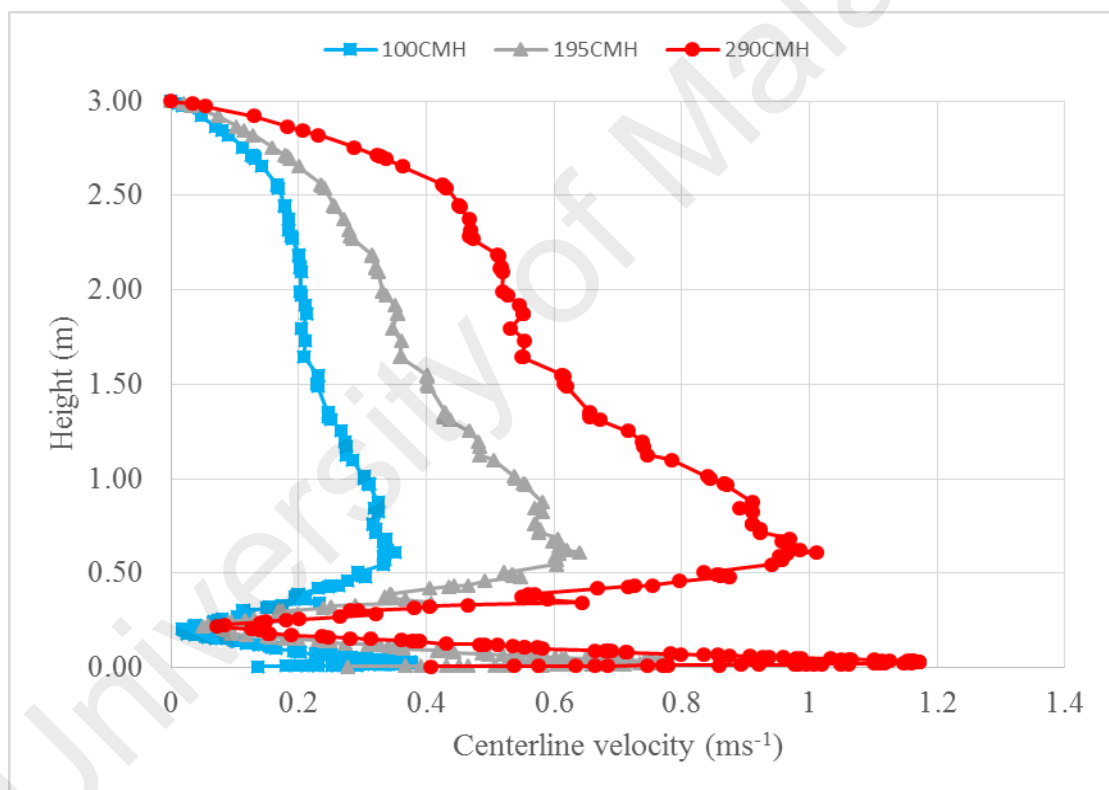
Figure 5.16: The centerline vertical air velocity profiles for airflow rate of 100, 195 and 290 CMH.

The characteristics of a pure jet are defined by thermal length scale, which is significant for thermal stratification. In UFAD systems where heat load is consistent, thermal stratification depends highly on the velocity of the supply air. The thermal length scale is defined as below (Arghand et al., 2015; Zhang et al., 2014a):

$$l_m = \frac{M_0^{3/4}}{B_0^{1/2}}$$

$$M_0 = Q_0 . u_0$$

$$B_0 = \frac{g . Q_0 . \Delta T_0}{T_r}$$

where l_m is the thermal length scale, M is the momentum flux, B is the buoyancy flux, Q is the volume flux, u is the supply air velocity, g is the gravitational acceleration, ΔT is the temperature difference between supply air of the diffuser and the room temperature and T_r is the reference air temperature.

For the case of 100 CMH, a terminal velocity of 0.25 ms^{-1} was reached at around 1.3 m above the floor swirl diffuser. It was the only case that achieved the requirement to receive the highest ventilation effectiveness of 1.2 according to ASHRAE Standard 62.1 (ASHRAE, 2013b). The terminal velocity for 195 CMH and 290 CMH was around 2.4 m and 2.8 m respectively. Due to the importance of supply air velocity towards thermal stratification as described earlier, it should be noted that the supply air velocity for the three cases were 1.73 ms^{-1}, 3.38 ms^{-1} and 5.03 ms^{-1} respectively.

Although the airflow rate of 100 CMH achieves a higher ventilation effectiveness, Figure 5.18 shows that the airflow rate was insufficient in reducing the temperature of the environment as effectively as airflow rates of 195 CMH and 290 CMH in Figure 5.20 and 5.22 respectively, where the surrounding space had a lower temperature around 298 K (25°C). Besides, the two cases with higher airflow rate create a greater air mixing in the area surrounding the diffuser's discharge outlet. The air movement is about 0.1 ms^{-1} which is slightly below the recommended air movement by Malaysian Standard (0.15 – 0.5 ms^{-1} for offices) (Department of Standards Malaysia, 2014). The plane air velocity profiles for 100, 195 and 290 CMH are shown in Figure 5.17, 5.19 and 5.21 respectively.

Figure 5.17: The plane air velocity profiles for airflow rate of 100 CMH.

Figure 5.18: The plane air temperature profiles for airflow rate of 100 CMH.
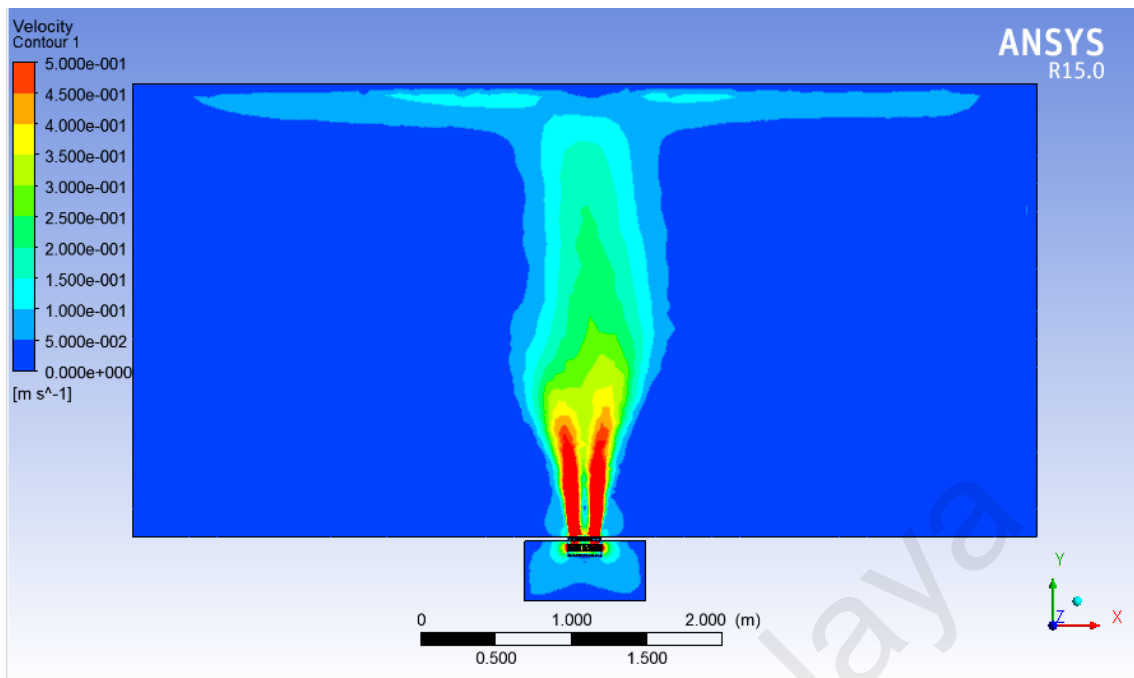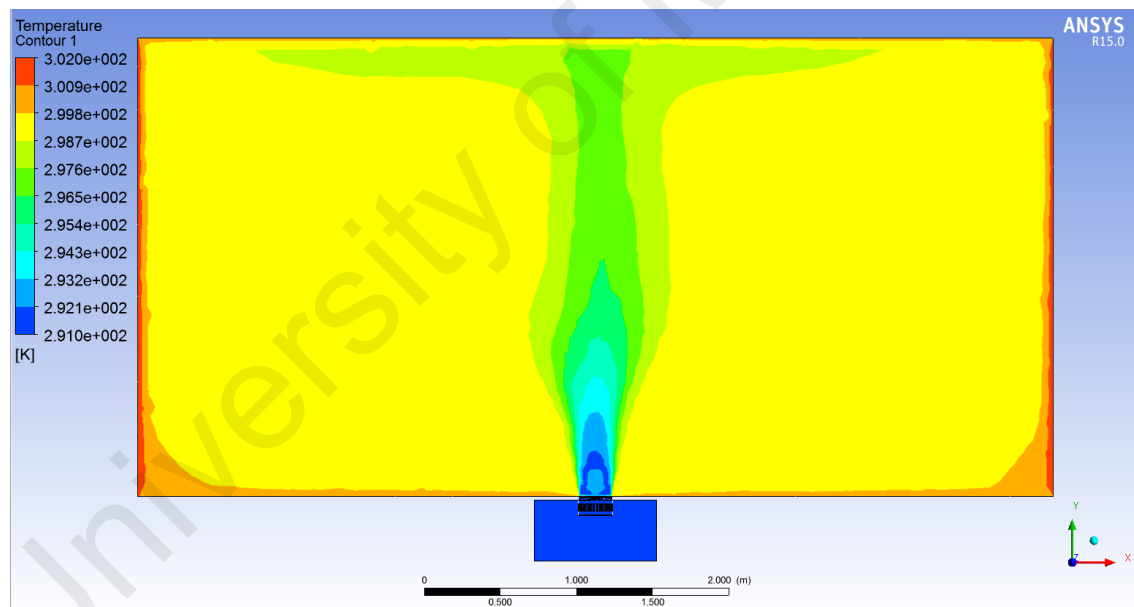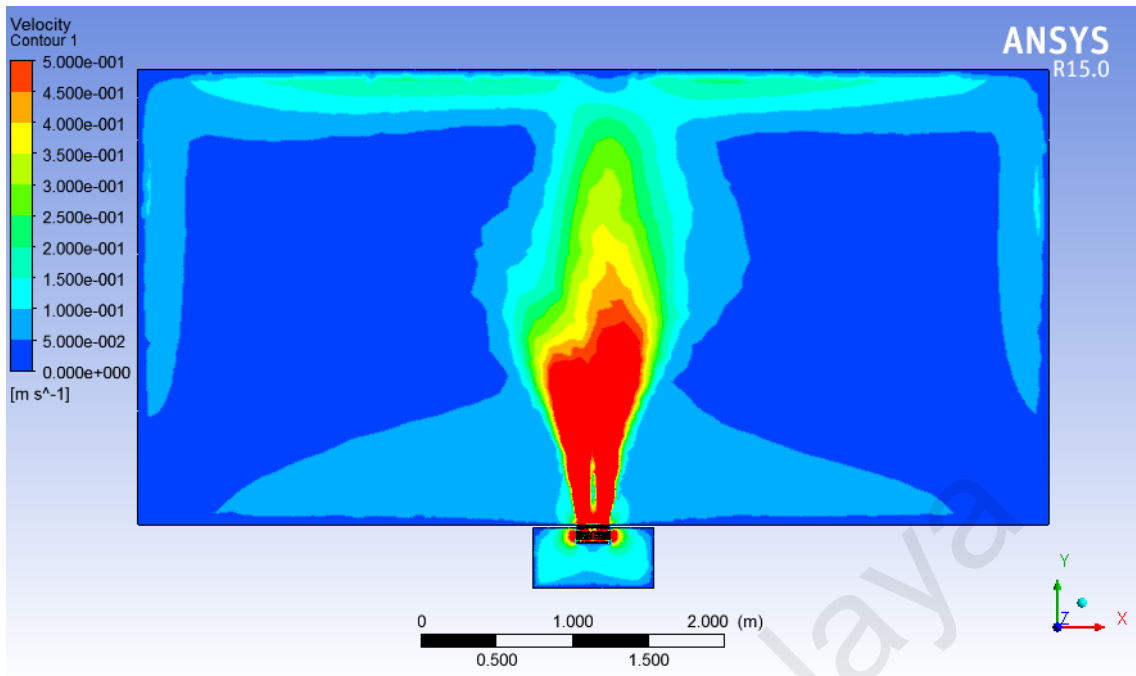
Figure 5.19: The plane air velocity profiles for airflow rate of 195 CMH.
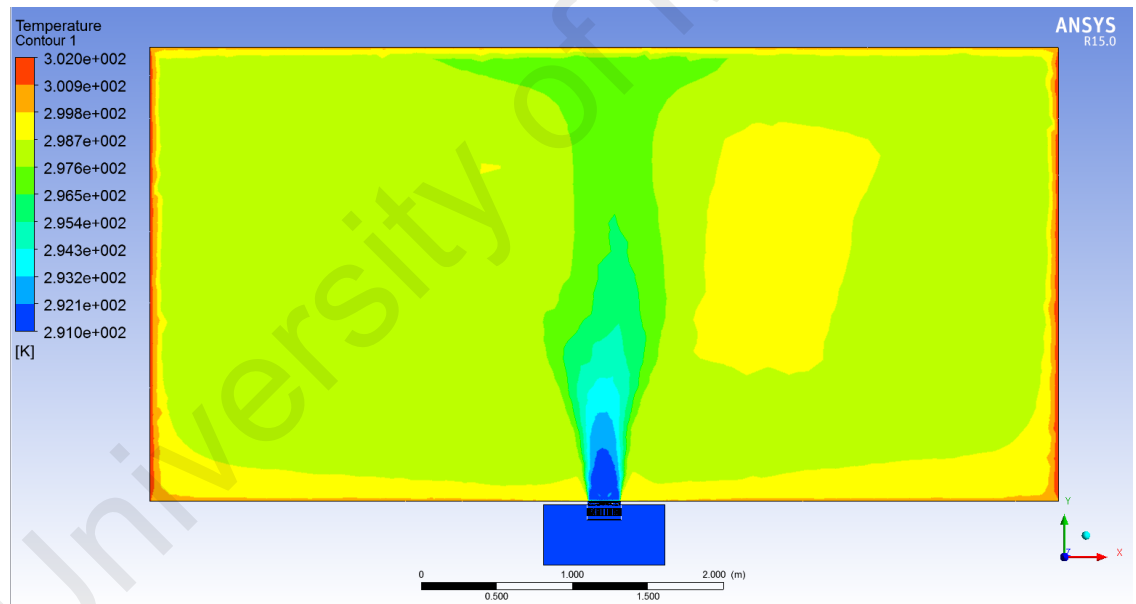
Figure 5.20: The plane air temperature profiles for airflow rate of 195 CMH.
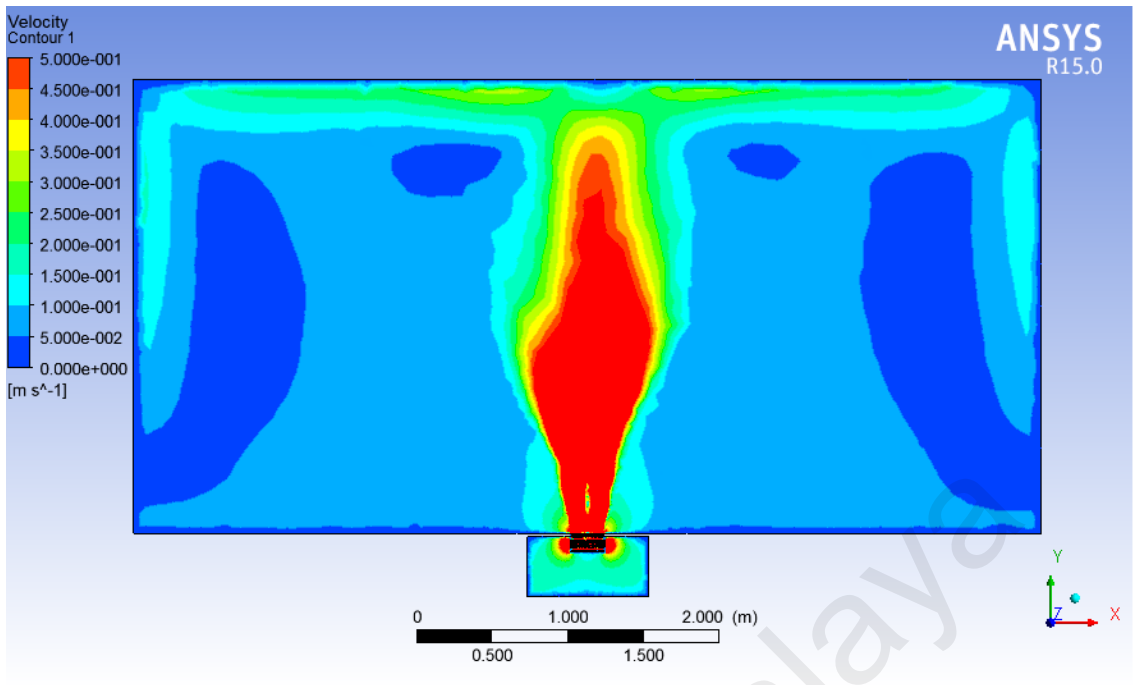
Figure 5.21: The plane air velocity profiles for airflow rate of 290 CMH.
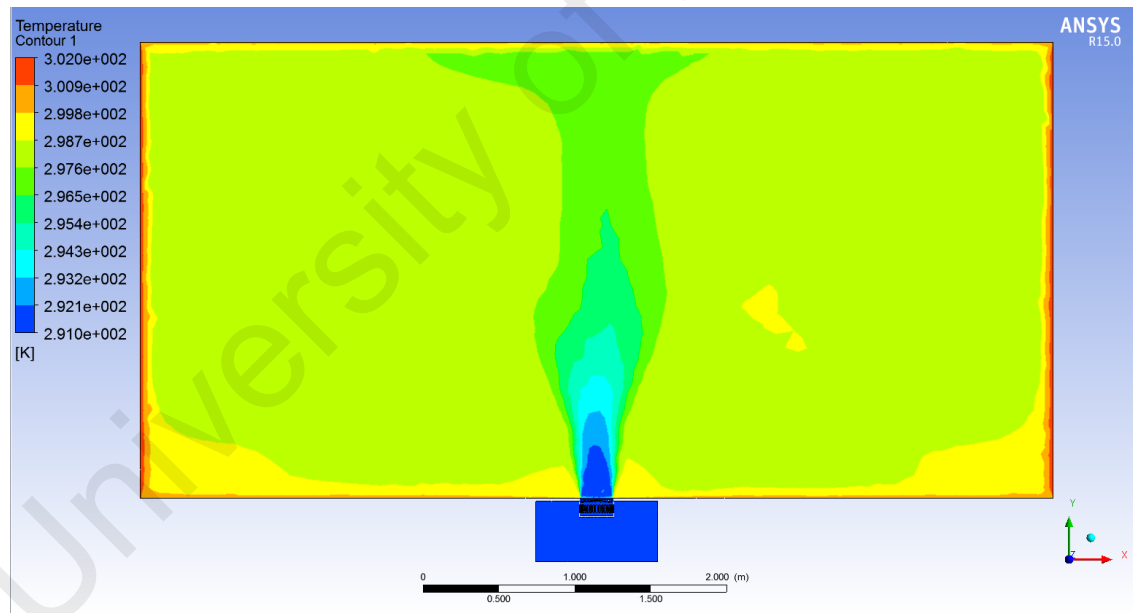
Figure 5.22: The plane air temperature profiles for airflow rate of 290 CMH.

5.4.5   The Effect of the Number of Diffuser Blades

This study examined the effect of the number of diffuser blades on the airflow pattern of the floor swirl diffuser. Diffusers with 12, 18 and 24 blades, as shown in Figure 5.23, were simulated separately at the same condition of 195 CMH. The 18 blade diffuser is used by various air terminal manufacturers. The percentage of the free area for 12, 18 and 24 blades is 43.27%, 18.86% and 5.51% respectively. The blade used in the study had a curvature profile adopted from the upper surface of airfoil NACA 0012 to enhance the aerodynamic airflow. The maximum air velocity that discharged from the under-floor swirl diffuser for 12, 18 and 24 blades were 3.24 ms^{-1}, 3.89 ms^{-1} and 4.19 ms^{-1} respectively.

| (a) | (b) | (c) |
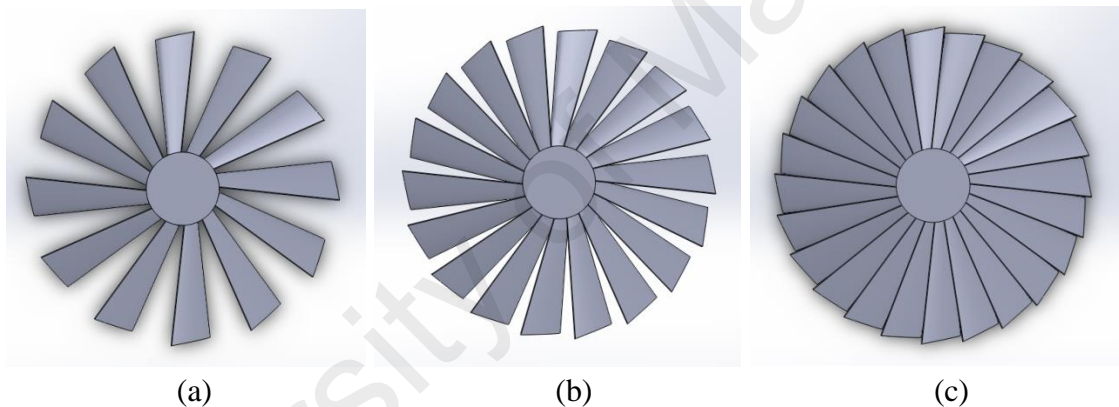
Figure 5.23: Diffuser's swirl mechanism with (a) 12 blades, (b) 18 blades and (c) 24 blades.

In the case of 12 blades swirl mechanism, almost half of the area is a free area. It makes the angled swirl blades ineffective in creating swirl effect. The primary air moves vertically like an air jet without expansion as shown in Figure 5.24. Secondary air movement is induced near to the primary air up to the ceiling height. The swirl air movement is seen after air discharged from the diffuser and disappeared shortly as shown in the streamline air velocity profiles in Figure 5.25.

The 18 blades swirl mechanism showed a well-developed plume air development due to the entrainment of room air. It reduced the velocity of the primary air significantly and shortened the throw as shown in Figure 5.26. Hence, secondary air movement was induced at a larger low level area of the room. Figure 5.27 shows that the 18 blade swirl mechanism createed a greater swirl air effect compared to the 12 blade swirl mechanism.

The 24 blade swirl mechanism had the most blades and the least free area. However, the primary air throws was higher compared to the case of 18 blades, as shown in Figure 5.28. The swirl effect, as shown in Figure 5.29, did not grow greater when compared to the case of 18 blades. This is due to the limited free area for the air to discharge and caused the air to be forced out from the diffuser at high velocity. In this case, the angled blades did not perform effectively in directing the air to flow in swirl effect.
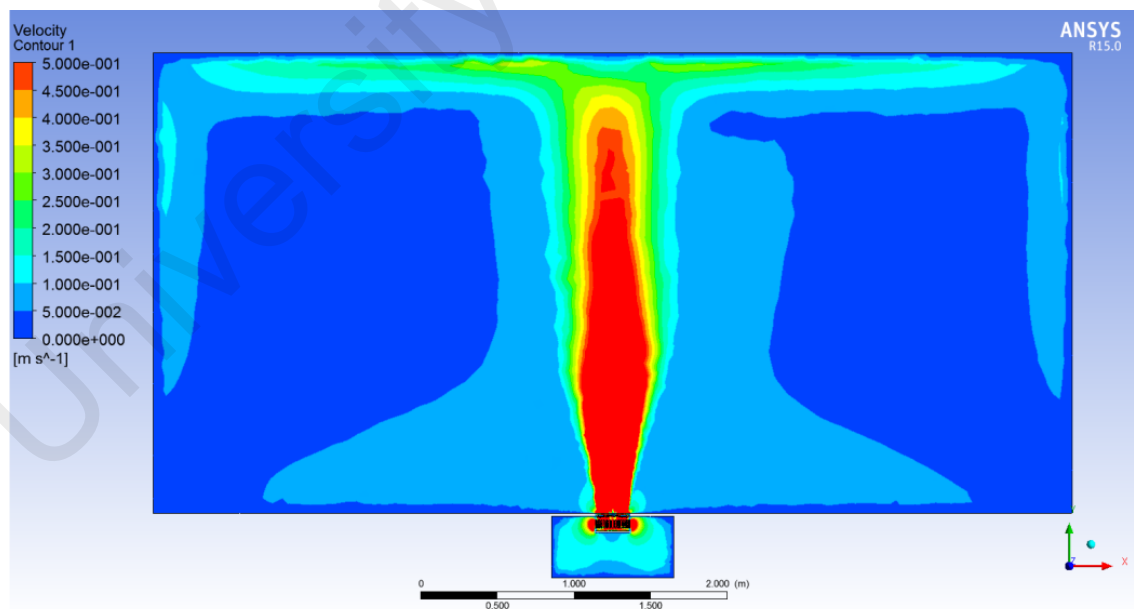
Figure 5.24: Plane air velocity profiles for 12 blades swirl mechanism.
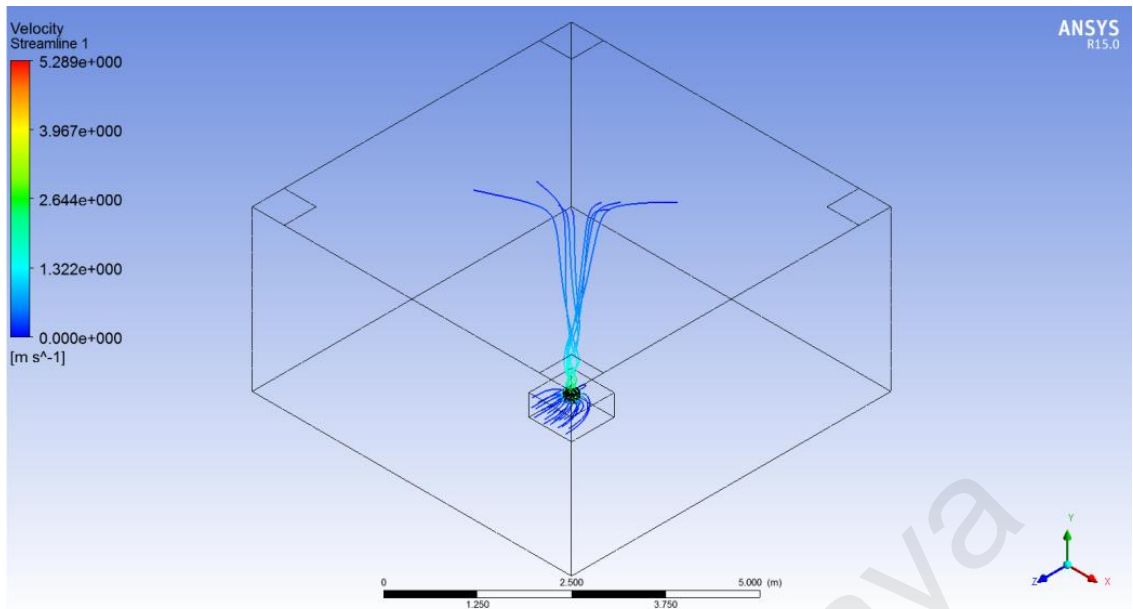
Figure 5.25: Streamline air velocity profiles for 12 blades swirl mechanism.
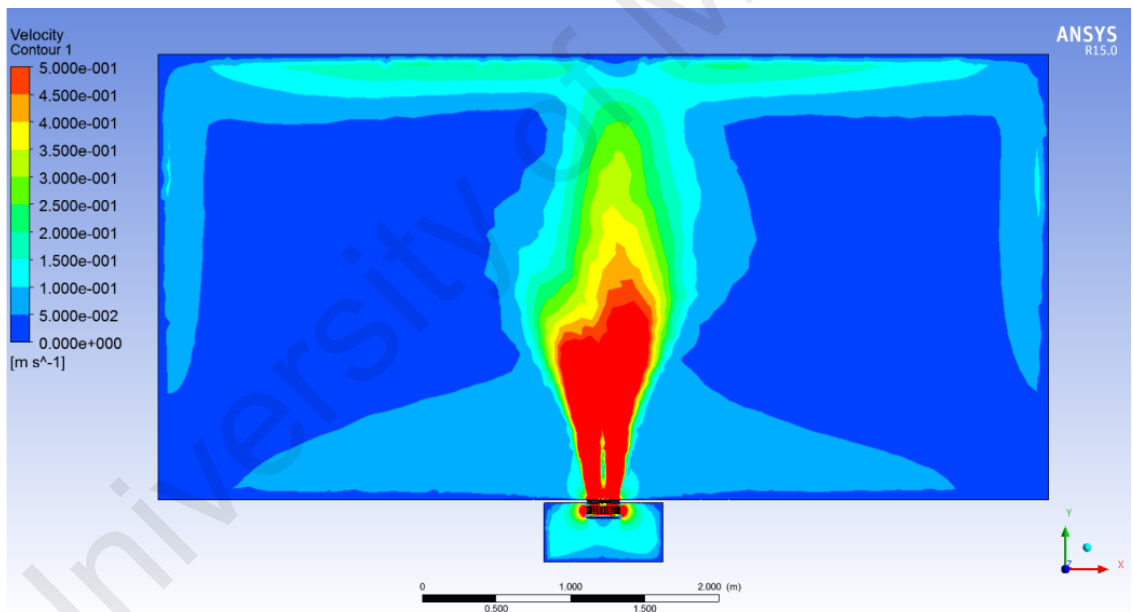
Figure 5.26: Plane air velocity profiles for 18 blades swirl mechanism.
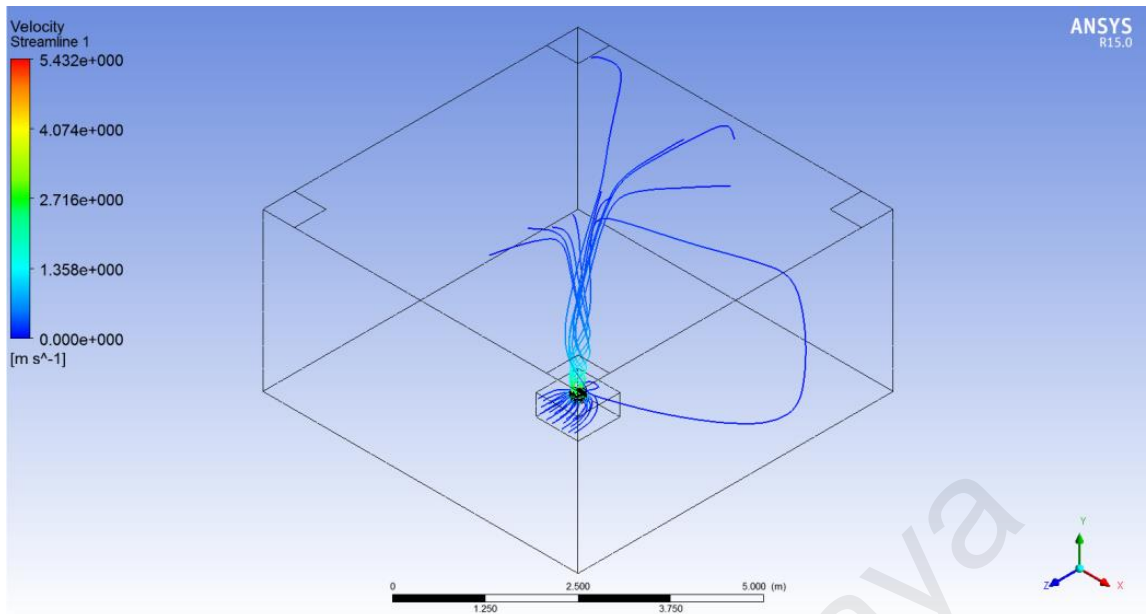
Figure 5.27: Streamline air velocity profiles for 18 blades swirl mechanism.
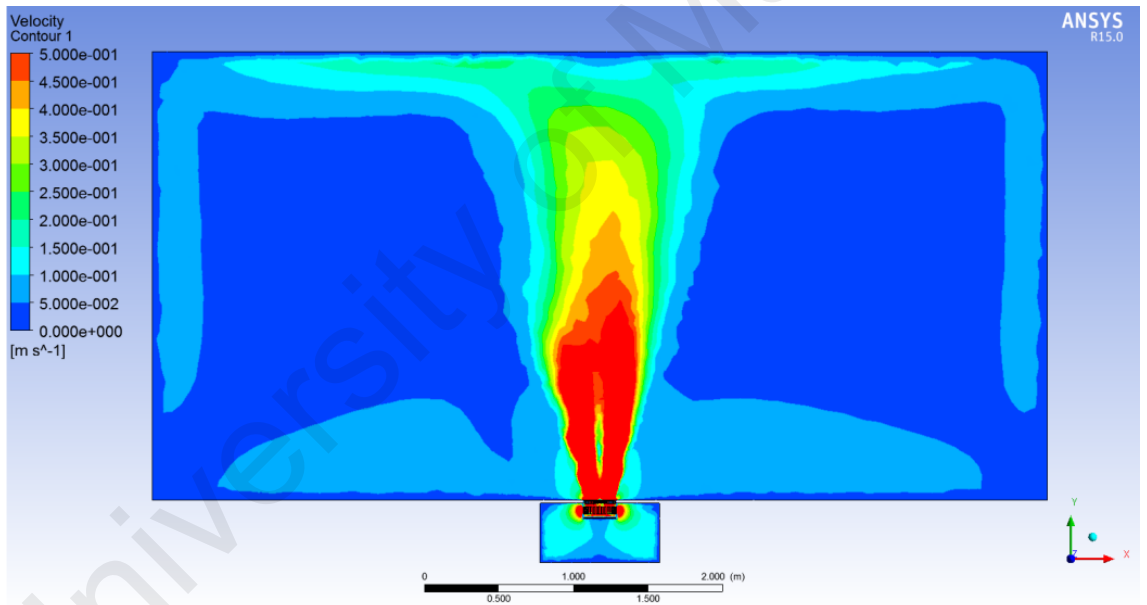
Figure 5.28: Plane air velocity profiles for 24 blades swirl mechanism.
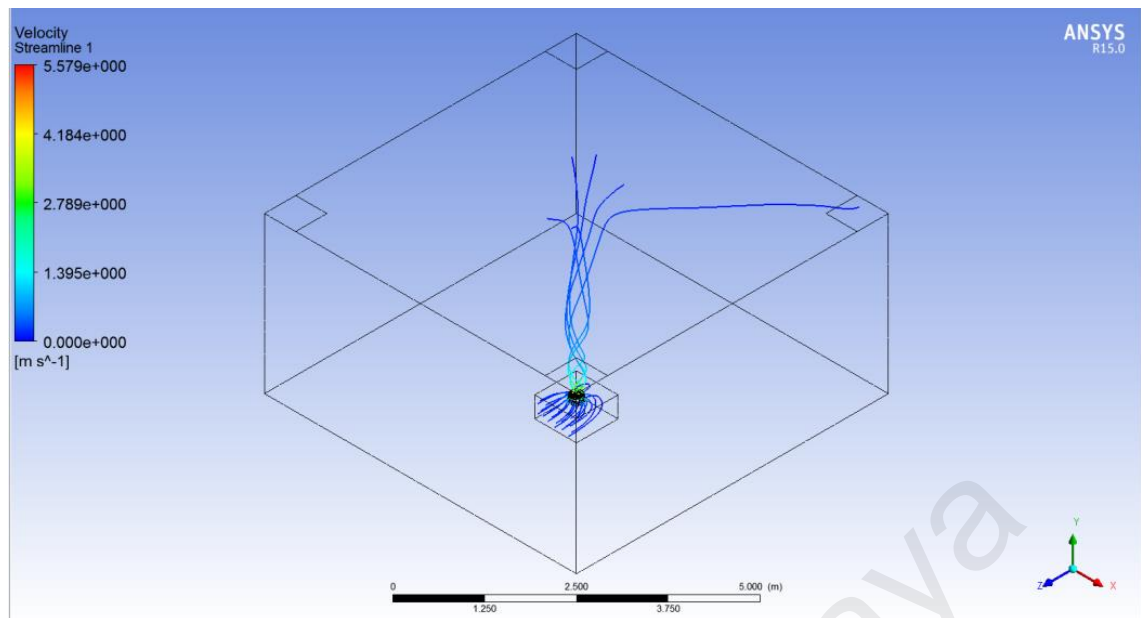
Figure 5.29: Streamline air velocity profiles for 24 blades swirl mechanism.

5.4.6 The Effect of Diffuser Blade's Angle of Attack

This study discussed the angle of attack that affects the room air movement and room temperature. The angles studied were 30°, 45° and 60°. Figure 5.30, 5.32 and 5.34 show the plane air velocity profiles while Figure 5.31, 5.33 and 5.35 shows the plane air temperature profiles for the angles of 30°, 45° and 60° respectively.

The airflow patterns in the case of 30° and 45° have a similar establishment. In both cases, the room at the lower level had induced air movement of about 0.1 ms^{-1}. In fact, the primary airflow in the case of 45° blade developed a greater air entrainment from the room air at the height of 1 – 2 meters above the diffuser. However, the 30° blade created a more evenly distributed temperature across the room compared with the other two cases. The primary airflow pattern in the 60° blade was similar to the case of the 12 blade diffuser where the air was moving vertically without expansion like an air jet. This caused the mixing of air at the higher level. The results were consistent with the findings by Sajadi et al. (2011) where the ceiling based swirl diffuser performed optimally at the swirl angle of 32°.
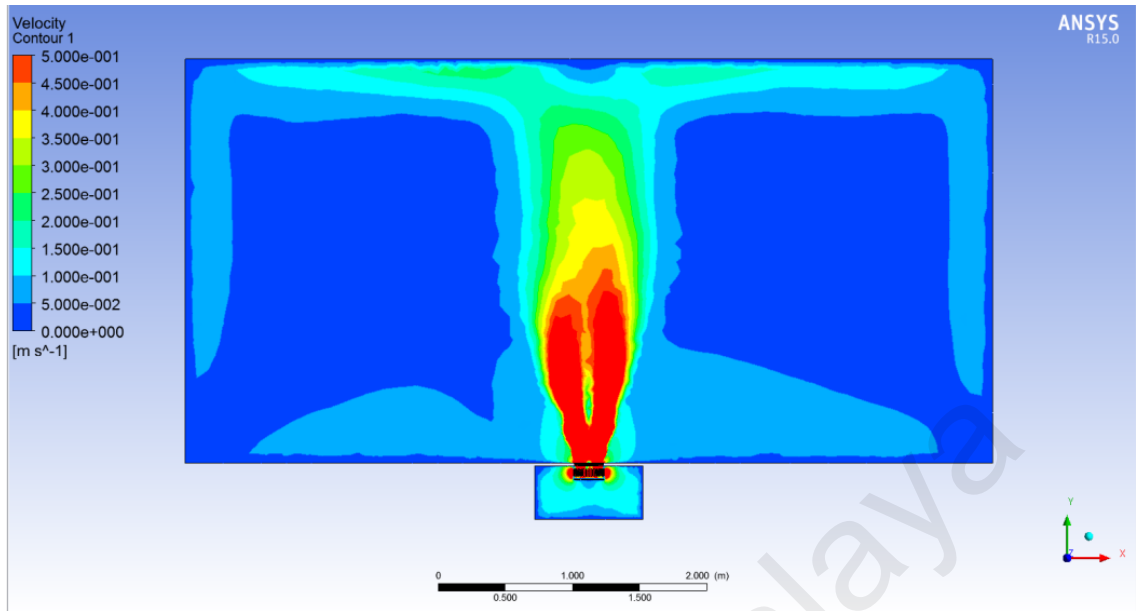
Figure 5.30: Plane air velocity profiles for diffuser blades at the angle of 30°.
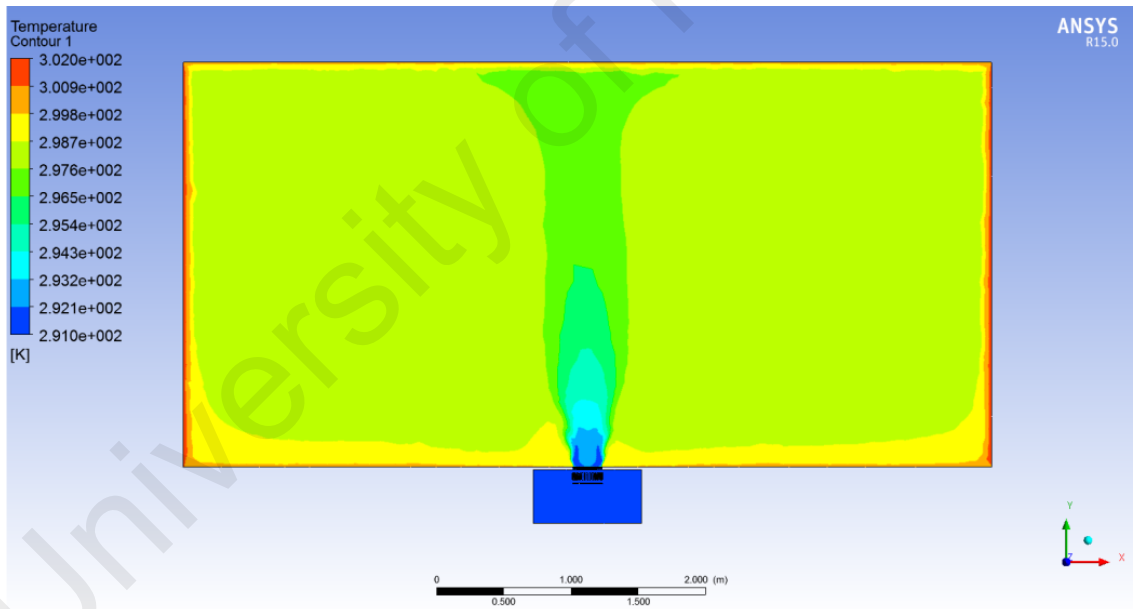
Figure 5.31: Plane air temperature profiles for diffuser blades at the angle of 30°.
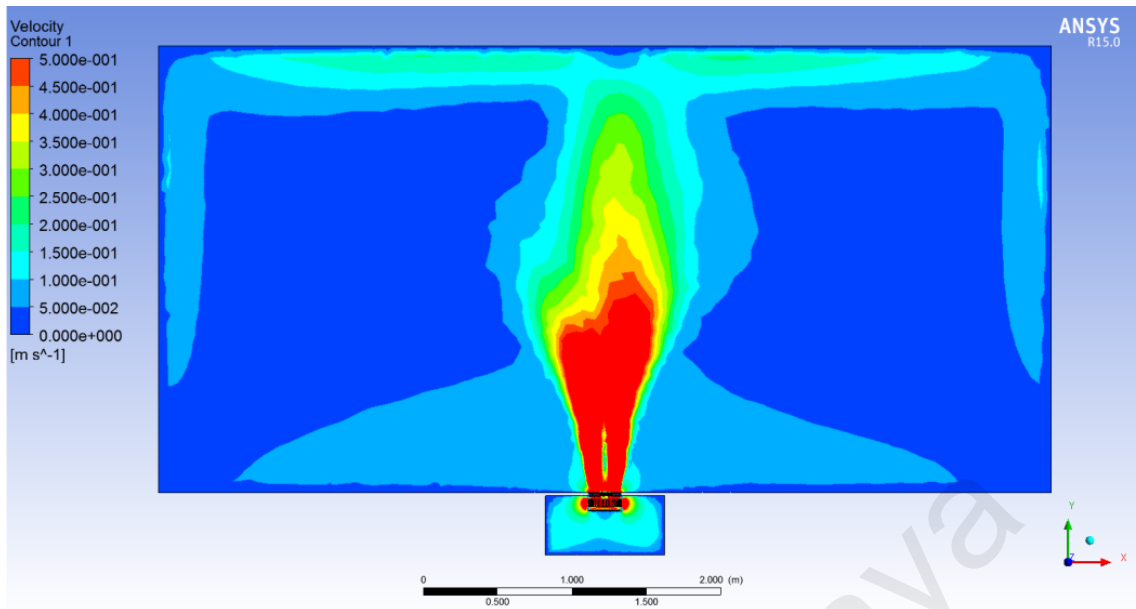
Figure 5.32: Plane air velocity profiles for diffuser blades at the angle of 45°.
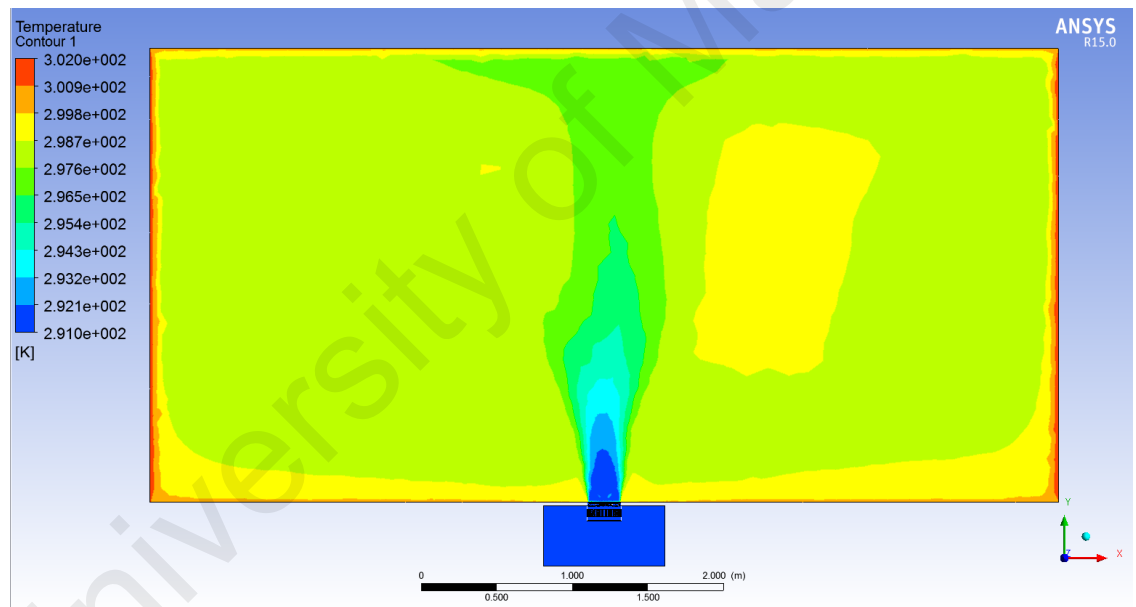
Figure 5.33: Plane air temperature profiles for diffuser blades at the angle of 45°.
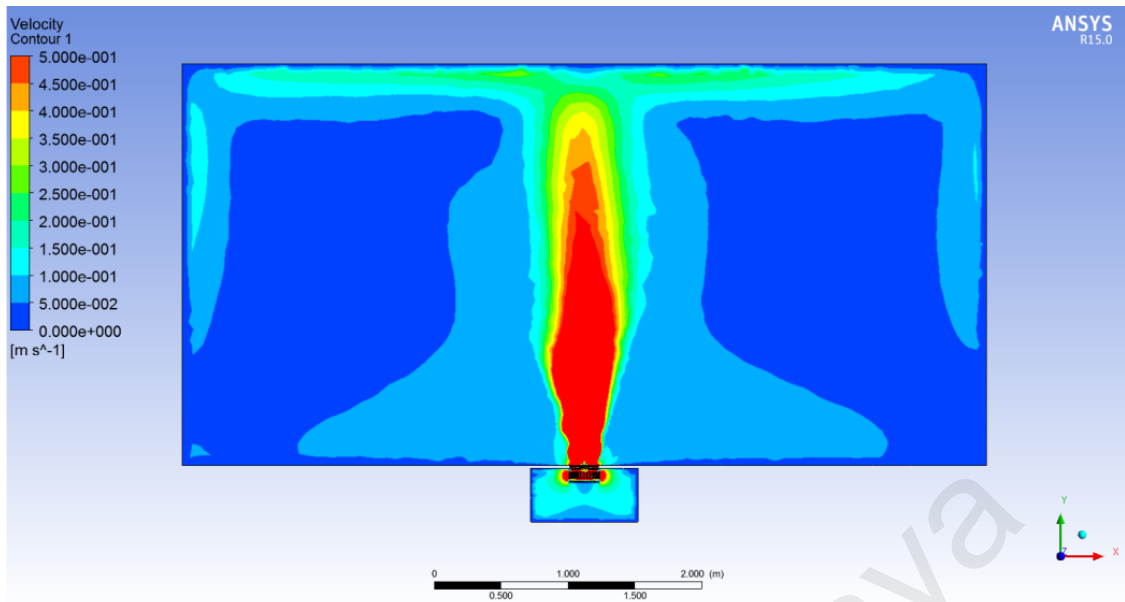
Figure 5.34: Plane air velocity profiles for diffuser blades at the angle of 60°.
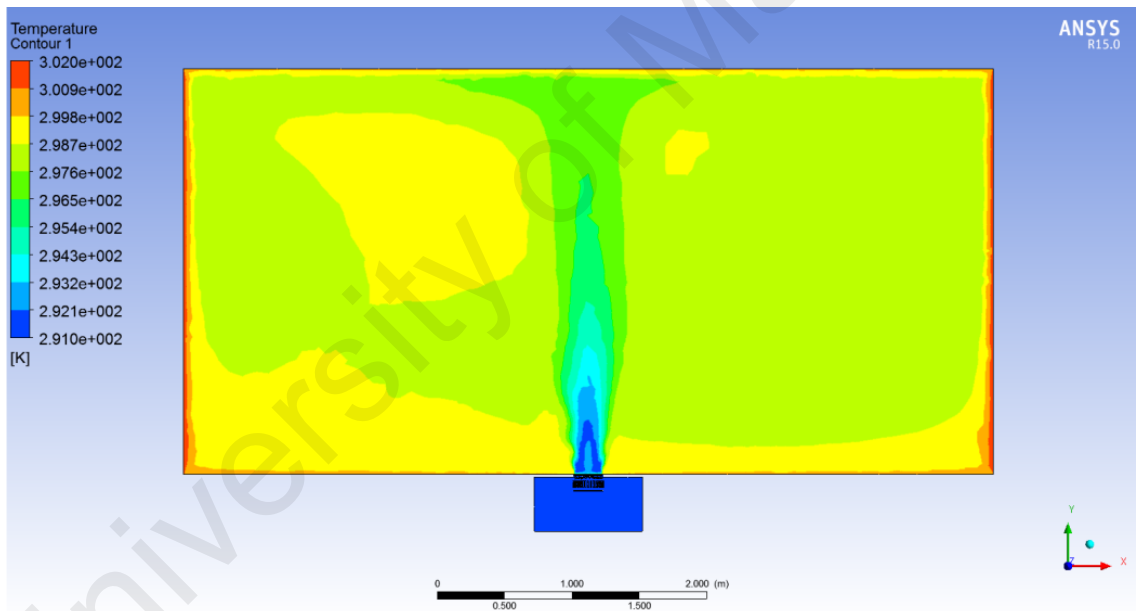
Figure 5.35: Plane air temperature profiles for diffuser blades at the angle of 60°.

5.4.7 The Effect of Diffuser and Grille Thickness

This study discussed the effects of the presence of diffuser blades and grille thickness that affects the airflow pattern in the room. The grille is required to have a minimum thickness in order for floor swirl diffusers to withstand the impact and load of a person or furniture. Although the design of the grille will affect the minimum grille thickness required, the impact and load study were not conducted in this study. The grille thickness test emphasized the airflow performance.

The five cases studied were no diffuser blades, no grille, 3 mm grille, 10 mm grille and 20 mm grille. A diffuser without a grille is not possible for UFAD system as the diffuser blades without a thick grille cannot withstand impact and load of a human or object. However, it was included in this study for comparison purposes in order to have a better understanding of the airflow patterns.

When there are no diffuser blades, the plane air velocity and temperature profiles are shown in Figure 5.36 and 5.37 respectively. The air was delivered to the space vertically upward like an air jet with minimum entrainment. The results a similar scenario to the case in Chapter 4 where thermal comfort was not achieved due to air stagnation.

The swirl angle of the diffuser plays a vital role in defining the characteristics of the swirl jet, especially when the grille was absent. The velocity profiles at the centerline, v_c, dropped below 0.57 ms^{-1} as shown in the plane air velocity profiles in Figure 5.38. A throw height of 0.25 ms^{-1} was reached at about 1.8 m above the floor. The primary air entrained the room air more effectively compared to other cases. This can be seen by the expansion of the plume air jet and the hollow cone pattern formed. The case is consistent to the swirl angle study performed by Tavakoli and Hosseini (2013) on the ceiling based

swirl diffuser. The plane air temperature profiles as shown in Figure 5.39 demonstrate that the room temperature was evenly distributed. The room was evenly cooled to 298 K (25°C).

Figures 5.40 – 5.45 show the plane air velocity and temperature profiles for the cases of 3 mm, 10 mm and 20 mm grille thickness. As the grille thickness increases, it was observed that the primary air was delivered into the space vertically upwards with higher air throw and velocities. The primary air jet induced secondary air flow near to the jet. However, the room temperature became uneven as the cold air was delivered straight to the return air grille.
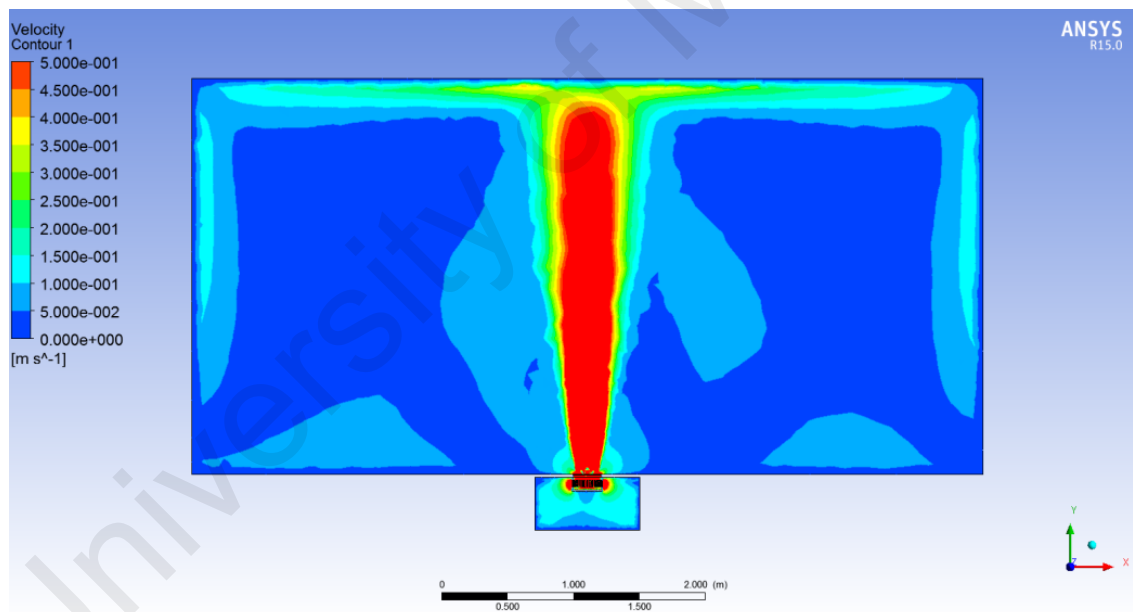
Figure 5.36: Plane air velocity profiles for the case without diffuser blades.
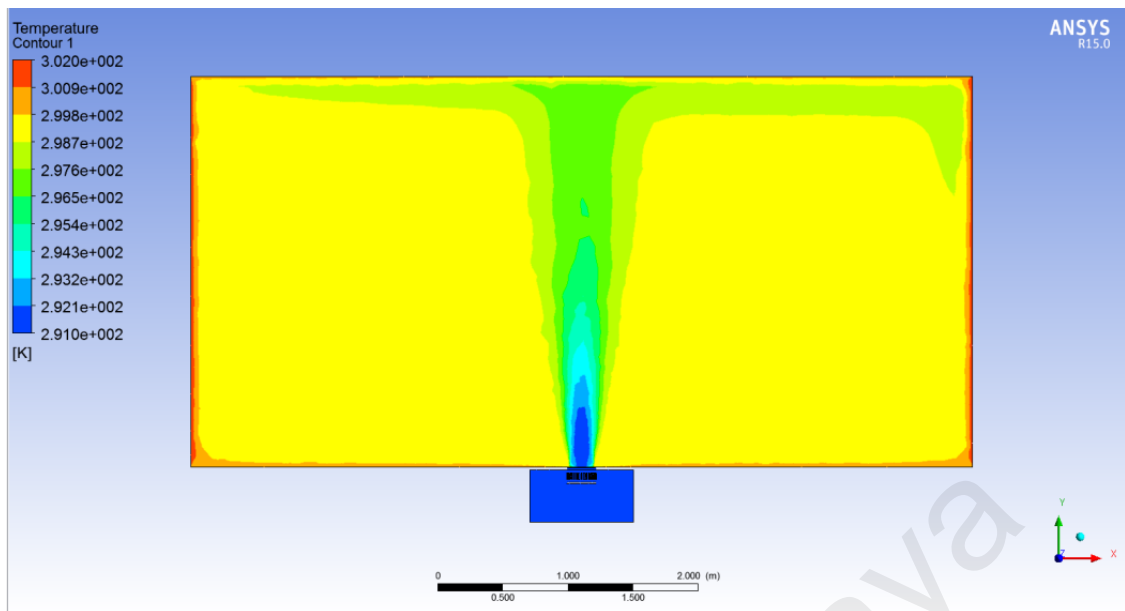
Figure 5.37: Plane air temperature profiles for the case without diffuser blades.
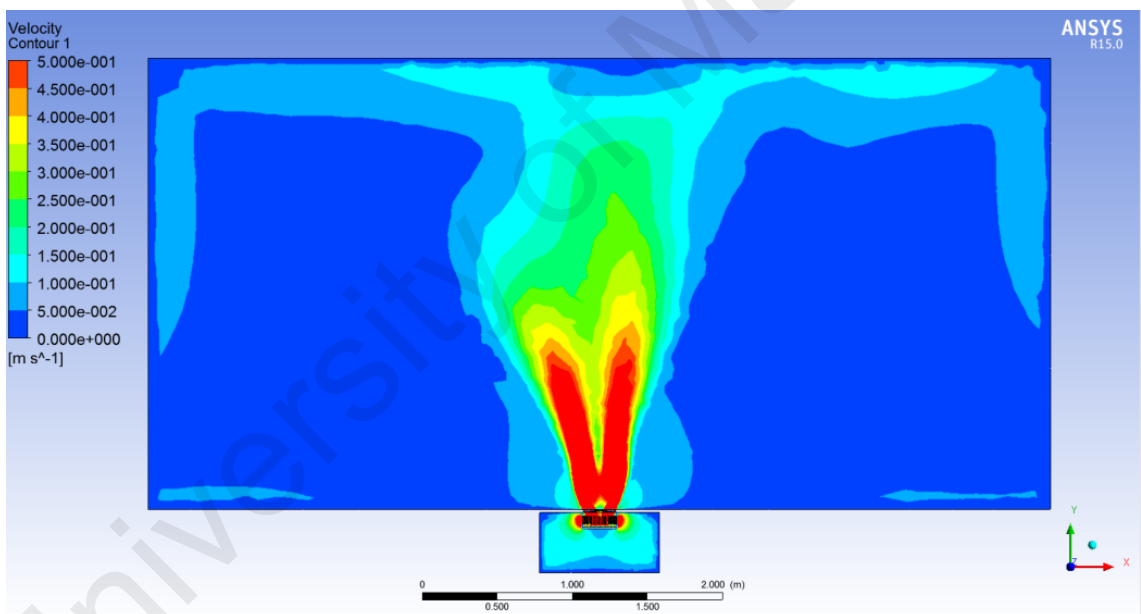
Figure 5.38: Plane air velocity profiles for the case without air grille.
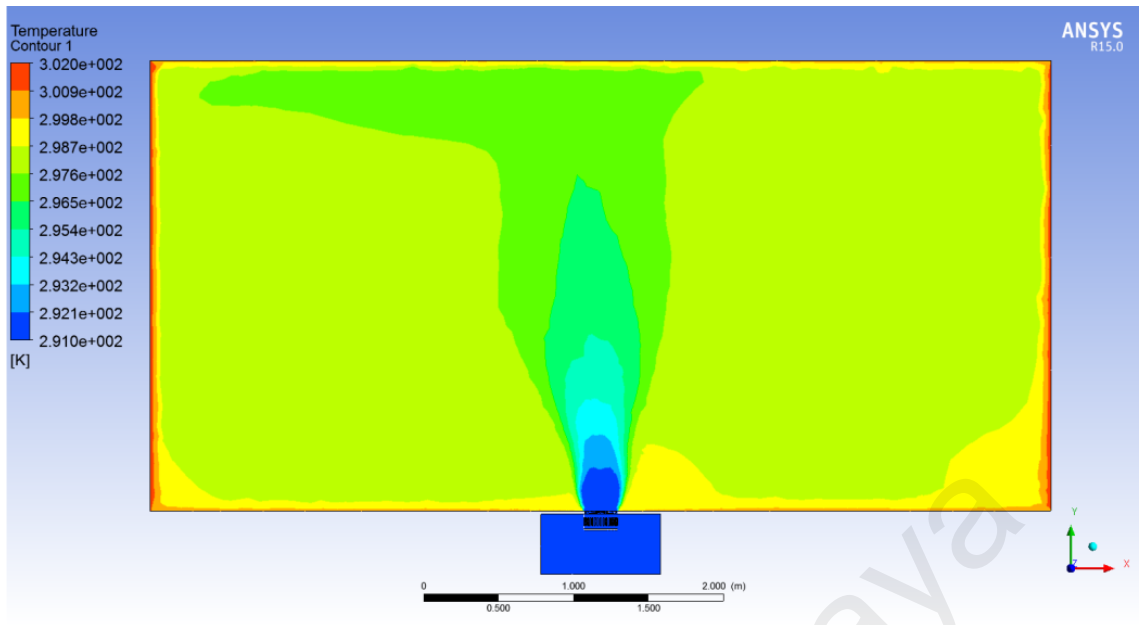
Figure 5.39: Plane air temperature profiles for the case without air grille.
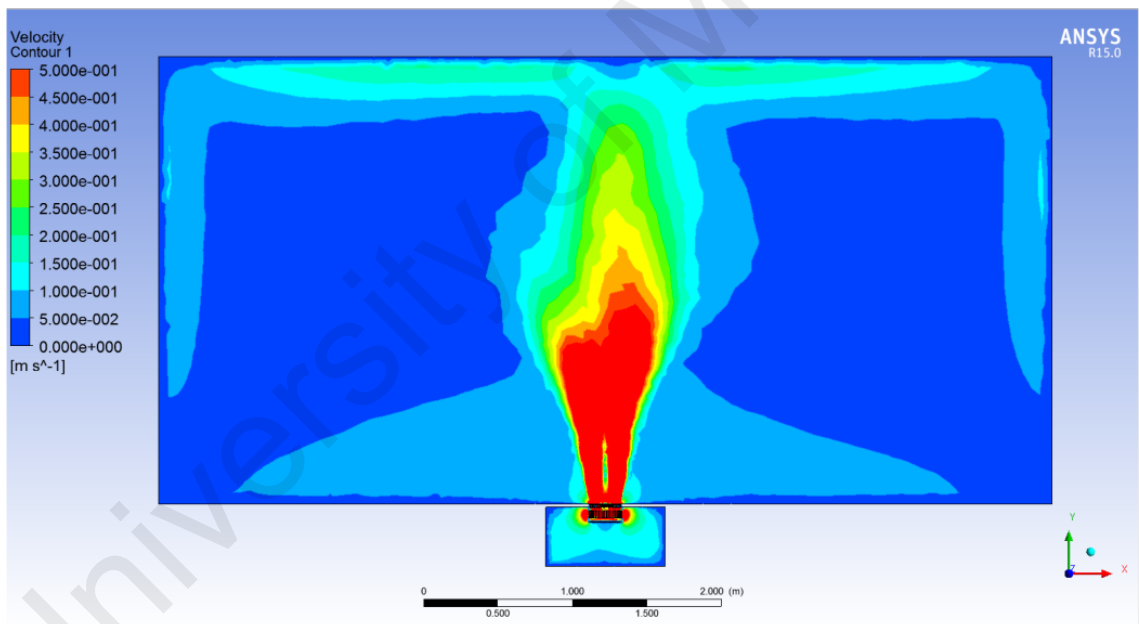
Figure 5.40: Plane air velocity profiles for the case with 3 mm air grille.
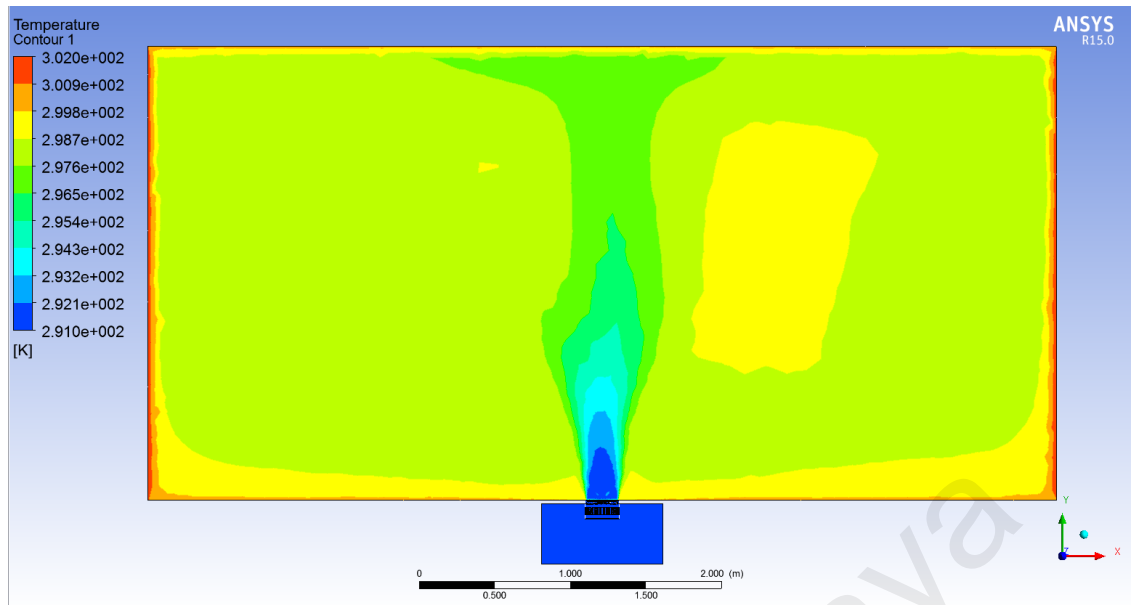
Figure 5.41: Plane air temperature profiles for the case with 3 mm air grille.
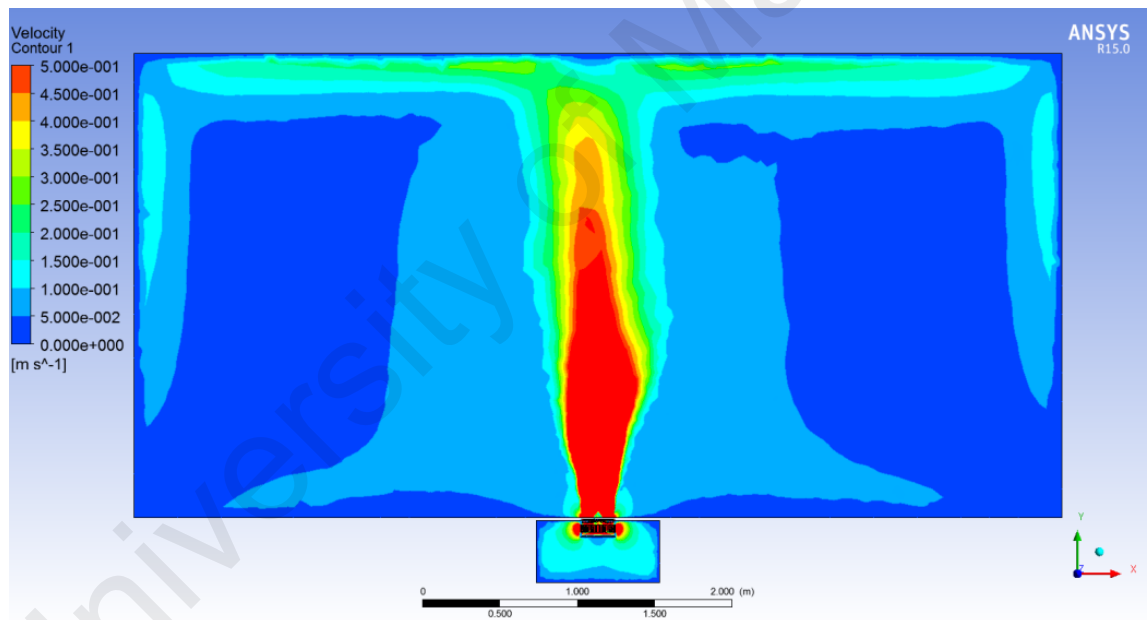
Figure 5.42: Plane air velocity profiles for the case with 10 mm air grille.
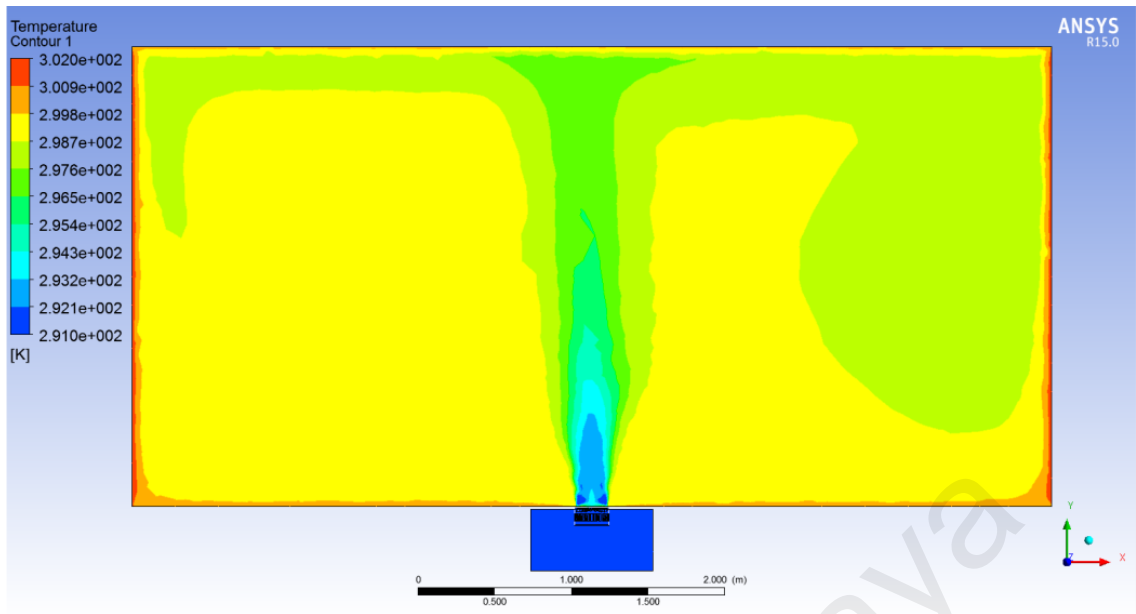
Figure 5.43: Plane air temperature profiles for the case with 10 mm air grille.
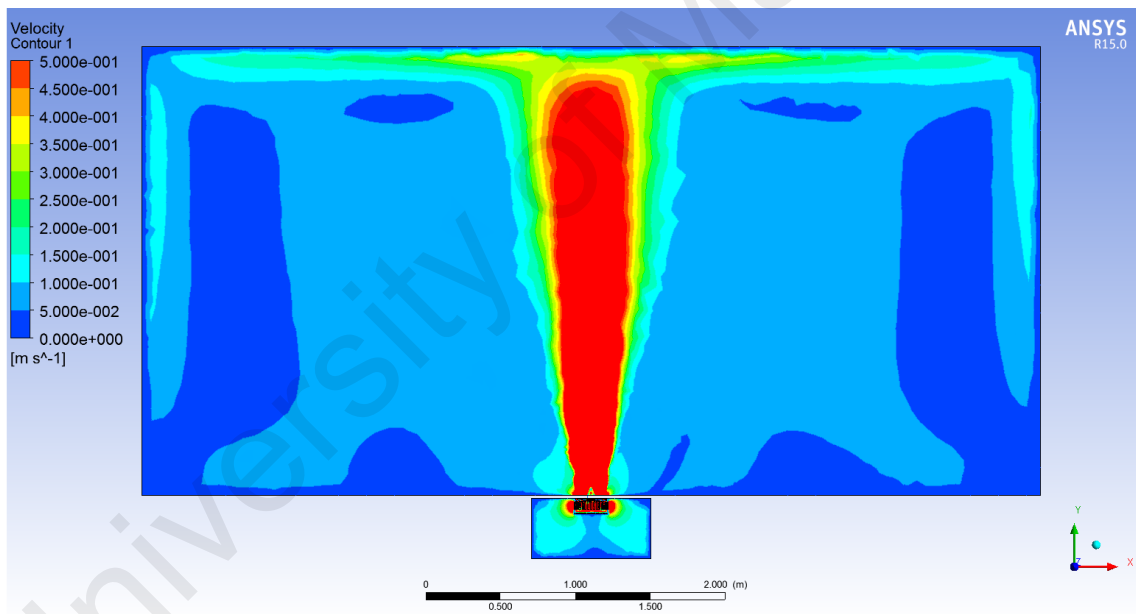
Figure 5.44: Plane air velocity profiles for the case with 20 mm air grille.
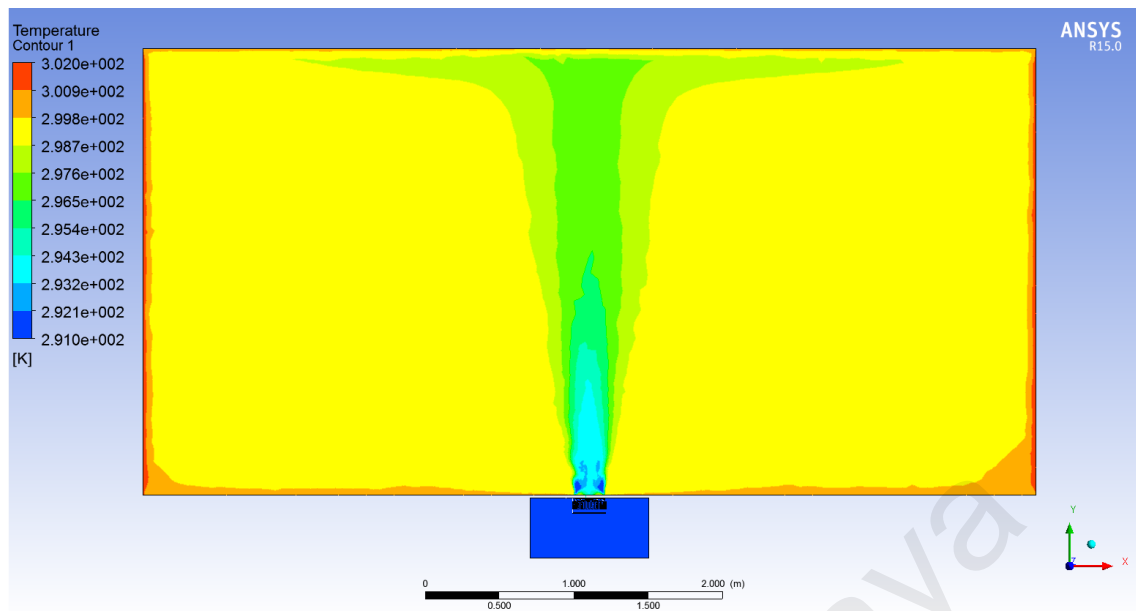
Figure 5.45: Plane air temperature profiles for the case with 20 mm air grille.

5.5   The Centerline Velocity

The case on 195 CMH is the default setting in comparison of other variations. This case has 18 blades of diffuser swirl mechanism, 45° angle of attack and 3mm thick grille. The simulation result showed a good agreement with experimental measurement. Figure 5.46 shows the centerline velocity of all the models through experimental measurement and simulation. It shows that the diffuser and grille thickness has the most impact on the centerline velocity compared to other geometrical variations such as airflow rate, number of diffuser blades and angle of diffuser blades. Thus, not having diffuser blades or having a thick grille is detrimental to the function of the floor swirl diffuser.
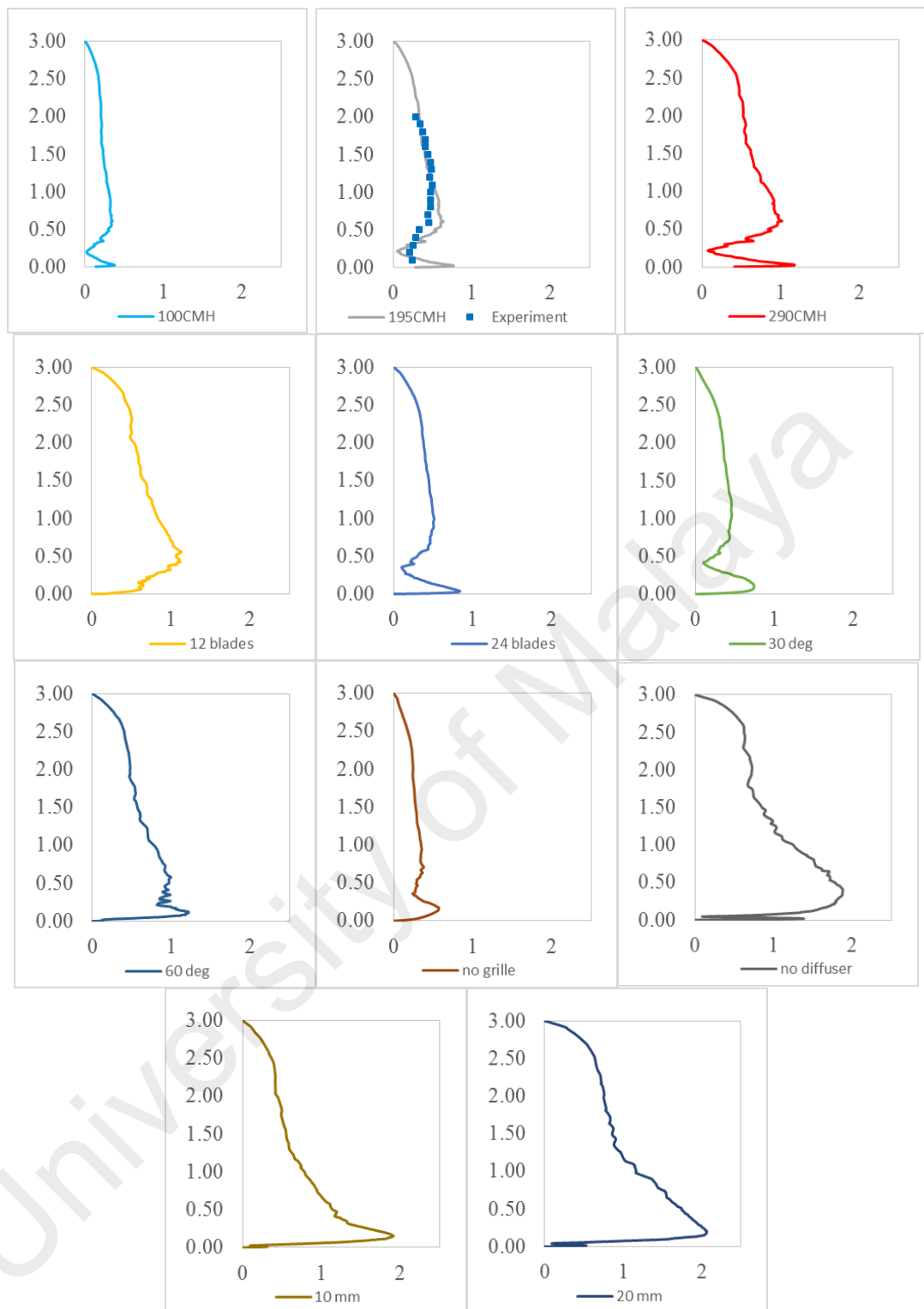
Figure 5.46: The centerline velocity (m/s) for all the geometrical variation of floor swirl diffuser from the floor level of 0 meter to 3 meters above floor level.

5.6   Summary

The several conclusions made according to the studies are:

- ➢ According to the airflow rate study, thermal stratification based on ASHRAE Standard 62.1 for the 250 mm nominal diameter floor swirl diffuser can be achieved at an airflow rate of 100 CMH and below, which translates to a supply air velocity of 1.73 ms^{-1}. The system will perform similarly to the OHAD mixing system with an airflow rate of 195 CMH and above. However, the lower airflow rate creates a lesser air mixing to the surrounding which could be uncomfortable to the occupants. Further study can be done on the thermal comfort.

- ➢ The optimum free area of the diffuser blades to create swirl effect is around 20%, which is closest to an 18 blade diffuser. A free area that is too large or too small could lead to ineffectiveness of using diffuser blades, similar to the system without diffuser blades.

- ➢ The swirl blades are important in rotating the discharged air to improve the mixing effect. At the low angles of attack of 30° and 45°, the air throw was lower compared to high angle of attack. The primary air was established and expanded by entraining room air. The room achieves an evenly distributed temperature profile at the low angle of attack due to the better air mixing effect.

- ➢ A thicker grille leads to air delivered as a straightened air jet into the space. The swirl effect from the diffuser blades is eliminated. Thus, minimum grille thickness should be developed without detrimental effects to the strength to withstand the impact and load of people and furniture.

CHAPTER 6 – FEASIBILITY STUDY OF SOLAR UNDER-FLOOR AIR DISTRIBUTION SYSTEM IN THE TROPICS

6.1 Overview

Solar energy is abundantly available in tropical countries. Solar irradiation in Malaysia's climates located at 3°08'N 101°42'E is studied as a representative of tropical climates. There are various types of light absorption materials that absorb photons and emit free electrons to generate electricity. The materials include amorphous silicon, monocrystalline silicon, multi-crystalline silicon, cadmium telluride (CdTe) and cadmium sulphide (CdS), organic and polymer cells, hybrid photovoltaic cell, and thin film technology (Parida et al., 2011). Multi-crystalline or poly crystalline was selected in this study due to the wide application in Malaysia's photovoltaic market.

A typical solar electrical cooling system was studied by Ashhab et al. (2013). In this study, the feasibility of a hybrid solar-powered under-floor air distribution (UFAD) system was studied in Malaysian weather. The difference of this study to a typical solar electrical cooling system is that electricity from the solar photovoltaic system was directly applied to the air handling unit (AHU) of the UFAD system. However, it does not associate to the energy consumption of the refrigeration cycle. The application is on a large scale HVAC system. This research work focused on the energy and cost investigation of using a solar photovoltaic system and evaluated the potential of incorporating it with UFAD system.

6.2 Assumptions

1. The initial cost of UFAD system is excluded from this study as it does not affect the comparison on overall payback period calculation of the systems.

2. The yearly maintenance cost of the solar photovoltaic system is assumed at 2.5% of the initial cost.

3. The performance degradation rate of solar panel is assumed to be at 0.8% per year.

4. The power consumption of AHU of the UFAD system is assumed constant.

5. The solar photovoltaic system is a product from China. Hence, the cost projection is assumed from literature.

6. The tariff charges for medium voltage general commercial tariff category is considered in this case study of an office building.

6.3   Solar Irradiation in Malaysia

Figure 6.1 shows the monthly average daily solar irradiation in the seven selected cities in Malaysia. The results showed that solar irradiation is higher at the northern region of Malaysia and East of Malaysia. The southern parts of Malaysia and high altitude regions have the lowest solar irradiation. Generally, higher solar irradiation is expected during the early months of the year and decreased slightly during the middle of the year. The results are similar to the conclusion that northern region of the peninsular Malaysia has a higher intensity of solar irradiation in the estimation of monthly average daily solar irradiation in the tropics (Shavalipour et al., 2013). The daily average solar irradiation throughout a year is ranged from 3.8 kWh/m² to 5.0 kWh/m².
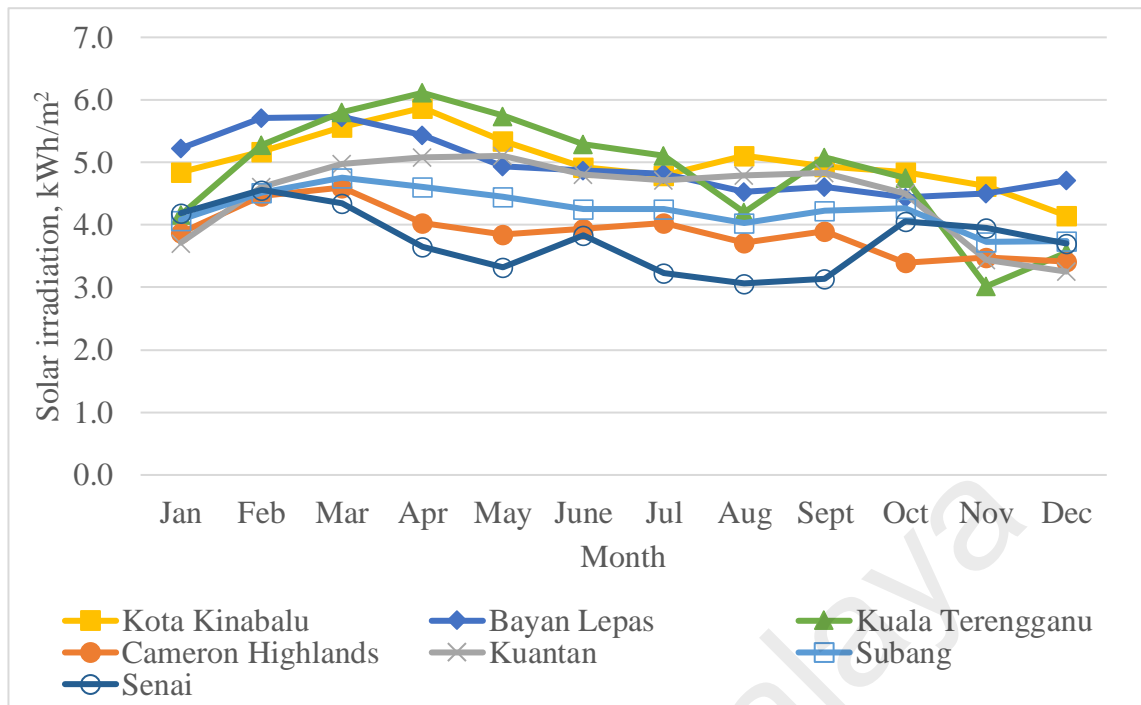
Figure 6.1: Monthly average daily solar irradiation in major cities in Malaysia.

The monthly average daily solar irradiation of 25 years data for tropical (Malaysia) and subtropical (Hong Kong) country is compared as shown in Figure 6.2. The data of the subtropical country is obtained from the research conducted by Chan et al. (2006). The results showed that a tropical country has a better advantage in harvesting solar irradiation compared to a subtropical country due to the stable energy output throughout the year. Subtropical countries receive a lower solar irradiation during the winter and spring seasons from November to April. Although the solar irradiation in tropical countries is relatively lower from the month of November to January, the difference is insignificant. Tropical countries receive an average of 4 kWh/m^2 to 5 kWh/m^2 daily throughout the year.
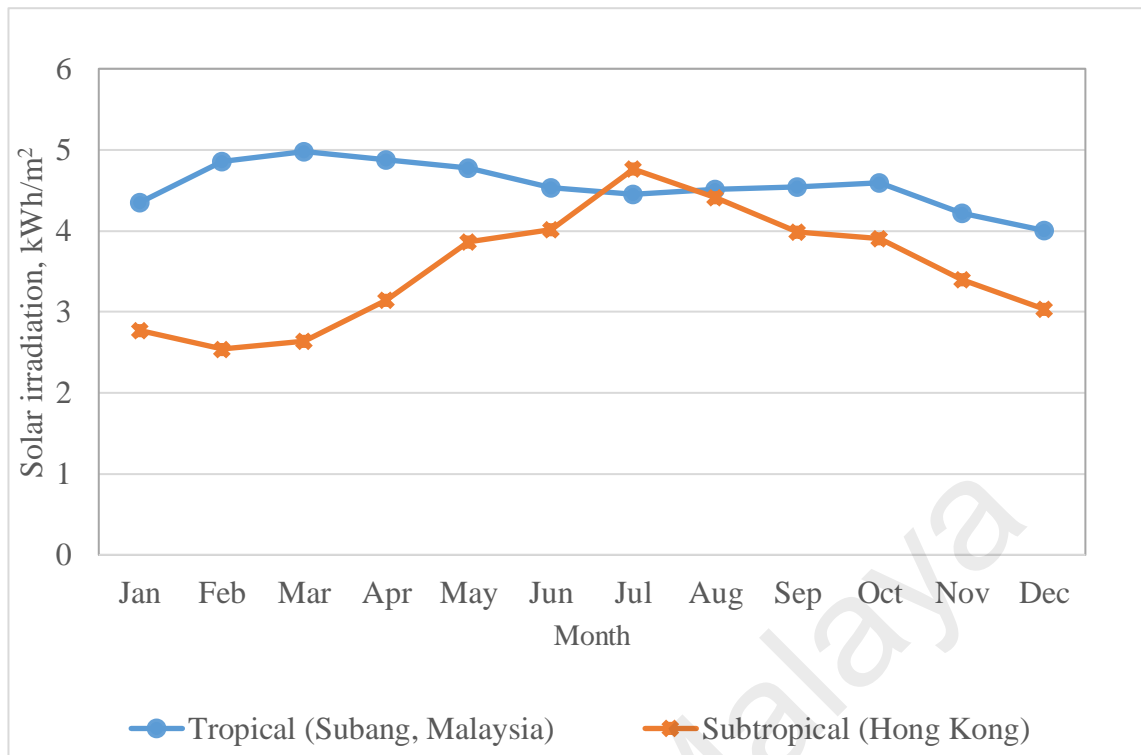
Figure 6.2: Monthly average daily solar irradiation in tropical and subtropical country.

Figure 6.3 shows the 25 year trend of monthly average daily solar irradiation in Subang, Malaysia from January 1988 to December 2012. It can be seen that the average solar irradiation is increasing at the rate of about 0.03 kWh/m^2 per year which is equivalent to 0.7% of the solar irradiation increase every year. The increasing solar irradiation is in association with the climate changes which is not discussed in this study (Yau and Pean, 2014).
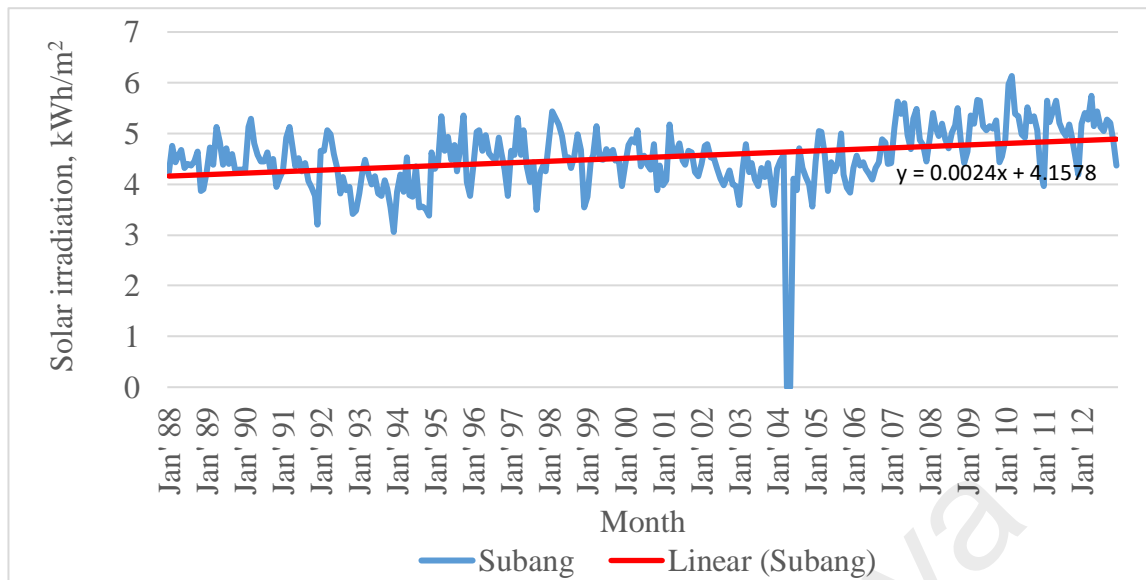
Figure 6.3: Monthly average daily solar irradiation in Subang, Malaysia from January 1988 to December 2012.

(Malaysian Meteorological Department, 2012)

6.4 Energy Output of Experimental Solar Photovoltaic System

Table 6.1 shows the daily electricity generation from the 1 kW on-grid solar photovoltaic system. There are some days where data was not collected due to the disconnection of the system. The maximum and minimum daily electricity output recorded are 7.2 kWh/day and 1.0 kWh/day respectively. The average daily electricity output ranged from 4.0 – 5.6 kWh. The area of the solar panel is 1.64 m^2. Thus, the daily average energy output is 2.76 kWh/m^2. The closest location of the solar irradiation data available to the experimental setup is Subang. Based on the solar irradiation data in Subang, the daily average solar irradiation is 4.52 kWh/m^2. Thus, the effectiveness of converting solar irradiation into electricity is about 61%.

Table 6.1: The daily energy output of solar photovoltaic system.

Date	Daily Energy Generation (kWh)											
	Jan	Feb	Mar	Apr	May	June	July	Aug	Sept	Oct	Nov	Dec
1	2.6	6.8	5.6	-	5.8	4.2	3.7	3.3	3.8	4.0	3.9	4.3
2	5.9	5.0	4.5	4.6	4.2	3.8	5.0	3.7	5.0	4.3	5.0	3.7
3	4.1	6.0	3.8	5.7	4.1	4.1	4.9	3.4	2.2	3.3	4.5	4.8
4	5.0	6.7	5.1	-	3.5	5.3	3.8	5.6	3.8	6.2	3.0	4.2
5	4.2	5.5	6.7	-	4.7	3.5	2.6	3.6	3.3	5.4	3.0	3.7
6	5.5	5.3	6.6	-	4.9	4.4	4.4	4.5	3.9	6.4	3.9	3.6
7	5.8	4.7	7.2	4.0	4.1	4.7	4.9	4.7	4.9	4.7	5.1	5.0
8	5.3	4.9	6.3	4.6	2.5	4.3	3.0	4.5	4.1	5.8	3.0	3.4
9	5.2	5.5	5.9	4.9	4.4	3.5	2.2	4.1	4.4	5.8	4.2	4.2
10	6.1	5.7	5.5	3.7	4.4	4.4	4.9	4.7	2.9	-	3.9	4.3
11	6.3	6.5	6.9	5.7	3.7	5.0	3.1	3.7	4.2	4.5	4.5	2.9
12	4.1	4.6	6.0	4.7	2.7	5.3	4.0	4.4	5.1	3.1	6.7	4.3
13	5.5	4.3	4.2	-	4.1	6.1	-	4.7	3.7	5.1	3.1	2.5
14	4.6	5.7	4.1	5.1	3.8	4.5	-	5.1	4.3	4.9	5.5	5.1
15	2.8	5.9	4.6	5.9	5.0	4.8	-	5.0	3.4	3.9	4.0	4.1
16	3.0	5.6	2.8	4.9	3.5	4.0	3.4	5.2	5.4	4.6	2.8	3.4
17	4.7	5.4	3.7	4.6	3.1	4.4	3.2	5.4	3.9	5.4	4.5	2.7
18	4.4	5.5	2.2	5.4	4.1	3.6	3.7	3.8	4.7	4.1	6.3	4.2
19	4.9	4.9	5.1	4.4	3.9	4.4	4.3	1.0	4.0	4.0	4.1	4.9
20	6.4	5.3	3.3	4.7	4.6	3.6	5.1	5.4	3.6	5.1	2.8	5.1
21	5.2	4.7	5.2	4.9	3.1	4.1	5.2	4.4	5.3	4.7	4.2	4.6
22	3.8	7.2	5.6	5.2	4.6	3.3	4.4	4.3	4.5	5.7	4.9	5.1
23	5.4	7.0	6.5	3.6	3.1	5.5	4.7	3.5	5.1	3.8	4.0	4.8
24	7.0	6.5	6.0	3.7	3.6	4.5	3.2	4.3	4.9	3.6	3.9	3.2
25	6.4	5.9	-	4.4	2.7	3.8	4.3	2.8	4.5	4.4	2.4	4.7
26	4.8	4.7	-	4.8	3.0	4.7	1.9	4.9	3.2	4.9	3.9	5.5
27	5.1	5.5	-	4.0	4.2	5.2	4.6	3.4	3.1	3.5	4.0	5.5
28	-	5.9	-	4.6	5.1	3.5	4.9	3.8	4.8	5.3	3.7	1.2
29	-	-	-	4.1	5.0	3.9	-	3.2	6.0	5.6	4.8	6.3
30	-	-	-	4.8	5.2	3.4	4.0	3.5	6.5	4.7	3.2	6.7
31	-	-	-	-	4.8	-	4.6	4.0	-	3.8	-	5.7
Average	5.0	5.6	5.1	4.7	4.0	4.3	4.0	4.1	4.3	4.7	4.1	4.3
Power Generation (kWh/m^2)	3.0	3.4	3.1	2.9	2.5	2.6	2.4	2.5	2.6	2.9	2.5	2.6

Figure 6.4 shows the moving average line of the solar energy generation. The daily electricity output from January to March is higher, in the range of about 5 – 6 kWh, while from April to December the range is about 4 – 5 kWh. For the simplicity in

123

calculation, the cash inflow of simple cash flow (SCF) is calculated using the yearly average daily solar energy generation of the solar photovoltaic system of 4.50 kWh/day.
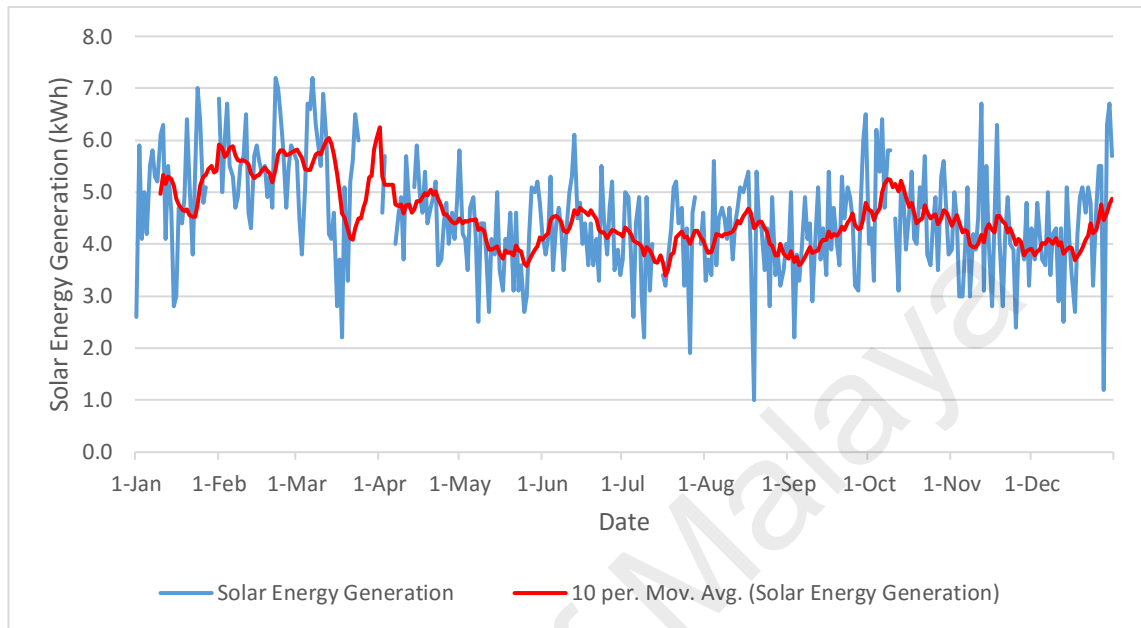
Figure 6.4: Solar energy generation from the 1 kW on-grid solar photovoltaic system.

6.5   Energy Consumption of UFAD system

The power consumption of the AHU for the UFAD system in TM Tower is measured using a power meter. Figure 6.5 shows the power consumption profiles of one AHU unit at Level 35 in TM Tower. The power consumption data is measured from 9am – 5pm of a usual working day. Since the AHU is a constant air volume (CAV) system with temperature control based on chilled water actuator regulation, the power consumption can be assumed constant. As proven in the power consumption profiles, the power consumption is in the range of 10.61 – 10.76 kW with an average of 10.69 kW. Due to access limitations of the site for investigation, the power consumptions of other hours were expanded from this average power consumption value. The normal office hours in Malaysia are 8 hours daily. Office staff often work longer than the office hours as overtime. Thus, the daily operation hours of the central HVAC system are usually 10 –

12 hours. In this study, the operation hours of central HVAC system are 10 hours from 8am to 6pm. Hence, the daily electricity consumption of one AHU is 106.9 kWh.
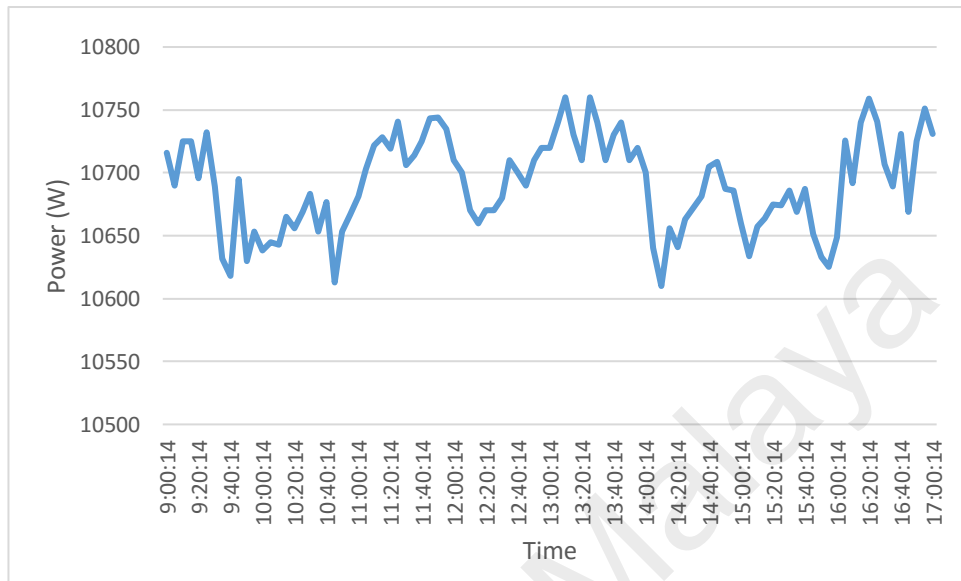
Figure 6.5: Power consumption of the AHU for UFAD system in TM Tower

6.6   Cost and Payback Period

6.6.1   Initial Cost of the Experimental On-grid Solar Photovoltaic System

The initial cost of the 1 kW experimental on-grid solar photovoltaic system is shown in Table 6.2. The cost includes the solar panels, solar inverter and installation on the grid system of the building. The total initial cost was RM 17,990.00, which is equivalent to about RM 13.00 per watt. Figure 6.6 shows the initial cost represented in percentage. The solar panels, solar inverter and installation cost account for 46.03%, 12.51% and 41.46% respectively. This shows that solar panels are the major cost of the system.

Table 6.2: The initial cost for the 1 kW experimental on-grid solar photovoltaic system

Descriptions	Qty	Unit Price (RM)	Total (RM)
Solar Panel SLP230-12	6	1380.00	8280.00
Solar Inverter GW-1500SS	1	2250.00	2250.00
Mounting Structure	1	600.00	600.00
DC & AC Cables	1	1860.00	1860.00
Combiner box, SPD, MCB and Others	1	2000.00	2000.00
Installation	1	1500.00	1500.00
Design, consultation, testing and commissioning	1	1500.00	1500.00
Total Cost			17990.00
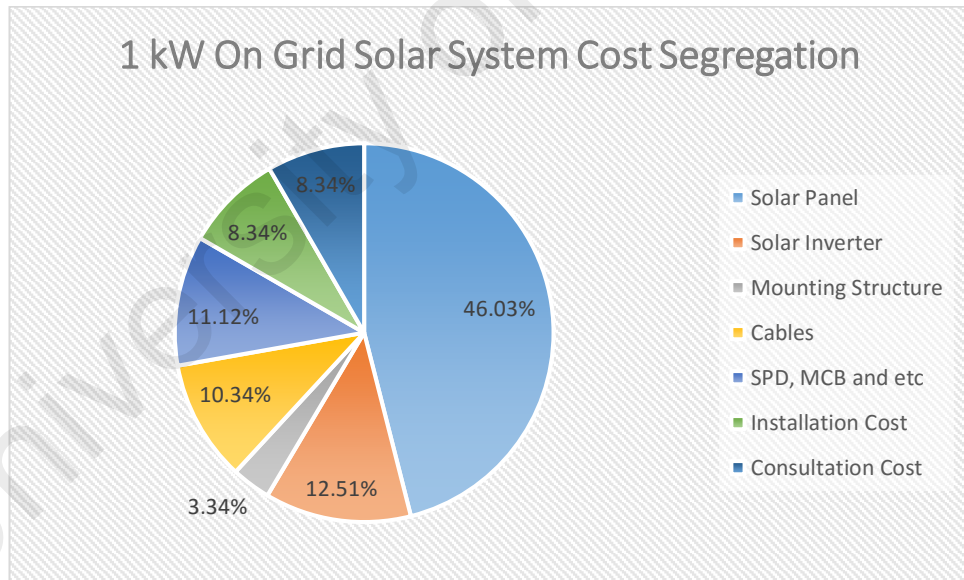
Figure 6.6: Cost segregation of the 1 kW experimental on-grid solar photovoltaic system.

6.6.2 Simple Payback Period (SPBP)

The solar photovoltaic system is a product and manufactured from China. Hence, the initial cost of 5 kW solar photovoltaic system is deduced from the aspect ratio of 1:4.13

obtained from Rodrigues et al. (2016). The FiT subsidy provided by SEDA is divided into two areas: basic FiT rates and bonus FiT rates. The rates for these cases are RM 0.8249/kWh and RM 0.155/kWh respectively. Hence, the total subsidy rate obtained was RM 0.9799/kWh. The subsidy provided is applicable for electricity produced for internal used and electricity returned to the grid-system. The tariff charges for medium voltage general commercial tariff category were considered in this case study. The tariff for all energy consumed is RM 0.365/kWh.

The energy consumption, solar energy generation, initial cost, operational cost, maintenance cost and all the related calculations of the three cases are presented in Table 6.3. The total accumulated cost represented all the cost used throughout the 21 years of system operations, including the initial cost, operational cost, maintenance cost and FiT subsidy. The daily and annual electricity consumptions of the three cases are the same. There are 243 actual working days per year in Malaysia, excluding Saturday, Sunday, and public holidays. The solar photovoltaic system operates throughout the year. Hence, the energy is collected even though the UFAD system is not operating.

The results showed that the total accumulated cost for 1 kW solar photovoltaic system, 5 kW solar photovoltaic system and conventional UFAD system after 21 years of operation are RM 182,728.93, RM 93,447.15 and RM 199,111.41 respectively. Figure 6.7 shows the annual accumulated cost of the three cases. The breakeven point, or the payback period, for 1 kW and 5 kW solar photovoltaic systems compared to conventional UFAD system without solar photovoltaic panels is 10.6 years and 8.3 years respectively. The 5 kW solar photovoltaic system showed a significant saving after 21 years of operation. The average annual return of investment is 4.3%. The annual return of investment for 1 kW solar photovoltaic system is 3.13%. The electricity energy savings

for 1 kW and 5 kW solar photovoltaic UFAD system in 21 years are 34,492.5 kWh and 172,462.5 kWh respectively. It is equivalent to CO_2 emission reductions of 23,917.79 kg and 119,588.96 kg, respectively, according to the CO_2 emissions per kWh electricity published in IEA (2015). The environmental effect is significant.

Table 6.3: The energy consumption, energy generation and related cost information of the three cases.

AHU	1 kW Solar PV	5 kW Solar PV	Conventional System
Daily Electricity Consumption of AHU unit (kWh)	106.90	106.90	106.90
Annual Electricity Consumption of AHU unit (kWh)[1]	25,976.70	25,976.70	25,976.70
Solar Photovoltaic System			
Initial Cost, I (RM)	17,990.00	74,375.00	-
Daily Solar Electricity Generation (kWh)	4.50	22.50	-
Annual Solar Electricity Generation (kWh)[2]	1,642.50	8,212.50	-
Percentage of Solar Electricity Consumption (%)	6.32	31.61	-
Cash Inflow, Cin			
Tariff for FiT, Tg (RM/kWh)	0.9799	0.9799	-
Annual Solar Electricity Generated, Eg (kWh)	1,642.50	8,212.50	-
Annual Cash Inflow, Tg x Eg (RM)	1,609.49	8,047.43	-
Annual Performance Degradation Rate (%)	-0.8%	-0.8%	-
Cash Outflow, Cout			
Tariff for Grid Electricity, Te (RM/kWh)	0.365	0.365	0.365
Annual Grid Electricity Consumption, Ee (kWh)	24,334.20	17,764.20	25,976.70
Annual Maintenance Cost, M (RM)	449.75	1,859.38	-
Annual Cash Outflow, (Te x Ee) + M (RM)	9331.733	8343.308	9481.4955
Simple Cash Flow, Cout - Cin (SCF)	7,722.25	295.88	9481.4955
Total Accumulated Cost in 21 years (T)	182,728.93	93,447.15	199,111.41

[1] 243 working days a year

[2] 365 days a year
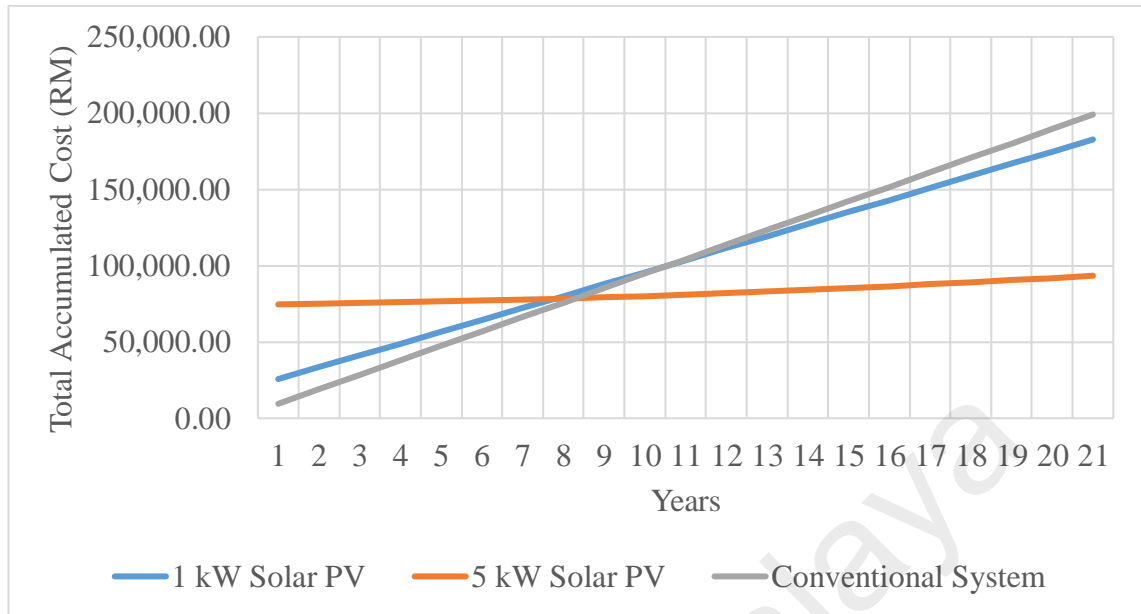
Figure 6.7: Annual accumulated cost of 1 kW solar PV, 5 kW solar PV and conventional UFAD system.

6.7 Summary

This chapter presented the solar potential of various cities in Malaysia and the economic analysis of solar photovoltaic UFAD system in Malaysia with the support of green energy policy FiT. The aim of this study was to analyze the potential application of hybrid solar-powered UFAD systems in the tropics. The focus of this study was on the energy saving and payback period. At the first part, the solar irradiation analysis showed that tropical countries have strong advantages to harvest solar irradiation throughout the year compared to subtropical countries. Tropical countries have a consistent solar irradiation of 4 – 5 kWh/m² throughout the year. In the comparison of different cities, the northern region and East of Malaysia such as Kuala Terengganu, Bayan Lepas and Kota Kinabalu have the highest intensity of solar irradiation. The daily average solar irradiation throughout a year is ranged from 3.8 kWh/m2 to 5.0 kWh/m2. From the study of cost and payback period calculation of the solar photovoltaic UFAD system, the payback periods for 1 kW and 5 kW solar photovoltaic UFAD systems are 10.6 years and 8.3 years

respectively. The returns of investment in 21 years are 3.13% for 1 kW solar photovoltaic system and 4.3% for 5 kW solar photovoltaic system. The investment of the solar photovoltaic system on the UFAD system is reasonable from the economic aspect. However, the 5 kW solar photovoltaic system needs a space of about 49 m^2 for solar panels, and it only supplied for one AHU in this study. Thus, space is a major concern when it comes to the application on high rise office building where space is limited. It can be applicable to offices where there is large roof space such as factory buildings. The office area in factory building is usually not more than 20% of the total factory area. In any event, economic consideration is still the market driving force of this technology. With the continuous decrease in the cost of solar photovoltaic, it remains optimistic that this technology is favorable.

CHAPTER 7 – CONCLUSION

7.1   Conclusions

The thermal environment and indoor air quality of the office floors served by UFAD system at TM Tower, Kuala Lumpur, Malaysia were investigated. The results show a few significant strategies that need the attention of the HVAC system designers and building's operation and maintenance team. The application of the floor swirl diffuser is totally different from the application of the ceiling type swirl diffuser or square diffuser. The floor swirl diffuser has a thick grille to support human and furniture weight. However, the grille support will affect the effectiveness of distributing treated air into the space. Air stagnation was found in the office area. The application of the diffuser blades is critical. Most of the SBS that occurred in the office area were due to maintenance issues. The malfunctioning chilled water valve actuators was the main reason why the high indoor RH exceeded 70% upper limits of local and international standards. Human maneuver on the fresh air supply pre-cooled AHU caused high indoor CO_2 levels. Formaldehyde is the major indoor air pollution after renovation. A proper IAQ management plan should be executed regularly on the building to ensure the health and well-being of the occupants are safeguarded.

The floor swirl diffuser is one of the most commonly used floor diffusers in UFAD system. From the experimental work and CFD simulations, the airflow rate and geometrical design of the diffuser, such as the number of blades, angle of attack of swirl blades and thickness of the grille directly affect the performance of the airflow pattern. This study on 250 mm floor swirl diffusers showed that the lowest airflow rate of 100 CMH can achieve thermal stratification. However, the air movement of the surrounding occupancy space is about 0.1 ms^{-1} which is below the standard's recommended values. The floor diffuser with 18 swirl blades has the most effective air distribution. The free

area of these swirl blades is about 20%. It should be noted that a large or small free area will lead to ineffective use of diffuser blades, and its performance is similar to the system without diffuser blades. A lower angle of attack of the swirl diffuser will reduce the air throw. It can compensate the shortcoming of high airflow rate which will impact the thermal stratification. Grille thickness is unavoidable in floor diffuser as it is necessary to support the load and impact of occupants and room furniture. However, this study found that a thicker grille, up to 20 mm, which is commonly used in the market, will straighten the airflow directly upwards. This defeated the purpose of using swirl diffuser blades. Thus, a thinner grille without detrimental to the strength to support loads is recommended.

On the aspect of energy consumption, HVAC systems account for half of the total energy consumption of a building. It is necessary to reduce the reliability on fuel-sourced electricity and seek for alternative sources of energy. The solar photovoltaic system is one of the prominent renewable energy suitable in a tropical country such as Malaysia. The solar irradiation throughout the year is consistently ranged from $4 - 5$ kWh/m^2 daily. However, the application can be varied from city to city. The case study showed that the payback period for 1 kW and 5 kW solar photovoltaic systems are 10.6 years and 8.3 years. The higher capacity solar photovoltaic system will have a better return of investment. However, large capacity solar panels require a larger space, which could be a shortfall for high-rise office buildings. The application for offices in factory buildings is more feasible due to the large factory rooftop area and small office area.

7.2 Recommendations

In this study, the research focus on a high-rise office building with a CAV type of UFAD system. Further study is required for other types of air distribution systems such as VAV type of UFAD system, OHAD system, etc. Besides, future study on thermal comfort, PMV and subjective measurement shall be conducted in order to have a complete understanding of the full system. The floor swirl diffuser is one of the most commonly used diffusers for UFAD system. With the increased application of the UFAD system in Malaysia, further research should cover all types of floor diffusers. Finally, a combined system (solar PV + UFAD) performance study is recommended to be conducted in the future with the existing data use for comparison so that a consolidate findings on energy saving potentials can be determined.

REFERENCES

Ahmad, S., Tahar, R. M., Muhammad-Sukki, F., Munir, A. B., & Rahim, R. A. (2015). Role of feed-in tariff policy in promoting solar photovoltaic investments in Malaysia: A system dynamics approach. *Energy, 84*, 808-815.

Ahmadzadehtalatapeh, M. (2011). *Measurements and modeling of the horizontal heat pipe heat exchangers for saving energy and improving thermal comfort in air-conditioning systems in the tropics.* (Doctor of Philosophy), University of Malaya, Kuala Lumpur.

AIAA. (1988). Guide for the verification and validation of computational fluid dynamics simulations *AIAA Standard G-077-1998*. Reston, VA: American Institute of Aeronautics and Astronautics.

Alajmi, A. F., Abou-Ziyan, H. Z., & El-Amer, W. (2013). Energy analysis of under-floor air distribution (UFAD) system: An office building case study. *Energy Conversion and Management, 73*(0), 78-85.

Alajmi, A. F., Baddar, F. A., & Bourisli, R. I. (2015). Thermal comfort assessment of an office building served by under-floor air distribution (UFAD) system – A case study. *Building and Environment, 85*(0), 153-159.

An, J.-Y., Kim, S., Kim, H.-J., & Seo, J. (2010). Emission behavior of formaldehyde and TVOC from engineered flooring in under heating and air circulation systems. *Building and Environment, 45*(8), 1826-1833.

ANSYS. (2013). *ANSYS Fluent Theory Guide*. Canonsburg, Pennsylvania: ANSYS Inc.

Arghand, T., Karimipanah, T., Awbi, H. B., Cehlin, M., Larsson, U., & Linden, E. (2015). An experimental investigation of the flow and comfort parameters for under-floor, confluent jets and mixing ventilation systems in an open-plan office. *Building and Environment, 92*(0), 48-60.

Ashhab, M. d. S. S., Kaylani, H., & Abdallah, A. (2013). PV solar system feasibility study. *Energy Conversion and Management, 65*, 777-782.

ASHRAE. (1992). ANSI/ASHRAE Standard 41.2 -1992 *Standard Methods for Laboratory Airflow Measurement*. Atlanta, GA: ASHRAE.

ASHRAE. (2009). *Fundamental Handbook, Chapter 13: Indoor environmental modeling*. Atlanta, GA: ASHRAE.

ASHRAE. (2013a). ANSI/ASHRAE Standard 55-2013 *Thermal Environmental Conditions for Human Occupancy* (pp. 52). Atlanta, GA: ASHRAE.

ASHRAE. (2013b). ANSI/ASHRAE Standard 62.1-2013 *Ventilation for Acceptable Indoor Air Quality* (pp. 52). Atlanta, GA: ASHRAE.

ASHRAE. (2013c). ANSI/ASHRAE Standard 113-2013 *Method of Testing for Room Air Diffusion*. Atlanta, GA: ASHRAE.

ASHRAE. (2013d). *UFAD Guide*. Atlanta, GA.

ASHRAE. (2015). *HVAC Applications Handbook, Chapter 57: Room Air Distribution*. Atlanta, GA: ASHRAE.

Aziz, M. A., Gad, I. A. M., Mohammed, E. S. F. A., & Mohammed, R. H. (2012). Experimental and numerical study of influence of air ceiling diffusers on room air flow characteristics. *Energy and Buildings, 55*, 738-746.

Bauman, F., & Webster, T. (2001). Outlook for Underfloor Air Distribution. *ASHRAE Journal*(June 2001), 8.

Bilgili, M. (2011). Hourly simulation and performance of solar electric-vapor compression refrigeration system. *Solar Energy, 85*(11), 2720-2731.

Burroughs, H. E., & Hansen, S. J. (2011). *Managing Indoor Air Quality* (Fifth Edition ed.). United States of America: The Fairmont Press, Inc.

Cao, G., Awbi, H., Yao, R., Fan, Y., Sirén, K., Kosonen, R., & Zhang, J. (2014). A review of the performance of different ventilation and airflow distribution systems in buildings. *Building and Environment, 73*(0), 171-186.

Chan, A. L. S., Chow, T. T., Fong, S. K. F., & Lin, J. Z. (2006). Generation of a typical meteorological year for Hong Kong. *Energy Conversion and Management, 47*(1), 87-96.

Cheong, K. W. D., & Lau, H. Y. T. (2003). Development and application of an indoor air quality audit to an air-conditioned tertiary institutional building in the tropics. *Building and Environment, 38*(4), 605-616.

Crook, B., & Burton, N. C. (2010). Indoor moulds, Sick Building Syndrome and building related illness. *Fungal Biology Reviews, 24*(3–4), 106-113.

David, J. (1984). Under floor air conditioning. *Journal of the Chartered Institution of Building Services*, 29-34.

Day, A. R., Jones, P. G., & Maidment, G. G. (2009). Forecasting future cooling demand in London. *Energy and Buildings, 41*(9), 942-948.

Department of Standards Malaysia, M. (2014). MS 1525:2014 *Code of Practice on Energy Efficiency and Use of Renewable Energy for Non-Residential Buildings* (pp. 46). Selangor, Malaysia: Department of Standards Malaysia.

DOSH. (2010). Industry Code of Practice on Indoor Air Quality (Vol. JKKP DP(S) 127/379/4-39, pp. 45). Malaysia: Department of Occupational Safety and Health, DOSH.

Fisk, W. J., Mirer, A. G., & Mendell, M. J. (2009). Quantitative relationship of sick building syndrome symptoms with ventilation rates. *Indoor Air, 19*(2), 159-165.

Fong, K. F., Chow, T. T., Lee, C. K., Lin, Z., & Chan, L. S. (2010). Comparative study of different solar cooling systems for buildings in subtropical city. *Solar Energy, 84*(2), 227-244.

Godish, T. (2001). *Indoor Environmental Quality*. United States of America: CRC Press.

Gül, H., Işsever, H., Ayraz, Ö., & Güngör, G. (2007). Occupational and Environmental Risk Factors for the Sick Building Syndrome in Modern Offices in Istanbul: A Cross Sectional Study. *Indoor and Built Environment, 16*(1), 47-54.

Gupta, V., & Woods, J. E. (2007). *The Performance of Underfloor Air Distribution Systems*. Paper presented at the High Performance Buildings Conference 2007, Nashville, Tennessee.

Hartmann, N., Glueck, C., & Schmidt, F. P. (2011). Solar cooling for small office buildings: Comparison of solar thermal and photovoltaic options for two different European climates. *Renewable Energy, 36*(5), 1329-1338.

Hoffmann, W. (2006). PV solar electricity industry: Market growth and perspective. *Solar Energy Materials and Solar Cells, 90*(18–19), 3285-3311.

Hu, S. C. (2003). Airflow characteristics in the outlet region of a vortex room air diffuser. *Building and Environment, 38*(4), 553-561.

Hwang, T., & Kim, J. T. (2013). Assessment of indoor environmental quality in open-plan offices. *Indoor and Built Environment, 22*(1), 139-156.

IARC. (2012) A review of human carcinogens.*: Vol. 100F. Part F: Chemical agents and related occupations* (pp. 567). Lyon, France: International Agency for Research on Cancer.

IEA. (2015). *CO2 Emissions From Fuel Combustion Highlights 2015*. Retrieved from France:

Ismail, A. M., Ramirez-Iniguez, R., Asif, M., Munir, A. B., & Muhammad-Sukki, F. (2015). Progress of solar photovoltaic in ASEAN countries: A review. *Renewable and Sustainable Energy Reviews, 48*, 399-412.

Khalid, F., Dincer, I., & Rosen, M. A. (2015). Development and analysis of sustainable energy systems for building HVAC applications. *Applied Thermal Engineering, 87*, 389-401.

Kilinc-Ata, N. (2016). The evaluation of renewable energy policies across EU countries and US states: An econometric approach. *Energy for Sustainable Development, 31*, 83-90.

Kim, D. S., & Infante Ferreira, C. A. (2008). Solar refrigeration options – a state-of-the-art review. *International Journal of Refrigeration, 31*(1), 3-15.

Kim, G., Schaefer, L., Lim, T. S., & Kim, J. T. (2013). Thermal comfort prediction of an underfloor air distribution system in a large indoor environment. *Energy and Buildings, 64*, 323-331.

Lee, K. H., Schiavon, S., Bauman, F., & Webster, T. (2012). Thermal decay in underfloor air distribution (UFAD) systems: Fundamentals and influence on system performance. *Applied Energy, 91*(1), 197-207.

Li, R., Sekhar, S. C., & Melikov, A. K. (2010). Thermal comfort and IAQ assessment of under-floor air distribution system integrated with personalized ventilation in hot and humid climate. *Building and Environment, 45*(9), 1906-1913.

Lin, Y. J. P., & Linden, P. F. (2005). A model for an under floor air distribution system. *Energy and Buildings, 37*(4), 399-409.

Lin, Y. J. P., & Tsai, T. Y. (2014). An experimental study on a full-scale indoor thermal environment using an Under-Floor Air Distribution system. *Energy and Buildings, 80*(0), 321-330.

Lin, Z., Chow, T. T., Tsang, C. F., Fong, K. F., Chan, L. S., Shum, W. S., & Tsai, L. (2009). Effect of internal partitions on the performance of under floor air supply ventilation in a typical office environment. *Building and Environment, 44*(3), 534-545.

Lin, Z., Lee, C. K., Fong, K. F., & Chow, T. T. (2011). Comparison of annual energy performances with different ventilation methods for temperature and humidity control. *Energy and Buildings, 43*(12), 3599-3608.

Liteplo, R. G., Beauchamp, R., Meek, M. E., & Chenier, R. (2002) Formaldehyde. *Vol. 40. Concise International Chemical Assessment Document* (pp. 74). Geneva, Switzerland: World Health Organization.

Liu, G., Rasul, M. G., Amanullah, M. T. O., & Khan, M. M. K. (2012). Techno-economic simulation and optimization of residential grid-connected PV system for the Queensland climate. *Renewable Energy, 45*(0), 146-155.

Malaysian Meteorological Department, M. (2012). *Solar Irradiation Hourly Data in Subang*.

Manzano-Agugliaro, F., Alcayde, A., Montoya, F. G., Zapata-Sierra, A., & Gil, C. (2013). Scientific production of renewable energies worldwide: An overview. *Renewable and Sustainable Energy Reviews, 18*, 134-143.

Maxwell, L. E. Facility Planning and Management Notes. In C. U. College of Human Ecology (Ed.), *Department of Design and Environmental Analysis* (Vol. 11). Ithaca, New York.

McQuiston, F. C., Parker, J. D., & Spitler, J. D. (2005). *Heating, Ventilating, and Air Conditioning - Analysis and Design* (6th ed.). New Jersey: John Wiley & Sons, Inc.

Mekhilef, S., Safari, A., Mustaffa, W. E. S., Saidur, R., Omar, R., & Younis, M. A. A. (2012). Solar energy in Malaysia: Current state and prospects. *Renewable and Sustainable Energy Reviews, 16*(1), 386-396.

Ministry of Science Technology and Innovation. (2012). General Climate of Malaysia. Retrieved from

http://www.met.gov.my/index.php?option=com_content&task=view&id=75&Ite mid=1089&limit=1&limitstart=2&lang=english

Ministry of the Environment, S. (1996). Guidelines for good indoor air quality in office premises. Singapore: Institute of Environmental Epidemiology.

Mohammed, R. H. (2013). A simplified method for modeling of round and square ceiling diffusers. *Energy and Buildings, 64*(0), 473-482.

Muhammad-Sukki, F., Munir, A. B., Ramirez-Iniguez, R., Abu-Bakar, S. H., Mohd Yasin, S. H., McMeekin, S. G., & Stewart, B. G. (2012). Solar photovoltaic in Malaysia: The way forward. *Renewable and Sustainable Energy Reviews, 16*(7), 5232-5244.

Nakaoka, H., Todaka, E., Seto, H., Saito, I., Hanazato, M., Watanabe, M., & Mori, C. (2014). Correlating the symptoms of sick-building syndrome to indoor VOCs concentration levels and odour. *Indoor and Built Environment, 23*(6), 804-813.

National Renewable Energy Laboratory. (2001). *Renewable Energy: An Overview*. Colorado, U.S.: U.S. Department of Energy.

OSHA. Formaldehyde *Occupational Safety and Health Standards* (Vol. 1910.1048). Washington, DC: U.S. Department of Labor.

Otanicar, T., Taylor, R. A., & Phelan, P. E. (2012). Prospects for solar cooling – An economic and environmental assessment. *Solar Energy, 86*(5), 1287-1299.

Pandey, A. K., Tyagi, V. V., Selvaraj, J. A. L., Rahim, N. A., & Tyagi, S. K. (2016). Recent advances in solar photovoltaic systems for emerging trends and advanced applications. *Renewable and Sustainable Energy Reviews, 53*, 859-884.

Parida, B., Iniyan, S., & Goic, R. (2011). A review of solar photovoltaic technologies. *Renewable and Sustainable Energy Reviews, 15*(3), 1625-1636.

Pasut, W., Bauman, F., & De Carli, M. (2014). The use of ducts to improve the control of supply air temperature rise in UFAD systems: CFD and lab study. *Applied Energy, 134*(0), 490-498.

Peng, J., Lu, L., & Yang, H. (2013). Review on life cycle assessment of energy payback and greenhouse gas emission of solar photovoltaic systems. *Renewable and Sustainable Energy Reviews, 19*(0), 255-274.

Pérez-Lombard, L., Ortiz, J., Coronel, J. F., & Maestre, I. R. (2011). A review of HVAC systems requirements in building energy regulations. *Energy and Buildings, 43*(2–3), 255-268.

Pérez-Lombard, L., Ortiz, J., & Pout, C. (2008). A review on buildings energy consumption information. *Energy and Buildings, 40*(3), 394-398.

Prudentaire. (2015). Floor Swirl Diffuser. Selangor, Malaysia: Prudentaire Marketing Sdn Bhd.

Pua, C. T. (2013). As-built layout plan (pp. Private communication). Kuala Lumpur: KVA Konsult Sdn Bhd.

Radhi, H. (2012). Trade-off between environmental and economic implications of PV systems integrated into the UAE residential sector. *Renewable and Sustainable Energy Reviews, 16*(5), 2468-2474.

Raftery, P., Bauman, F., Schiavon, S., & Epp, T. (2015). Laboratory testing of a displacement ventilation diffuser for underfloor air distribution systems. *Energy and Buildings, 108*, 82-91.

Redlich, C. A., Sparer, J., & Cullen, M. R. (1997). Sick-building syndrome. *The Lancet, 349*(9057), 1013-1016.

Rim, D., Schiavon, S., & Nazaroff, W. W. (2015). Energy and cost associated with ventilating office buildings in a tropical climate. *PLoS ONE, 10*(3).

Rodrigues, S., Torabikalaki, R., Faria, F., Cafôfo, N., Chen, X., Ivaki, A. R., . . . Morgado-Dias, F. (2016). Economic feasibility analysis of small scale PV systems in different countries. *Solar Energy, 131*, 81-95.

Sajadi, B., Saidi, M. H., & Mohebbian, A. (2011). Numerical investigation of the swirling air diffuser: Parametric study and optimization. *Energy and Buildings, 43*(6), 1329-1333.

Salthammer, T., Mentese, S., & Marutzky, R. (2010). Formaldehyde in the Indoor Environment. *Chemical Reviews, 110*(4), 2536-2572.

Schiavon, S., Lee, K. H., Bauman, F., & Webster, T. (2011). Simplified calculation method for design cooling loads in underfloor air distribution (UFAD) systems. *Energy and Buildings, 43*(2–3), 517-528.

Schiavon, S., Webster, T., Dickerhoff, D., & Bauman, F. (2014). Stratification prediction model for perimeter zone UFAD diffusers based on laboratory testing with solar simulator. *Energy and Buildings, 82*(0), 786-794.

SCOEL. (2008). Recommendation from the Scientific Committee on Occupational Exposure Limits for Formaldehyde. Italy: SCOEL.

SEDA. (2015). *Annual Report 2014*. Retrieved from Putrajaya, Malaysia:

Sekhar, S. C., & Ching, C. S. (2002). Indoor air quality and thermal comfort studies of an under-floor air-conditioning system in the tropics. *Energy and Buildings, 34*(5), 431-444.

Sekhar, S. C., & Goh, S. E. (2011). Thermal comfort and IAQ characteristics of naturally/mechanically ventilated and air-conditioned bedrooms in a hot and humid climate. *Building and Environment, 46*(10), 1905-1916.

Shavalipour, A., Hakemzadeh, M. H., Sopian, K., Haris, S. M., & Zaidi, S. H. (2013). New Formulation for the Estimation of Monthly Average Daily Solar Irradiation for the Tropics: A Case Study of Peninsular Malaysia. *International Journal of Photoenergy, 2013*, 6.

Solarland. (2012). SLP230-20 High Efficiency Multicrystalline PV Module.

Srebric, J., & Chen, Q. (2002). Simplified numerical models for complex air supply diffusers. *HVAC&R Research, 8*(3), 227-294.

Stamou, A., & Katsiris, I. (2006). Verification of a CFD model for indoor airflow and heat transfer. *Building and Environment, 41*(9), 1171-1181.

Tang, X., Bai, Y., Duong, A., Smith, M. T., Li, L., & Zhang, L. (2009). Formaldehyde in China: Production, consumption, exposure levels, and health effects. *Environment International, 35*(8), 1210-1224.

Tavakoli, E., & Hosseini, R. (2013). Large eddy simulation of turbulent flow and mass transfer in far-field of swirl diffusers. *Energy and Buildings, 59*(0), 194-202.

Trox. (2015). Floor Diffusers   Retrieved from https://www.troxapo.com/air-diffusers/floor-diffusers-debfe1d830db0666. Retrieved 31.07.2015, from Trox Malaysia   https://www.troxapo.com/air-diffusers/floor-diffusers-debfe1d830db0666

TSI. (2012). Alnor Electronic Balancing Tool Models EBT730/EBT731 Owner's Manual.

Tu, J., Yeoh, G.-H., & Liu, C. (2013). *Computational Fluid Dynamics - A Practical Approach* (2nd ed.). United Kingdom: Butterworth-Heinemann.

Turanjanin, V., Vučićević, B., Jovanović, M., Mirkov, N., & Lazović, I. (2014). Indoor CO2 measurements in Serbian schools and ventilation rate calculation. *Energy, 77*(0), 290-296.

Ürge-Vorsatz, D., Cabeza, L. F., Serrano, S., Barreneche, C., & Petrichenko, K. (2015). Heating and cooling energy trends and drivers in buildings. *Renewable and Sustainable Energy Reviews, 41*, 85-98.

Webster, T., Bauman, F., & Reese, J. (2002). Underfloor air distribution: Thermal stratification. *ASHRAE Journal, 44*(5), 28-30+32+34+36.

WHO. (2010). WHO guidelines for indoor air quality *Selected pollutants* (pp. 454). Copenhagen, Denmark: World Health Organization.

Wilcox, D. C. (2006). *Turbulence modeling for CFD* (3rd ed.). La Canada, Califonia: DCW Industries, Inc.

Xue, Y., & Chen, Q. (2014). Influence of floor plenum on energy performance of buildings with UFAD systems. *Energy and Buildings, 79*(0), 74-83.

Ya, Y. H., & Poh, K. S. (2015). Thermal environmental case study of an existing underfloor air distribution (UFAD) system in a high-rise building in the tropics. *IOP Conference Series: Materials Science and Engineering, 88*(1), 012064.

Yau, Y. H., Chew, B. T., & Saifullah, A. Z. A. (2013). A field study on thermal comfort of occupants and acceptable neutral temperature at the national museum in malaysia. *Indoor and Built Environment, 22*(2), 433-444.

Yau, Y. H., & Ding, L. C. (2014). A case study on the air distribution in an operating room at Sarawak General Hospital Heart Centre (SGHHC) in Malaysia. *Indoor and Built Environment, 23*(8), 1129-1141.

Yau, Y. H., & Pean, H. L. (2014). The performance study of a split type air conditioning system in the tropics, as affected by weather. *Energy and Buildings, 72*(0), 1-7.

Yu, C. W. F., & Jeong Tai Kim. (2011). Building Environmental Assessment Schemes for Rating of IAQ in Sustainable Buildings. *Indoor and Built Environment, 20*(1), 5-15.

Yun, G. Y., & Kim, J. T. (2014). Creating Sustainable Building through Exploiting Human Comfort. *Energy Procedia, 62*(0), 590-594.

Zhang, K., Zhang, X., Li, S., & Jin, X. (2014a). Experimental study on the characteristics of supply air for UFAD system with perforated tiles. *Energy and Buildings, 80*(0), 1-6.

Zhang, K., Zhang, X., Li, S., & Jin, X. (2014b). Review of underfloor air distribution technology. *Energy and Buildings, 85*(0), 180-186.

Zogou, O., & Stapountzis, H. (2011). Energy analysis of an improved concept of integrated PV panels in an office building in central Greece. *Applied Energy, 88*(3), 853-866.

Zuraimi, M. S., & Tham, K. W. (2008). Indoor air quality and its determinants in tropical child care centers. *Atmospheric Environment, 42*(9), 2225-2239.